Inverse source problem and inverse diffusion coefficient problem for parabolic equations with applications in geology

by

Sedar Ngoma

A dissertation submitted to the Graduate Faculty of
Auburn University
in partial fulfillment of the
requirements for the Degree of
Doctor of Philosophy

Auburn, Alabama
August 05, 2017

Keywords: inverse problems, parabolic equation, Rothe's method, fixed point theory, semigroup theory, geochronology

Copyright 2017 by Sedar Ngoma

Approved by

Dmitry Glotov, Co-Chair, Associate Professor of Mathematics and Statistics
Amnon J. Meir, Co-Chair, Professor of Mathematics, Southern Methodist University, and Professor Emeritus of Mathematics and Statistics, Auburn University
Wenxian Shen, Professor of Mathematics and Statistics
Paul G. Schmidt, Professor of Mathematics and Statistics
Willis E. Hames, Professor of Geosciences

Abstract

This dissertation deals with inverse problems for parabolic partial differential equations with an integral constraint and their applications in geology. We employ analytical and numerical methods to analyze and approximate solutions of these inverse problems. We consider an inverse diffusion coefficient problem for a parabolic equation that arises in science and engineering, specifically, in geochronology, a branch of geology in which radiometric ages are determined for rock formations and geological events. We investigate the corresponding direct problem, where we use a finite element approximation for a 2D model to describe the distribution of argon in mica crystals. Using a fixed point method, we show that the inverse coefficient problem has a unique classical solution that depends continuously on the data. We also consider an inverse source problem for a parabolic equation with Dirichlet and Neumann boundary conditions. We prove the existence of both weak and classical solutions to the inverse source problem subject to the Dirichlet boundary condition by means of the Rothe method and the semigroup method, respectively. An energy method is used to show uniqueness. In addition, we establish the existence and uniqueness of solutions to the inverse source problem with the Neumann boundary condition. We derive and implement numerical schemes that are used to compute approximate solutions of the inverse diffusion coefficient problem and solutions of the inverse source problem with the Dirichlet boundary condition. Our numerical algorithms employ a finite element discretization in space and the implicit Euler method in time. To assess the accuracy of the approximation, we compute the errors and estimate the rates of convergence. We conducted numerical experiments using the mathematical programming software MATLAB. We finally outline a discussion of possible future work.

Acknowledgments

I would like to thank my advisors, Dr. Dmitry Glotov and Dr. A. J. Meir for their support, availability and advice throughout my dissertation period. At any moment, they are always willing to help, direct, discuss, suggest, and comment. This work could not be possible without them. I am very thankful and pride to be advised by two very good hearted persons who always share their knowledge and expertise. I take this opportunity to express my gratitude to the committee members, Dr. Wenxian Shen, Dr. Paul G. Schmidt and Dr. Willis E. Hames for their availability, time, willingness to help and for their useful comments and suggestions. I thank Dr. Wenxian Shen for giving me the idea to solve the inverse source problem found in Chapter 4 via the semigroup approach. Thank you to Dr. Willis E. Hames for providing the geology background, samples and histories to perform the numerical computations. I thank Dr. Lorraine Wolf for the time and availability to serve as the University reader for my dissertation and for her important comments and suggestions.

I am grateful to Auburn University in general and to the Department of Mathematics and Statistics, in particular. My thanks to Dr. Greg Harris, Dr. Herman Pat Goeters, Dr. Ash Abebe, Dr. Geraldo De Souza, Dr. Overtoun Jenda, and the Department of Mathematics and Statistics staff, Ms. Malory Lipscomb, Ms. Carolyn Donegan, Ms. Gwen Kirk, and Ms. Lori Bell for their assistance and support.

I cannot hold my appreciation to many friends of mine at Auburn and everywhere else. Thank you for being good friends.

My thanks to my mother Elisabeth Sandza Ngoma, my sisters Pauline and Constantine Ngoma, my brother Fabien Ngoma, and my brother in law, Tsoumou Ntoutou. Thank you to my extended family, Emile Massala, Hermann Mvouala, Gilfery Ngamboulou, Henriette Inzoungou and their families, and others. Above all, let the glory be to the Almighty God.

Table of Contents

List of Figures

List of Tables

Chapter 1

Introduction

We are interested in two inverse problems arising in geochronology: in one problem, the source and in the other the diffusion coefficient is unknown. We start with a brief introduction to direct and inverse problems.

1.1 Direct and inverse problems

Inverse problems are widely used in science and engineering. We give a brief overview of inverse problems and contrast them with direct problems. In direct problems, one tries to determine exact or approximate functions that describe various quantities such as the concentration of a chemical, the propagation of sound, heat, or seismic waves, and many others. In direct problems the media properties of a given model described by equations, the initial state of the process under investigation (in the case of a non-stationary process) and its properties on the boundary (if considered in domains with boundaries) are known. However, media properties are often not readily observable. This lack of specification in the model leads to inverse problems, in which one is required to find, for example, equation coefficients from the information about solutions of the direct problem. These coefficients usually represent important media properties such as the heat conductivity, electrical conductivity, activation energy and frequency factor for diffusion, etc. Other types of inverse problems deal with determining the depth-time history of geologic units that formed deeply within Earth's crust. We refer to [30] for more examples. We provide an elementary example to illustrate the formulation of a direct and inverse problems. Later, we will return to this example to derive a formula for the age of a mineral.

Example 1. *Radioactive decay is a classical example for the separation of variables method in ordinary differential equations (ODEs). In that process, the rate of radioactive decay is proportional to the amount of the radioactive substance. It is described by the solution of the Cauchy problem for an ordinary differential equation*

$$\frac{dN}{dt} = -\lambda N(t), \quad t \geq 0,$$

and

$$N(0) = N_0,$$

where $N(t)$ is the amount of radioactive substance at a given time t, N_0 is the amount of substance at the initial time, and λ is the decay constant. The direct problem *is as follows: given the initial amount N_0 and the decay constant λ, determine how the amount of substance $N(t)$ changes with time. The solution is written explicitly as*

$$N(t) = N_0 e^{-\lambda t}, \quad t \geq 0.$$

Assume now that the decay constant λ and the initial amount N_0 are not known, but we can measure the amount of the radioactive substance $N(t)$ for certain values of t, namely

$$N(t_k) = f_k, \quad k = 1, 2, \cdots, \tilde{N}, \tag{1.1}$$

where f_k is known for all $k = 1, 2, \cdots, \tilde{N}$, with $\tilde{N}$ some positive integer. A possible inverse problem *is to determine the initial amount N_0 and the decay constant λ from the data* (1.1).

We now begin to describe the model we will use in this dissertation.

1.2 Model description

Our primary focus is on the following system

$$\partial_t u(x,t) - c(t)\Delta u(x,t) = f(x,t), \quad \text{in } \Omega \times (0, T_f], \tag{1.2}$$

$$u(x,t) = g(x,t), \quad \text{on } \partial\Omega \times [0, T_f], \tag{1.3}$$

and

$$u(x,0) = u_0(x), \quad \text{in } \Omega, \tag{1.4}$$

where Ω is a bounded open set in $\mathbb{R}^d$, $d \geq 1$, with a C^2 boundary $\partial\Omega$. The model describes the evolution in time of the concentration $u(x,t)$ of a chemical throughout this dissertation. In this chapter, T_f denotes the final time to distinguish it from the temperature T. In the rest of the dissertation however, the final time will be denoted by T. The function u_0 is the initial condition, g is the boundary condition, f is the source function, and c is the diffusion coefficient. For given c, f, g, and u_0, the problem of finding u from the equations (1.2)–(1.4) is the direct problem.

System (1.2)–(1.4) arises in the Potassium-Argon (K-Ar) methods of geochronology as applied to measuring the ages of micas. These methods are based on the radioactive decay of ^{40}K to stable ^{40}Ar. Isotopes are defined as atoms of the same element with equal number of protons but different number of neutrons in their nuclei. A stable isotope is an isotope that does not change over a long period of time while an unstable or parent isotope is the one that spontaneously changes the number of protons and/or neutrons by radioactive decay. A daughter isotope is a stable isotope produced by the radioactive decay of a parent isotope. In the K-Ar methods, the daughter isotope ^{40}Ar can escape the molten rock, but begins to accumulate as the rock crystallizes and cools. To calculate the time since cooling and onset of ^{40}Ar retention, a measurement of the ratio of the amount of ^{40}Ar accumulated to the amount of ^{40}K remaining is taken [34]. In order to obtain this ratio, the amounts of argon and potassium are measured by mass spectrometry of the gasses released when a rock sample

is melted in vacuum. Directly measuring the amount of ^{40}K is inconvenient, suggesting that a different method should be used instead. The ^{40}Ar/^{39}Ar dating method is a variation of the K-Ar method in which ^{39}Ar serves as a proxy for ^{40}K. A sample is crushed and partial crystals of the mineral are hand-selected for analysis and then irradiated with fast neutrons to produce ^{39}Ar from ^{39}K. The sample is then degassed in a high vacuum system. The crystal structure of the mineral degrades due to heat, and as the sample melts, trapped gases ^{40}Ar and the derived ^{39}Ar are released and their amounts are measured.

Common micas (e.g., muscovite with chemical composition $K_2Al_4Si_6Al_2O_{20}(OH,F)_4$) are silicate minerals with nearly perfect basal cleavage, whose shape can be described as a domain $\Omega \subset \mathbb{R}^d$, $d = 2$ or $d = 3$. By cleavage we mean the tendency of crystalline materials to split along a definite crystallographic structural planes. The geometry of these planes defines the structure of material parameters of micas (an application of Neumann's principle in mineralogy) such as diffusion coefficients. The cleavage in micas allows us to consider and analyze models in $\mathbb{R}^2$.

The function $u(\cdot, t)$ represents the concentration of argon within a mica at time t. Argon is the most abundant noble gas in the Earth's crust and the third most abundant gas in the Earth's atmosphere. Almost all of the argon in the atmosphere is radiogenic ^{40}Ar, produced by the radioactive decay of potassium ^{40}K in the Earth's crust, which itself is an isotope found in mica crystals. A mica crystal has the structure of layers with crystal lattice composed of aluminium and silicon and the atoms of ^{40}K and ^{40}Ar sandwiched between these layers. The diffusion of argon is more rapid parallel to these layers than perpendicular to them. Figure 1.1 shows the images of mixed polyhedral and atomic ('ball and stick') representations of a phlogopite structure, a mica with chemical composition $K_2Mg_6Si_6Al_2O_{20}(OH)_4$, drawn with the *Crystalmaker software package*. The tetrahedra-octahedra-tetrahedra layers are filled with silica and aluminum (blue tetrahedra) and magnesium (yellow octahedra). Oxygen and hydroxyl (OH) are at the vertices of the polyhedra and they bind the layers together. The interlayer sites are each formed by two six-sided rings of tetrahedra and are filled with

potassium (purple). For a brief overview of types of micas including their chemical formulas, see [34, p.25-27].

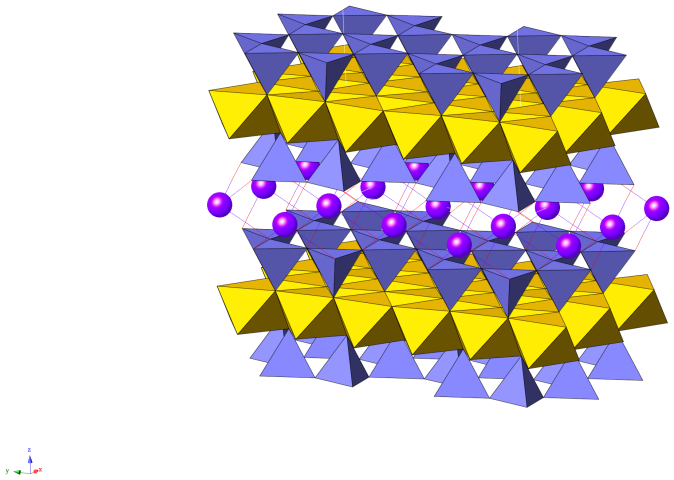

Figure 1.1: Phlogopite rendered with Crystalmaker.

The coefficient c is a composition of a function $D(\cdot)$ and the temperature, which itself is a function of time, that is, $c(t) = D(T(t))$, and the dependence of D on the temperature T is given by the Arrhenius law

$$D(T) = D_0 e^{-E/RT}, \tag{1.5}$$

where D_0 is the pre-exponential factor also called the frequency factor, E is the activation energy which is the energy necessary for diffusion, and R is the gas constant. The gas constant is the same for all chemicals including argon and it has the value $R = 8.314$. The constants D_0 and E are unique for every diffusant and are estimated from experiments or postulated based on empirical data.

The thermal history is significant in studies of the Earth's crust history due to the proxy relationship between depth and temperature beneath Earth's surface. Restricting the temperature of geologic samples as a function of time permits us to reconstruct the different

processes they have undergone and to better understand the Earth's history. The source term that takes into account the production of argon within the crystal can be considered in the general form $f(x,t)$. We often consider the specific form:

$$f(t) = \lambda_{\mathrm{K}} f_{\mathrm{Ar}} e^{-\lambda_{\mathrm{K}} t}, \tag{1.6}$$

where λ_{K} is the rate of radiogenic decay of ^{40}K and f_{Ar} is the fraction of ^{40}K that yields ^{40}Ar.

The problem of finding the diffusion coefficient c (or the source function f) from (1.2)–(1.4) for given f, g and u_0 (or, for given c, g and u_0) is underdetermined, since we now have two unknowns u and c (respectively, u and f). Additional data that we refer to as an *overdetermination condition* is required. The additional data we consider throughout this dissertation is in the form of an integral constraint given by

$$\int_\Omega u(x,t)\,dx = \mu(t), \quad \text{for all } t \in [0, T_f]. \tag{1.7}$$

Other common types of overdetermination conditions include (but are not limited to) the solution $u(x,T_f)$ at final time, the solution $u(x_0,t)$ evaluated at an interior point $x_0 \in \Omega$ or the normal derivative of the solution $\partial u(x_0,t)/\partial\nu$ at a boundary point $x_0 \in \partial\Omega$ for all times $0 < t < T_f$, where ν is the outward unit vector normal to the boundary $\partial\Omega$. The problem of determining c or f, together with u from (1.2)–(1.4) and (1.7) is the inverse diffusion coefficient problem or the inverse source problem, respectively. For the inverse source with a Neumann boundary condition, we replace the Dirichlet boundary data (1.3) by a condition of the form

$$\frac{\partial u}{\partial \nu}(x,t) = g(x,t) \quad \text{on } \partial\Omega. \tag{1.8}$$

The rest of this chapter is organized as follows: in Section 1.3, we recall the known results for the direct problem (1.2)–(1.4) and present details of numerical studies of approximate

solutions to the direct problem (1.2)–(1.4). In Section 1.4, we establish a link between the inverse source problem and the inverse diffusion coefficient problem, and motivate the integral constraint. A literature review appears in Section 1.5. In Section 1.6, we summarize the notation used throughout this dissertation.

1.3 The direct problem

We now investigate the determination of the concentration of argon from system (1.2)–(1.4), which we will convert into apparent age as explained later. We also provide a geological literature review, and a brief description of the finite element method and some numerical results. The source function is taken in the form (1.6). We assume that the concentration of argon is zero on the boundary. We also suppose that argon has zero initial concentration. That is, we consider the system

$$\partial_t u(x,t) - c(t)\Delta u(x,t) = f(t), \quad \text{in } \Omega \times (0, T_f], \tag{1.9}$$

$$u(x,t) = 0, \qquad \text{on } \partial\Omega \times [0, T_f], \tag{1.10}$$

and

$$u(x,0) = 0, \qquad \text{in } \Omega, \tag{1.11}$$

where the final time T_f, the diffusion coefficient c and the source function f are given, and $u : \bar{\Omega} \times [0, T_f] \to \mathbb{R}$ is the unknown. Again, $c(t) = D(T(t))$, and the dependence of D on the temperature T is given by the Arrhenius law (1.5). The system is a special case of the problem considered in [14, p. 372],

$$\partial_t u + Lu = s, \quad \text{in } \Omega \times (0, T_f], \tag{1.12}$$

$$u = 0, \quad \text{on } \partial\Omega \times [0, T_f], \tag{1.13}$$

and

$$u = h, \quad \text{in } \Omega \times \{t = 0\}, \tag{1.14}$$

where L is a second-order partial differential operator having the form

$$Lu = -\sum_{i,j=1}^{d} (c^{ij}(x,t)u_{x_i})_{x_j} + \sum_{i=1}^{d} b^i(x,t)u_{x_i} + a(x,t)u,$$

for given source $s : \Omega \times (0, T_f] \to \mathbb{R}$, initial data $h : \Omega \to \mathbb{R}$, and coefficients c^{ij}, b^i, a $(i, j = 1, \cdots, d)$. Under the assumptions

$$c^{ij}, b^i, a \in L^\infty(\Omega \times (0, T_f]) \quad (i, j = 1, \cdots, d),$$
$$s \in L^2(\Omega \times (0, T_f]),$$

and

$$h \in L^2(\Omega),$$

the existence and uniqueness of weak solutions to (1.12)–(1.14) are established by the Galerkin's method and an energy method, respectively. See [14, Theorem 3, p. 378] for existence and [14, Theorem 4, p. 379] for uniqueness. A function $u \in L^2(0, T_f; H^1(\Omega))$, with $u' \in L^2(0, T_f; H^{-1}(\Omega))$ is a *weak solution* of (1.12)–(1.14) provided

i. the weak equation $\langle u', v\rangle + B[u, v; t] = (s, v)$ holds

for all $v \in H_0^1(\Omega)$ and a.e. $0 \le t \le T_f$ and

ii. the initial condition $u(0) = h$ is satisfied in $C([0, T]; L^2(\Omega))$.

Here, B is the time-dependent bilinear form

$$B[u, v; t] = \int_\Omega \sum_{i,j=1}^{d} c^{ij}(\cdot, t)u_{x_i}v_{x_j} + \sum_{i=1}^{d} b^i(\cdot, t)u_{x_i}v + a(\cdot, t)uv\, dx,$$

which is defined for all $u, v \in H_0^1(\Omega)$ and a.e. $0 \le t \le T_f$. See the definition in [14, p. 374]. The notation $L^2(0, T_f; H^1(\Omega))$, $L^2(0, T_f; H^{-1}(\Omega))$, $H_0^1(\Omega)$, and $C([0, T]; L^2(\Omega))$ is standard.

Geologists use the concentration of argon and potassium to determine the apparent age of rocks. In this paragraph, we derive a formula for the apparent age of a mineral as a function of the ratio of a radiogenic daughter product to its parent as widely used in geochronology. Continuing with Example 1 of the radioactive decay, let N denote the number of radioactive atoms of the parent potassium ^{40}K and let D be the number of daughter atoms ^{40}Ar. These quantities satisfy a conservation of mass law, that is, $N_0 = N + D$, where N_0 is the initial number of radioactive atoms. Thus, $N = (N + D)e^{-\lambda_{\mathrm{K}} t}$ or $e^{\lambda_{\mathrm{K}} t} = 1 + \frac{D}{N}$. Taking the natural logarithm of both sides, we obtain a basic equation used in geochronology [34, p. 18]:

$$t = \frac{1}{\lambda_{\mathrm{K}}} \ln\left(1 + \frac{D}{N}\right).$$

To take into account the fact that ^{40}K decays to ^{40}Ca and ^{40}Ar, the basic equation needs to be modified. Namely, let f_{Ar} denote the fraction of the ^{40}K decays that yields ^{40}Ar. It is the ratio of the relevant partial decay constants to the ^{40}K decay constant. It follows from the basic equation that, for the K-Ar dating method,

$$\frac{D}{N} = \frac{1}{f_{\mathrm{Ar}}} \frac{^{40}\mathrm{Ar}*}{^{40}\mathrm{K}},$$

where $\frac{^{40}\mathrm{Ar}*}{^{40}\mathrm{K}}$ represents the ratio of radiogenic ^{40}Ar to ^{40}K present in the sample. In the notation of (1.2)–(1.4), let u denote the concentration of argon at location x in the sample at the final time. Denote by v the concentration of ^{40}K at the final time. Then the apparent age $A(x)$ as a function of u and v is given by the formula

$$A(x) = \frac{1}{\lambda_{\mathrm{K}}} \ln\left(1 + \frac{1}{f_{\mathrm{Ar}}} \frac{u}{v}\right). \tag{1.15}$$

We recall some results related to the direct problem (1.9)–(1.11) that appeared in the geological literature. Much attention has been devoted to the one dimensional case.

In a seminal paper [11], Dodson introduced the concept of *closure temperature* defined as the temperature of a mineral at the time corresponding to its apparent age, to take into account the dependence of the diffusion coefficient D on temperature in (1.5). The closure temperature is a function of the pre-exponential factor, the activation energy, the diffusion radius, and the cooling rate of the rock. The relation between the apparent ages of K-bearing minerals and the temperatures in plutonic rocks that cooled over millions of years supports the closure temperature concept and shows ranges of closure temperatures for various minerals (for instance, 350-400°C for muscovite, 300-350°C for biotite with a diffusion radius of ca. 100 μm.)

Dodson's model is applicable for histories linear in $1/T$. Also, Dodson's derivation of the closure temperature value for a mineral assumes that the argon concentration at the grain boundary is zero, or equivalently, the diffusant is quickly lost once it reaches the grain boundary by lattice diffusion. This assumption is reasonable if argon transport is faster in the grain boundary network than it is within the lattice, and if high concentrations of ^{40}Ar are never retained within the pathways along which radiogenic argon escapes in the atmosphere. However, there are many observations that imply exceptions to these criteria. In some cases, biotite is apparently older than muscovite, or there may be wide variations in apparent ages in small areas [45, p. 920]. Moreover, many metamorphic mineral grains display complex intracrystalline age patterns. In the case of mica, for example, there may be more ^{40}Ar at the edge of the grain than in the center, a condition most easily explained by diffusion of argon from the grain boundary network into the crystal, which is excess argon. Other possible explanations for such behavior include the facts that the thermal history of rocks is complex and may involve reheating events. Finally, if grains crystalize from a ^{40}Ar-rich fluid, they could incorporate ^{40}Ar during growth. If ^{40}Ar is not easily lost from the grain

boundary, then this will inhibit ^{40}Ar loss from the grain interiors. See [45] and references therein for more on diffusion mechanisms.

Among results of computational nature, J. Wheeler [45] developed DIFFARG, a program written in MATLAB to compute apparent age profiles within grains and model them as a function of any thermal history and boundary conditions. The core algorithm of the program is a routine to approximate solutions of the diffusion equation in one dimension by one of the two finite difference schemes: a fully explicit algorithm and a Crank-Nicholson algorithm. DIFFARG is intended to be used for fitting observed apparent age profiles with computed profiles by varying thermal history when the assumption of homogeneous volume diffusion of argon is considered appropriate. It serves as a tool to explore general aspects of ^{40}Ar diffusion in minerals and their implications for geochronology. Infinite plane sheet, cylindrical, and spherical model diffusion geometries may be selected. To model the diffusion of excess argon in the surroundings, the diffusant concentration at the edge of the grain can vary with time. The temperature history may be specified as a linear or any other monotonically decreasing function of time to simulate rapid or slow cooling, it may incorporate a temperature pulse to simulate a reheating event, or it can be arbitrarily defined by a user.

In [44], Watson, Wanser, and Farley developed general analytical solutions to the anisotropic diffusion equation for a finite cylinder that capture both the internal distribution of diffusant as a function of time and the fraction of diffusant lost during a specified thermal history. These solutions were shown to conform to the existing analytical expressions for limiting cases of diffusion in an infinite slab and infinite cylinder. Moreover, the authors computed solutions by the finite difference method and observed a good match of the numerical output with their analytical expressions. Their computations allowed to go beyond some of the limitations of the analytical solutions and simulate complex natural scenarios including non-zero and time-dependent boundary conditions and arbitrary initial distribution of diffusant within the cylinder. However, their model does not allow evaluation of the effects of a crystal geometry different from a cylinder.

Meanwhile, in the geological literature, Hames and Hodges [22], Hames and Andresen [23], and Hodges, Hames, and Bowring [27] examined samples for which the contours of age show asymmetry that is not consistent with the assumption of radial symmetry imposed by cylindrical geometry imposed in the previous papers.

Using the finite element method, we developed a 2-D model to describe argon diffusion in mica crystals that are dominated by diffusion within the layers. This model allows modeling of a user-defined thermal history and crystal shape. We evaluate this model by comparing direct or *in situ*, laser based measurements of argon apparent age gradients with the output of the program. As we will see in Section 1.3.2, modeling of previously published *in situ* laser $^{40}\mathrm{Ar}/^{39}\mathrm{Ar}$ apparent age gradients in actual micas with this model allows for reasonably accurate approximation. In the following two sections, we will provide a brief description of the finite element method and present the numerical results.

1.3.1 The finite element method

We start by deriving the weak form of equation (1.9). To that end, we multiply it by a function $v \in H_0^1(\Omega)$, integrate by parts in the second term on the left, and use the boundary condition (1.10) to obtain the weak form of equation (1.9):

$$\int_\Omega \partial_t uv\,dx + \int_\Omega c(t)\nabla u\cdot\nabla v\,dx = \int_\Omega f(t)v\,dx \quad \text{for all } v \in H_0^1(\Omega), \quad \text{and} \quad 0 < t \le T_f. \tag{1.16}$$

We discretize problem (1.9)–(1.11), first in the spatial variable x, solving which results in an approximate solution $u_h(\cdot, t)$ that belongs to a finite dimensional, linear space V_h of functions of x, called the finite element space. The function u_h, which in the simplest case, is a continuous, piecewise linear function on some partition of Ω, is a solution of an initial value problem for a finite number of ODEs. The fully discrete approximation of this initial value problem is obtained by approximating the time derivative using finite differences.

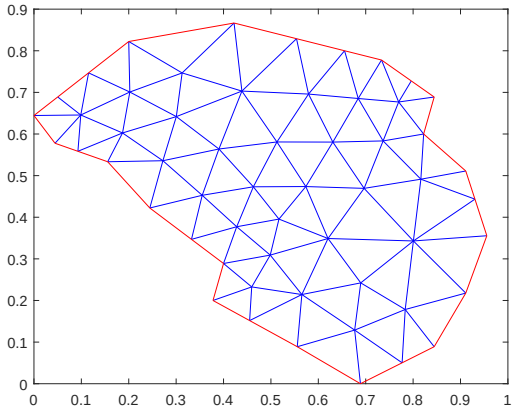

Figure 1.2: Triangulation of a domain.

We now construct the finite element space V_h. Let Ω be a polygonal domain and let T_h denote a partition of Ω, or triangulation, into a set of non-overlapping triangles such that no vertex of one triangle lies in the interior of the edge of another triangle. Let h denote the maximum length of the edges of triangles in the triangulation T_h (also called maximum mesh size). A plot of an example of a triangulation with maximum mesh size $h = 0.5$ appears in Figure 1.2. Denote by V_h the space of continuous functions on $\overline{\Omega}$ (the closure of Ω) which are linear on each triangle of T_h and which vanish on the boundary $\partial\Omega$. Let $\{x_j\}_{j=1}^{N_p}$ be the vertices interior to Ω called nodes or points of T_h. Let N_p be the number of nodes. A function in V_h is then uniquely determined by its values at the nodes x_j and therefore depends on N_p parameters. Let ϕ_j be the function in V_h that takes the value 1 at x_j but vanishes at all other vertices. Then $\{\phi_j\}_{j=1}^{N_p}$ forms a basis for V_h, and every function $v \in V_h$ has a unique representation in terms of this basis. The spatially discrete problem, based on the weak formulation (1.16) is to find $u_h(t) = u_h(\cdot, t)$, which belongs to V_h for all $t \in [0, T_f]$, such that

$$\int_\Omega \partial_t u_h v \, dx + \int_\Omega c(t) \nabla u_h \cdot \nabla v \, dx = \int_\Omega f(t) v \, dx, \tag{1.17}$$

for all $v \in V_h$, and $0 < t \leq T_f$ with $u_h(0) = 0$. Using the basis $\{\phi_j\}_{j=1}^{N_p}$ for V_h, we construct a discrete approximation of the solution in the form

$$u_h(x,t) = \sum_{j=1}^{N_p} U_j(t)\phi_j(x) \quad \text{with} \quad U_j(t) = u_h(x_j,t), \tag{1.18}$$

where $U_j(t)$ are differentiable functions for $j = 1, 2, \cdots, N_p$. Substituting $v(x) = \phi_i(x)$ in (1.17) and using (1.18) we obtain a system of ODEs,

$$\sum_{j=1}^{N_p} \frac{dU_j(t)}{dt} \int_\Omega \phi_j(x)\phi_i(x)\,dx + c(t) \sum_{j=1}^{N_p} U_j(t) \int_\Omega \nabla\phi_j(x) \cdot \nabla\phi_i(x)\,dx = f(t) \int_\Omega \phi_j(x)\,dx.$$

for $i = 1, 2, \cdots, N_p$. In matrix form, this system of ODEs can be written as

$$M\frac{dU}{dt} + KU = F,$$

for all $t \in (0, T_f]$, with $U(0) = 0$. We used the notation

$U = (U_i)^t$ unknown solution vector,

$M = (M_{ij})$, $M_{ij} = \int_\Omega \phi_j(x)\phi_i(x)\,dx$ mass matrix and its elements,

$K = (K_{ij})$, $K_{ij} = c(t) \int_\Omega \nabla\phi_j(x) \cdot \nabla\phi_i(x)\,dx$ stiffness matrix and its elements,

and

$F = (F_i)$, $F_i = f(t) \int_\Omega \phi_j(x)\,dx$ load vector and its elements.

The superscript t denotes the matrix transpose. The mass and the stiffness matrices can be shown to be positive definite. Thus the above system of ODEs can be rewritten as

$$\frac{dU}{dt} + M^{-1}KU = M^{-1}F,$$

for all $t \in (0, T_f]$, with $U(0) = 0$. Here, M^{-1} denotes the matrix inverse of M. This system has a unique solution for all $t \in (0, T_f]$. For details on the finite element method, including error estimates see, for instance [43, Chapter 1] and [3, 8, 20, 33].

1.3.2 Numerical studies

In this section, we present some numerical results on the direct problem (1.9)–(1.11). While MATLAB allows entering parameters of a model, including the equations and the description of the domain using a graphical user interface, we implemented the description of the polygonal domain and the construction of the approximate discrete solution programmatically. We use the built-in MATLAB functions *decsg* to construct the $2D$ polygonal domain Ω, *initmesh* to generate a triangular mesh on the domain Ω, *assempde* to assemble the finite element matrices that represent the discretization of the PDE (M, K, F above), and *parabolic* to produce the solution to the finite element approximation of the PDE (1.9)–(1.11). For an illustration of the finite element approximation, we consider two muscovite crystals with *in situ* $^{40}\mathrm{Ar}/^{39}\mathrm{Ar}$ age distribution and geometries described in the paper by Hames and Andresen [23] (Figure 1.3), with nonlinear time-temperature histories postulated on the basis of the samples' geologic context (left column in Figure 1.4) and the resulting apparent age distribution in model crystals (right column in Figure 1.4). We note that these two muscovite crystals came from two different geologic structural levels of an area and experienced different time-temperature histories. (See [23] and references therein for description of geological analytical methods and procedures used to determine $^{40}\mathrm{Ar}/^{39}\mathrm{Ar}$ ages.) For the crystal in Figure 1.3 A, we prescribed the zero Neumann boundary condition (a condition of the form (1.8) with $g = 0$) on the boundary segments along which the sample was cut as illustrated in Figure 1.3 A and the homogeneous Dirichlet boundary condition on the remaining edges. We specified the homogeneous Dirichlet boundary condition for the crystal in Figure 1.3 B; the half-life of $^{40}\mathrm{K}$ is $H = 1250 \times 10^6$ and we use the diffusion parameters from Hames and Bowring [21]: $E = 52$ kcal/mol and $D_0 = 0.04$ cm^2/s. For the muscovite

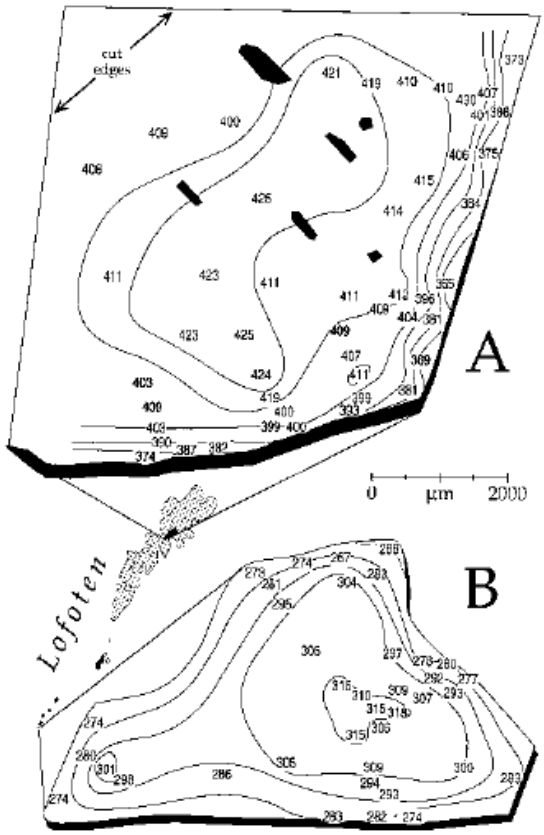

Figure 1.3: *In situ* $^{40}Ar/^{39}Ar$ age distribution in muscovite crystals from Hames and Andresen [23]. A: Laser fusion $^{40}Ar/^{39}Ar$ ages for spot analyses within a muscovite porphyroblast from Vestvågøy island, Lofoten, Norway. B: Laser $^{40}Ar/^{39}Ar$ fusion ages for a muscovite porphyroblast in Røst island, Lofoten, Norway. Numerical values are ages in millions of years with an analytical spot size of approximately 100 μm.

in Figure 1.4 (b), we show level curves for ages 375, 390, 405, and 420 Ma. We display level curves for ages 270, 280, 290, 300, and 310 for the muscovite in Figure 1.4 (d). The resulting apparent age in millions of years (Ma) is computed using formula (1.15) and can be read on the accompanying color bar plot . We summarize in Table 1.1 the mesh sizes, the number of elements (triangles) and the number of unknowns used in the finite element discretization. Visual inspection of the age gradients in Figure 1.3 and the model results in Figure 1.4 are in good agreement. Shaded areas in Figure 1.3 A indicate the positions of spot-fusion analyses used to construct the age contours. We note that the zero Dirichlet boundary condition imposes argon loss from the crystal edge at all times for all temperatures. Consequently, there

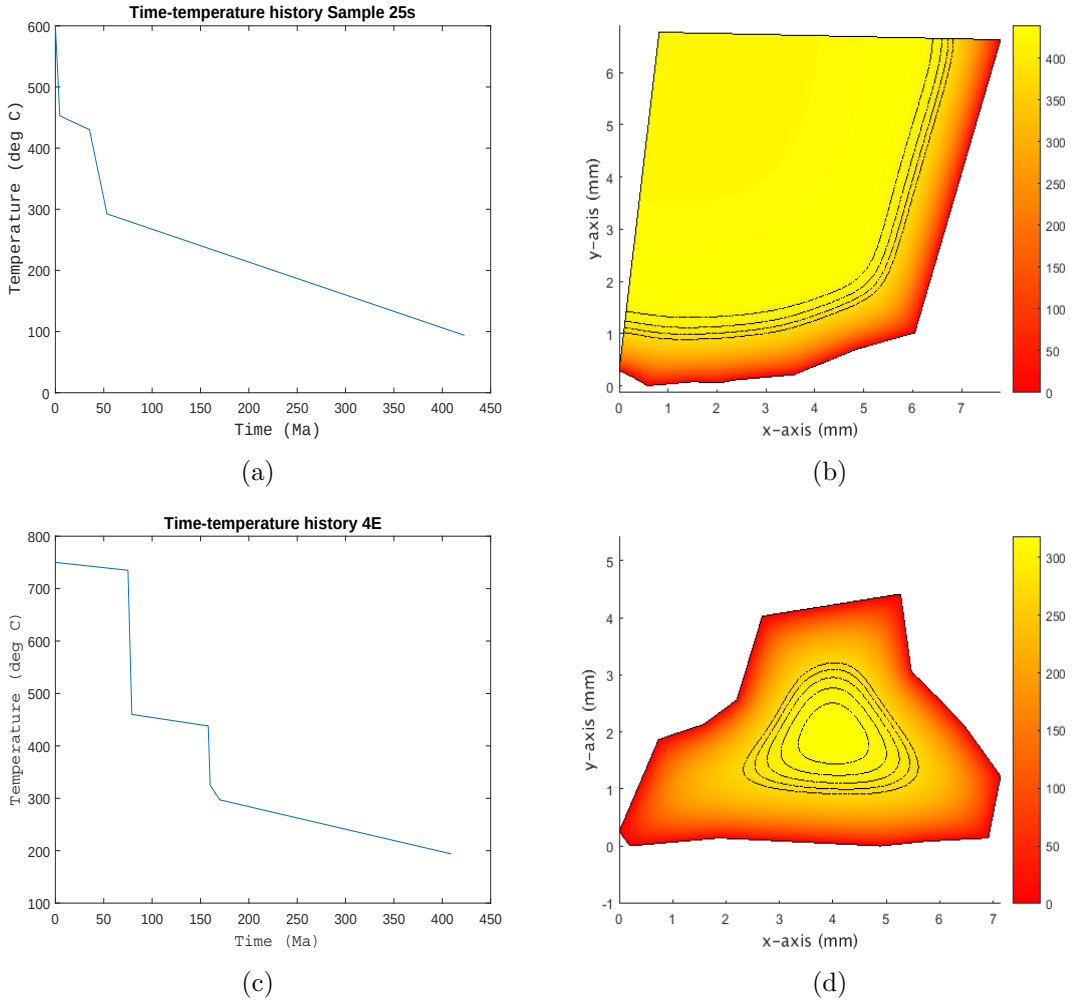

Figure 1.4: (a) Postulated T-t history *25s* for muscovite crystal A in Figure 1.3; (b) apparent age distribution in model for muscovite crystal A from Figure 1.3; (c) postulated T-t history *4E* for muscovite crystal B in Figure 1.3; and (d) apparent age distribution in model for muscovite crystal B from Figure 1.3.
The age values on the color bar are in Ma.

Table 1.1: Model sources, mesh sizes, number of elements and unknowns.

Samples	Hames and Andresen [23], A	Hames and Andresen [23], B	Hodges, Hames, and Bowring [27]
Maximum mesh size	0.05	0.05	0.011
Number of elements	56,094	27,888	13,374
Number of unknowns	28,307	14,145	6,820

is a limitation on argon accumulation throughout the crystal resulting in younger age range in Figure 1.4 (b) and in Figure 1.4 (d) than observed in Figure 1.3 (notice the age range in Figure 1.3 A, about 435 to 360 Ma and about 320 to 270 Ma in Figure 1.3 B). We also consider a biotite crystal with *in situ* $^{40}\mathrm{Ar}/^{39}\mathrm{Ar}$ age distribution and geometry reported in the paper by Hodges, Hames, and Bowring [27] (Figure 1.5 (c)). The nonlinear time-temperature history is postulated on the basis of the sample's geologic context (Figure 1.5 (a)). The resulting apparent age distribution in the model crystal appears in Figure 1.5 (b). This biotite is from a low-pressure, high-temperature metamorphic area in central Arizona. For a more detailed description of the geological methods and procedures used, see [27]. For this model, we prescribe the homogeneous Dirichlet boundary condition and we use the diffusion parameters from Harrison, Duncan, and McDougall [24]: $D_0 = 0.077$ cm^2/s and $E = 46.1$ kcal/mol. We display the level curves for ages 1200, 1250, 1300, 1350 and 1400 Ma (again, note the age range of about 1400 to 1200 Ma in Figure 1.5 (c)). The mesh size and the resulting number of triangles and unknowns used in the finite element approximation are as in Table 1.1. The agreement between the author's initial interpretation of age gradients [27] and the model results appears to be quite good by visual inspection. The purpose of these studies is to demonstrate the ability of numerical modeling to describe intracrystalline age gradients in actual micas with complex geometric shapes formed by diffusion over geologic histories of interest.

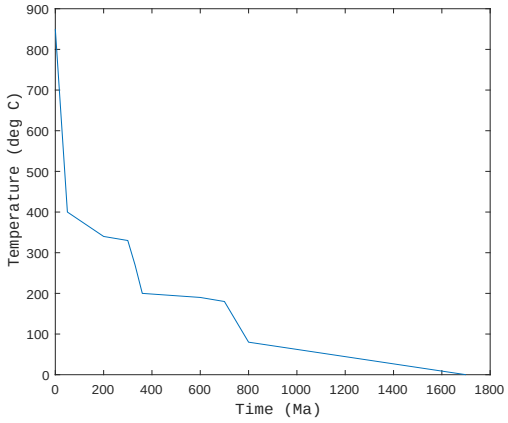

(a)

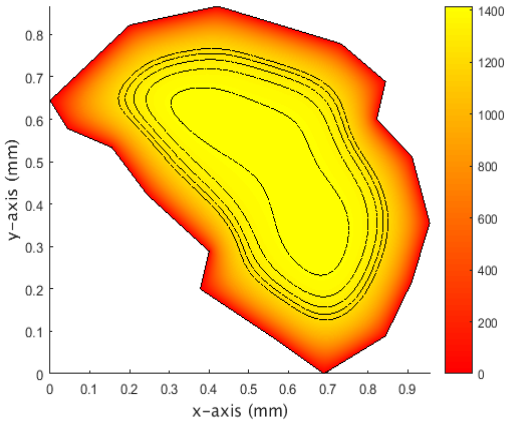

(b)

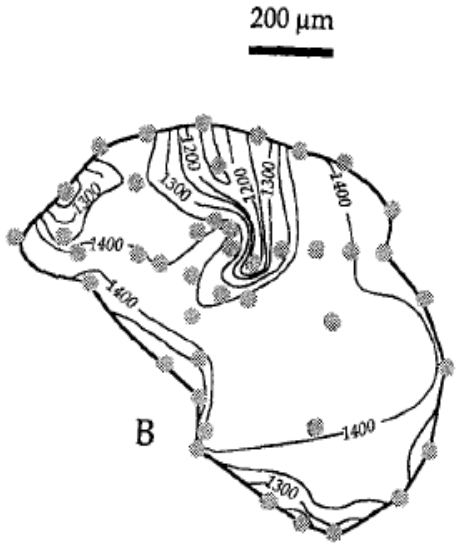

(c)

Figure 1.5: (a) Postulated temperature-time history for biotite crystal in Hodges, Hames, and Bowring [27]; (b) apparent age distribution in biotite crystal from Hodges, Hames, and Bowring [27]; and (c) *in situ* $^{40}Ar/^{39}Ar$ age distribution in biotite crystal from Hodges, Hames, and Bowring [27].

1.4 Inverse diffusion coefficient and inverse source problems

We now turn to inverse problems, which is the main focus of this dissertation. Before proceeding to the inverse problems, in Section 1.4.1, we first provide a motivation for the integral constraint based on the kind of data available to geologists. Then in Section 1.4.2, we outline the connection between the problem with unknown source and the problem with unknown diffusion coefficient. We conclude this section by introducing the inverse diffusion coefficient problem and the inverse source problem.

1.4.1 Motivation for the integral constraint

As we mentioned earlier, in order to recover from (1.2)–(1.4) the diffusion coefficient c together with the concentration u for given data in the form of a source f, an initial condition u_0, and a boundary condition g, we need additional information on the solution of the direct problem u. Similarly, for given coefficient c, initial data u_0, and boundary condition g from (1.2)–(1.4), the recovery of the source f together with the concentration u requires additional data. The additional information of our choice is the integral constraint given by (1.7). This condition can be interpreted as the total mass of argon contained in the spatial domain Ω.

We next describe how this type of data appears or is obtained in geochronology. We evoke the description of the $^{40}\mathrm{Ar}/^{39}\mathrm{Ar}$ dating technique, a variation of the K-Ar dating method, as described in Section 1.2. This method allows the measurements of the amounts of the trapped gases $^{40}\mathrm{Ar}$ and $^{39}\mathrm{Ar}$ released when a sample is crushed and fragmentary crystals of the mineral are hand-selected for analysis, then exposed to radiation with fast neutrons and degassed in a high vacuum system. The function u represents the concentration of argon at the final time, which once obtained is converted by geologists into apparent age by a version of formula (1.15) that includes a proportionality constant for $^{39}\mathrm{Ar}$ production [34]. Thus the integral of $u(x,t)$ over Ω (or the function $\mu(t)$ in (1.7)) corresponds to the measured bulk age of the crystal.

As a specific example, Eusden and Lux in [13] reported $^{40}Ar/^{39}Ar$ mineral ages from muscovite in rocks exposed on Mount Washington, New Hampshire. These geologists showed that the bulk ages of muscovite increase progressively from the bottom to the top of the mountain. They used this relation to determine the exhumation rates of rocks. Exhumation is the process by which rocks approach Earth's surface. In that work, muscovite from each sample was analyzed using the $^{40}Ar/^{39}Ar$ incremental heating method. See Figure 1.6 for a plot of the reported data. The data were fit with a line whose slope is interpreted as the exhumation rate. See Chapter 6 for another brief overview of applications of the integral overdetermination condition.

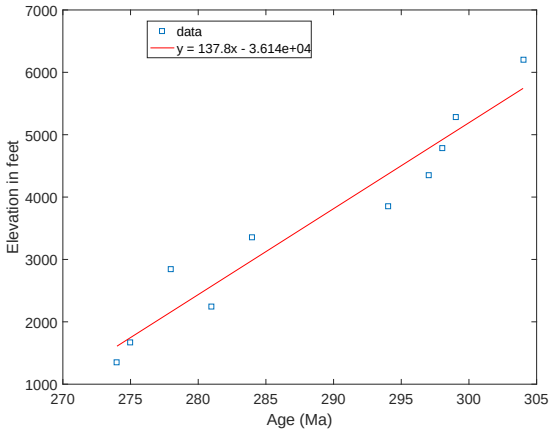

Figure 1.6: Age vs. elevation plot through relief of Mount Washington, New Hampshire with data from Eusden and Lux [13].

1.4.2 Unknown source vs. unknown diffusion coefficient

We now establish a connection between the diffusion coefficient and the source. The equation with a known time-dependent diffusion coefficient

$$\partial_t u(x,t) - c(t)\Delta u(x,t) = f(t), \tag{1.19}$$

can be transformed into an equation with a constant diffusion coefficient via a change of the time variable. The transformation is inspired by [9, p. 4]. We point out that the following

method is limited to the case of the diffusion coefficient term being a function only of time. We consider the special case when the source is of the form $f(t) = \lambda_{\mathrm{K}} f_{\mathrm{Ar}} e^{-\lambda_{\mathrm{K}} t}$, where λ_{K} is the rate of decay of ^{40}K and f_{Ar} is the fraction of ^{40}K that yield ^{40}Ar. A change of the time variable in the more general case where $f = f(x,t)$ is considered in Chapter 2. For a given coefficient c, let φ be the solution of the problem

$$c(\varphi(t))\varphi'(t) = 1, \quad \varphi(0) = 0, \tag{1.20}$$

and let $v(x,t) = u(x,\varphi(t))$. Then v satisfies the equation

$$\partial_t v(x,t) - \Delta v(x,t) = s(t), \quad \text{where } s(t) = \frac{f(\varphi(t))}{c(\varphi(t))}. \tag{1.21}$$

Starting with equation (1.21), suppose we can find $s(t)$ that satisfies (1.21). We determine the unknown coefficient c in (1.19) as follows. From (1.20) and (1.21) we have that $f(\varphi(t))\varphi'(t) = s(t)$. Integrating and using the form of the source we obtain that

$$\int_0^t \lambda_{\mathrm{K}} f_{\mathrm{Ar}} e^{-\lambda_{\mathrm{K}}\varphi(\tau)}\varphi'(\tau)\,d\tau = \int_0^t s(\tau)\,d\tau \quad \text{or} \quad -f_{\mathrm{Ar}}\int_0^t \left[e^{-\lambda_{\mathrm{K}}\varphi(\tau)}\right]' d\tau = \int_0^t s(\tau)\,d\tau.$$

It follows that

$$\varphi(t) = -\frac{1}{\lambda_{\mathrm{K}}}\ln\left(1 - \frac{1}{f_{\mathrm{Ar}}}\int_0^t s(\tau)\,d\tau\right),$$

and

$$c(\varphi(t)) = \frac{f(\varphi(t))}{s(t)} = \frac{\lambda_{\mathrm{K}} f_{\mathrm{Ar}}}{s(t)} e^{-\lambda_{\mathrm{K}}\varphi(t)} = \frac{\lambda_{\mathrm{K}}}{s(t)}\left(f_{\mathrm{Ar}} - \int_0^t s(\tau)\,d\tau\right).$$

1.5 Review of mathematical literature

In this section, we summarize results available for the inverse diffusion coefficient and the inverse source problems. First, we review what is known about the former. Cannon

and Rundell [5] treated this inverse problem with a homogeneous source ($f = 0$), nonhomogeneous boundary conditions, superharmonic initial condition and an overdetermination condition (1.7) being the normal derivative evaluated at a boundary point, that is, with additional data of the form

$$\frac{\partial u}{\partial \nu}(x_0, t) = g(t), \quad x_0 \in \partial\Omega, \quad 0 \leq t \leq T_f.$$

Under the assumption that g is continuous on $[0, T_f]$, they proved existence and uniqueness of classical solutions using a contraction mapping principle by introducing a compact mapping in partially ordered Banach spaces. In addition, they obtained a stability result. They argued that their method could be extended to the integral data in the form (1.7). We follow their general outline and supply detailed arguments in Chapter 2. Specifically, we will show the existence, uniqueness, and stability of classical solutions to the inverse diffusion coefficient problem with a subharmonic initial condition using the Banach fixed point theorem in partially ordered Banach spaces under the condition $\mu \in C^1[0, T_f]$. We will also provide numerical approximations of solutions. In [19], we considered the inverse diffusion coefficient problem with time-dependent source $f = f(t)$. Under the condition $\mu \in C^1[0, T_f]$, we established the existence of weak solutions using Rothe's method. Moreover, we provided numerical results using a finite element discretization in space and the implicit Euler method in time. Ivanchov [29] investigated the problem of recovering the unknown diffusion coefficient in the one-dimensional case for non-local boundary conditions and established the existence by means of the Schauder fixed point theorem. The method of separation of variables was used by Kanca and Ismailov [31] to establish well-posedness in one dimension. An unknown diffusion coefficient also appears in elliptic problems, famously in the inverse conductivity problem for the electric potential. This problem is investigated, for example, in the book by Isakov [28]. Other types of inverse coefficient problems in elliptic and parabolic equations are considered, for instance, in the book by Choulli [7].

We conclude this section with a review of available results for the inverse source problem. Švadlenka and Omata [42] investigated the existence and regularity, and presented results of numerical studies of an inverse time-dependent source problem with an integral constraint that is constant in time. Ginder [17] developed the case of a non-constant integral constraint and proved the existence of Hölder continuous weak solutions under the assumption that $\mu \in C^1[0, T_f]$. In both papers [42] and [17], the authors used the discrete Morse flow, in which the parabolic problem is discretized in time and one searches for a minimizer of the functional corresponding to the discretized problem. In [10], Dehghan developed finite difference schemes and presented numerical results in the case of dimension 2. An application of the boundary element method in one dimension is considered by Hazanee, Ismailov, Lesnic, and Kerimov in [26]. Optimal control theory was used by Cao, Gunzburger and Turner [6] to establish the existence of an inverse source problem with final overdetermination, in which the source function depends on both time and space. Rundell [41] investigated parabolic and pseudo-parabolic inverse source problems with final time overdetermination in which the sources depend only on the time variable or only on the space variables or for a multiplicative source with unknown time-dependent term. An inverse source problem with internal measurement is considered by Yang, Dehghan, Yu, and Luo in [46], and an inverse source problem involving both the final time and internal measurements using the semigroup method is treated by Hasanov and Slodička in [25]. Meir and Yavneh [35] solved an elliptic problem with an integral constraint. In [18], we proved the existence and uniqueness of weak solutions of the inverse source problem using Rothe's method under the condition that μ is Lipschitz continuous on $[0, T_f]$ and presented results of numerical studies. These results appear in Chapter 3. Merazga and Bouziani [36] recovered a time-dependent function on the boundary in a two-dimensional parabolic equation with a Neumann boundary condition and integral overdetermination. The authors proved the existence, uniqueness, and continuous dependence on data using the Rothe method.

The rest of this dissertation is organized as follows. In Chapter 2, we will consider the inverse diffusion coefficient problem (1.2)–(1.4) and (1.7) with $g = 0$. Given the final time T_f, the source f, the initial data u_0, and the integral data μ, we are required to determine the time-dependent coefficient $c(t)$ together with the concentration u. In the geochronology applications, the diffusion coefficient is temperature-dependent and the temperature itself is a function of time. Thus, solving the inverse diffusion coefficient problem is equivalent to reconstructing the temperature history of rocks. In fact since $c(t) = D(T(t))$ and the Arrhenius law gives $D(T(t)) = D_0 e^{-E/RT(t)}$, once we determine $c(t)$, we recover the temperature.

In Chapters 3, 4, and 5, we consider the inverse source problem for the model (1.2)–(1.4) and (1.7). Based on the applications in geochronology as described before, the source function depends only on time, that is $f = f(t)$. In Chapter 3, we take $g(x,t) = 0$ for all $(x,t) \in \partial\Omega \times (0, T_f)$ and $u_0(x) = 0$ for all $x \in \Omega$ and use Rothe's method and an energy method to show the existence and uniqueness of weak solutions, respectively. Moreover, we develop and implement a numerical scheme that can be used to approximate solutions of this problem. Chapter 4 is dedicated to the existence and uniqueness of classical solutions via semigroup theory and an energy method, respectively. Finally, Chapter 5 deals with the inverse source problem with a Neumann boundary condition.

1.6 Notation

For the remainder of this dissertation, T denotes the final time, and throughout this dissertation, we denote by

- $L^2(\Omega)$: the space of square integrable functions defined on Ω with values in $\mathbb{R}$;
- $H^1(\Omega)$: the Sobolev space $W^{1,2}(\Omega)$ of locally summable functions $u : \Omega \to \mathbb{R}$ such that $u \in L^2(\Omega)$, the weak derivative ∇u exists in the weak sense and belongs to $L^2(\Omega)$;

- $H_0^1(\Omega)$: the closure of $C_c^\infty(\Omega)$ in $H^1(\Omega)$, where $C_c^\infty(\Omega)$ is the space of infinitely differentiable functions $\phi : \Omega \to \mathbb{R}$, with compact support in Ω. The trace inequalities allow us to interpret $H_0^1(\Omega)$ as the space of functions $u \in H^1(\Omega)$ such that $u = 0$ on $\partial\Omega$.

- $H^{-1}(\Omega)$: the dual space to $H_0^1(\Omega)$;

- $L^2(0,T;V)$: the space of strongly measurable functions $u : [0,T] \to V$ with

$$\|u\|_{L^2(0,T;V)} := \left(\int_0^T \|u(t)\|_V^2 \, dt \right)^{1/2} < \infty,$$

  where V is a real Hilbert space with norm $\|\cdot\|_V$. We often choose V to be $H^1(\Omega)$, $H_0^1(\Omega)$, or $L^2(\Omega)$; a function $u : [0,T] \to V$ is strongly measurable *if there exist simple functions* s_k such that $s_k(t) \to u(t)$ for a.e. $0 \le t \le T$.

- $C([0,T];V)$: the space of continuous functions $u : [0,T] \to V$ with the norm

$$\|u\|_{C([0,T];V)} := \max_{0 \le t \le T} \|u(t)\|_V < \infty;$$

- $(\cdot,\cdot)$: the scalar product in $L^2(\Omega)$;

- $\|\cdot\|$: the norm in $L^2(\Omega)$;

- $\langle \cdot,\cdot \rangle$: the duality pairing between functions in a space V and functions in its dual V^*.

Chapter 2

Fixed point method for inverse diffusion coefficient problem

2.1 Problem statement

We now consider the system

$$\partial_t u(x,t) - c(t)\Delta u(x,t) = f(x,t), \quad (x,t) \in \Omega \times (0,T], \tag{2.1}$$

$$u(x,t) = 0, \qquad (x,t) \in \partial\Omega \times [0,T], \tag{2.2}$$

$$u(x,0) = u_0(x), \qquad x \in \Omega, \tag{2.3}$$

and

$$\int_\Omega u(x,t)\,dx = \mu(t), \qquad t \in [0,T]. \tag{2.4}$$

where Ω is a domain in $\mathbb{R}^d$, $d \geq 1$ with a C^2 boundary $\partial\Omega$. The problem we solve is as follows: given the source function $f : \Omega \times [0,T] \to \mathbb{R}$, the initial data $u_0 : \Omega \to \mathbb{R}$, and the integral data $\mu : [0,T] \to \mathbb{R}$, find the positive, time-dependent, coefficient $c : [0,T] \to (0,\infty)$ together with the concentration $u : \overline{\Omega} \times [0,T] \to \mathbb{R}$ satisfying (2.1)–(2.4). Note that the source is a function of space and time.

We define a solution as follows.

Definition 2.1. The pair (u,c) is a solution of (2.1)–(2.4) if:

1. The function $c(t)$ is continuous for $0 \leq t \leq T$, and satisfies the bounds $0 < \underline{c} \leq c(t) \leq \bar{c}$, for some constants $\bar{c}$ and $\underline{c}$.

2. The concentration $u(x,t)$ is continuous for $(x,t) \in \overline{\Omega} \times [0,T]$.

3. The derivatives $\partial_t u$, ∇u, $\partial^2 u/\partial x_i \partial x_j$ exist and are continuous for $(x,t) \in \overline{\Omega} \times (0,T)$, $1 \le i,j \le d$.

4. Equations (2.1)–(2.4) hold in the classical sense.

We assume the following conditions on the data:

A1.
- The source $f(x,t)$ is locally Hölder continuous in $x \in \Omega$ with exponent β, uniformly with respect to t.
- The source $f(x,t)$ is twice continuously differentiable in $x \in \Omega$ for all $t \in [0,T]$, continuous in $[0,T]$ for all $x \in \Omega$ and $\Delta f(x,t) \le 0$ for all $t \in [0,T]$.
- The source $f(x,t) > 0$ for $(x,t) \in \partial\Omega \times [0,T]$.

A2. The initial condition $u_0 \in C^2(\Omega)$ satisfies $\Delta u_0 < 0$ in Ω and the compatibility condition $\mu(0) = \int_\Omega u_0(x)\,dx$ holds.

For a given function $c(t)$, we denote by $u(x,t;c)$ the solution of the direct problem (2.1)–(2.3). We assume the following on the integral data:

A3. The data $\mu \in C^1[0,T]$ satisfies for all $0 \le t \le T$ the estimate

$$\bar{c} \int_\Omega \Delta u(x,t;\bar{c})\,dx \le \mu'(t) - \int_\Omega f(x,t)\,dx \le \underline{c} \int_\Omega \Delta u(x,t;\underline{c})\,dx$$

for some positive constants $\bar{c}$ and $\underline{c}$.

Following [1], we denote by $E[a,b]$ the ordered Banach space $C[a,b]$ equipped with the positive cone $P = \{f \in C[a,b] : f \ge 0\}$. The partial order in P is given by: $f \ge g$ if $f(x) \ge g(x)$ for all $x \in [a,b]$.

We make the following transformation, as in [9, p. 4],

$$\tau = \alpha(t) = \int_0^t c(s)\,ds,$$

and set

$$\tilde{u}(x,\tau;c) = u(x,t;c).$$

For $c(t) > 0$, the mapping $\alpha(t)$ is one-to-one. An application of the chain rule and the fact that $\alpha'(t) = c(t)$ yield

$$\partial_\tau \tilde{u}(x,\tau) - \Delta\tilde{u}(x,\tau) = \frac{1}{c(\alpha^{-1}(\tau))}\left(\partial_t u(x,\alpha^{-1}(\tau)) - c(\alpha^{-1}(\tau))\Delta u(x,\alpha^{-1}(\tau))\right),$$

so that $\tilde{u}$ then satisfies the system

$$\partial_\tau \tilde{u}(x,\tau) - \Delta\tilde{u}(x,\tau) = \frac{f(x,\alpha^{-1}(\tau))}{c(\alpha^{-1}(\tau))}, \quad (x,\tau) \in \Omega \times (0,\alpha(T)], \tag{2.5}$$

$$\tilde{u}(x,\tau) = 0, \qquad (x,\tau) \in \partial\Omega \times [0,\alpha(T)], \tag{2.6}$$

and

$$\tilde{u}(x,0) = u_0(x), \qquad x \in \Omega. \tag{2.7}$$

In order to make use of the overdetermination condition (2.4), we define a map

$$\mathcal{T} : c \mapsto \frac{\mu'(t) - \int_\Omega f(x,t)\,dx}{\int_\Omega \Delta u(x,t;c)\,dx}, \quad \text{for } c \in C([0,T];[\underline{c},\bar{c}]).$$

In view of this definition, we see that, if the overdetermination condition (2.4) is satisfied for some function $c(t)$, then we must have $c = \mathcal{T}c$. In fact, integrating (2.1) over Ω and using (2.4), we obtain that

$$c(t) = \frac{\mu'(t) - \int_\Omega f(x,t)\,dx}{\int_\Omega \Delta u(x,t;c)\,dx} = \mathcal{T}c(t). \tag{2.8}$$

Conversely, if $\mathcal{T}$ has a fixed point c, then (2.4) must hold for this function c. To see this, note that, from the definition of $\mathcal{T}$, we obtain that $\mu'(t) = \int_\Omega f(x,t) + c(t)\int_\Omega \Delta u(x,t;c)\,dx$.

From (2.1) it follows that

$$\int_\Omega \partial_t u(x,t;c)\,dx = \int_\Omega f(x,t) + c(t)\int_\Omega \Delta u(x,t;c)\,dx.$$

Using $\mu'(t) = \int_\Omega \partial_t u(x,t;c)\,dx$ and integrating, we obtain that

$$\mu(t) - \mu(0) = \int_\Omega u(x,t;c)\,dx - \int_\Omega u_0(x)\,dx.$$

The integral constraint (2.4) is satisfied thanks to the compatibility condition A2.

2.2 Technical lemmas

In view of the goal to determine the function $c(t)$ from the overdetermination condition (2.4), our approach is to show that $\mathcal{T}$ is a contraction mapping and apply the Banach fixed point theorem to prove that $\mathcal{T}$ has a unique fixed point. In order to show that $\mathcal{T}$ is a contraction, we will first establish in Lemmas 2.1, 2.2, and 2.3 various properties of this mapping. We first demonstrate that the mapping $\mathcal{T}$ is well defined.

Lemma 2.1. *Suppose that Assumptions A1 and A2 hold. For $c \in C([0,T];[\underline{c},\bar{c}])$ we have that*

$$\Delta u(x,t;c) < 0, \quad \textit{for all} \quad 0 \le t \le T. \tag{2.9}$$

In particular, the mapping $\mathcal{T}$ is well defined and maps continuous functions into continuous functions.

Proof. The idea is to apply the Laplace operator to the differential equation and use the maximum principle for Δu. To that end, we first show that $u \in C^4(\Omega)$ for all $0 \le t \le T$. This follows from the regularity of the source f. In fact, let w and $\overline{w}$ be the solutions of the

problems

$$\begin{aligned} \partial_t w(x,t;c) - c(t)\Delta w(x,t;c) &= f(x,t), \quad (x,t) \in \Omega \times (0,T], \\ w(x,t;c) &= 0, \qquad\quad (x,t) \in \partial\Omega \times [0,T], \end{aligned}$$

and

$$w(x,0;c) = 0, \qquad x \in \Omega,$$

and

$$\begin{aligned} \partial_t \overline{w}(x,t;c) - c(t)\Delta \overline{w}(x,t;c) &= 0, \qquad (x,t) \in \Omega \times (0,T], \\ \overline{w}(x,t;c) &= 0, \qquad (x,t) \in \partial\Omega \times [0,T], \end{aligned} \tag{2.10}$$

and

$$\overline{w}(x,0;c) = u_0(x), \quad x \in \Omega.$$

Since $f \in C^2(\Omega)$ for all $0 \le t \le T$, it is well known [4, p. 343] that $\partial_t w$ and Δw are also $C^2(\Omega)$ for all $0 \le t \le T$. So, $w \in C^4(\Omega)$ for all $0 \le t \le T$. Moreover, $\overline{w} \in C^\infty(\Omega \times (0,T])$ by [14, Theorem 8, p. 59]. Thus, $\partial_t \overline{w} \in C^\infty(\Omega)$ for all $0 \le t \le T$. Consequently, we get that $u(x,t;c) = w(x,t;c) + \overline{w}(x,t;c)$ is $C^4(\Omega)$ for all $0 \le t \le T$. Furthermore, since $f \in C[0,T]$ for all $x \in \Omega$, it follows that $\partial_t w \in C[0,T]$ and $\partial_t u(x,t;c) = \partial_t w(x,t;c) + \partial_t \overline{w}(x,t;c) \in C[0,T]$ for all $x \in \Omega$. Hence $u \in C^1[0,T]$ for all $x \in \Omega$.

Applying the Laplace operator to the left-hand sides and right-hand sides of (2.1) and (2.3), then using (2.2) with (2.1), we obtain that

$$\begin{aligned} \partial_t \Delta u(x,t) - c(t)\Delta(\Delta u(x,t)) &= \Delta f(x,t), \qquad (x,t) \in \Omega \times (0,T], \\ \Delta u(x,t;c) &= -\frac{1}{c(t)} f(x,t), \quad (x,t) \in \partial\Omega \times [0,T], \end{aligned}$$

and

$$\Delta u(x,0) = \Delta u_0(x), \qquad x \in \Omega.$$

The conclusion of the lemma follows by using Assumptions A1 and A2 and the maximum principle. In particular, we have that

$$\int_\Omega \Delta u(x,t;c)\,dx < 0, \quad \text{for all } 0 \le t \le T. \tag{2.11}$$

□

Next, we show that the map $\mathcal{T}$ is increasing.

Lemma 2.2. *Suppose Assumptions A1 and A2 are satisfied. For $c \in C([0,T];[\underline{c},\bar{c}])$ we have that*

$$\int_\Omega \Delta u(x,t;c)\,dx \quad \textit{is an increasing function of } c.$$

In particular, the map $\mathcal{T}$ is increasing.

Proof. Let $c_1(t) \le c_2(t)$ for all $t \in [0,T]$ and put $v(x,t) = u(x,t;c_1) - u(x,t;c_2)$. Then v satisfies

$$\begin{aligned}
\partial_t v - c_1(t)\Delta v &= (\partial_t u(x,t;c_1) - c_1(t)\Delta u(x,t;c_1)) \\
&\quad - (\partial_t u(x,t;c_2) - c_2(t)\Delta u(x,t;c_2)) \\
&\quad + (c_1(t) - c_2(t))\Delta u(x,t;c_2) \\
&= (c_1(t) - c_2(t))\Delta u(x,t;c_2) \ge 0,
\end{aligned}$$

where the last inequality follows from Lemma 2.1. Also, $v(x,0) = 0$ in Ω and $v(x,t) = 0$ on $\partial\Omega \times (0,T]$. Thus, by the maximum principle, we have that $v(x,t) \ge 0$ in $\overline{\Omega} \times [0,T]$ and therefore,

$$0 \ge \int_{\partial\Omega} \frac{\partial v}{\partial \nu}\,dS(x) = \int_\Omega \Delta v\,dx = \int_\Omega \Delta u(x,t;c_1)\,dx - \int_\Omega \Delta u(x,t;c_2)\,dx,$$

where ν denotes the outward unit normal to the boundary $\partial\Omega$. It follows that

$$\mathcal{T}[c_1] = \frac{\mu'(t) - \int_\Omega f(x,t)\,dx}{\int_\Omega \Delta u(x,t;c_1)\,dx} \leq \frac{\mu'(t) - \int_\Omega f(x,t)\,dx}{\int_\Omega \Delta u(x,t;c_2)\,dx} = \mathcal{T}[c_2].$$

□

Lemma 2.3. *Suppose Assumptions A1, A2 and A3 hold. Then the mapping $\mathcal{T}$ maps functions with values in the interval $[\underline{c}, \bar{c}]$ into functions with values in the interval $[\underline{c}, \bar{c}]$.*

Proof. Due to the monotonicity of $\mathcal{T}$, it is enough to show that

$$\mathcal{T}\underline{c} \geq \underline{c} \quad \text{and} \quad \mathcal{T}\bar{c} \leq \bar{c}. \tag{2.12}$$

These two inequalities follow from the assumption on the integral constraint μ. Indeed using Assumption A3 and (2.11), we obtain that

$$\underline{c} \leq \frac{\mu'(t) - \int_\Omega f(x,t)\,dx}{\int_\Omega \Delta u(x,t;\underline{c})\,dx} = \mathcal{T}\underline{c} \quad \text{and} \quad \bar{c} \geq \frac{\mu'(t) - \int_\Omega f(x,t)\,dx}{\int_\Omega \Delta u(x,t;\bar{c})\,dx} = \mathcal{T}\bar{c}.$$

□

2.3 Well-posedness of the problem

We now turn to the main result of this chapter, namely the existence and uniqueness of solutions to the inverse coefficient problem. The result is stated in the following theorem.

Theorem 2.4. *Suppose Assumptions A1, A2, and A3 hold. Then there exists a unique solution $(u(x,t), c(t))$ in the sense of Definition 2.1 to the inverse coefficient problem (2.1)–(2.4) for all $t \in [0,T]$. Moreover, the bounds for $c(t)$ in Definition 2.1 correspond to $\underline{c}$ and $\bar{c}$ in Assumption A3.*

Proof. We first prove that the mapping $\mathcal{T}$ is a contraction on $C([0,T_0];[\underline{c},\bar{c}])$ for a sufficiently small T_0 and then extend the solution smoothly by uniqueness to the interval $[0,T]$. To that

end, note that from (2.5)–(2.7), $\tilde{u}$ has a representation

$$\tilde{u}(x,\tau;c) = I(x,\tau) + \int_0^\tau \int_\Omega G(x,y;\tau,s)\frac{f(y,\alpha^{-1}(s))}{c(\alpha^{-1}(s))}\,dy\,ds, \tag{2.13}$$

for $c \in C([0,T];[\underline{c},\bar{c}])$, where G denotes the Green function for the heat equation with the Dirichlet boundary condition, and I denotes the contribution from the initial data. See [12, p. 180] for a derivation of such a representation formula. Then I has the form

$$I(x,\tau) = \sum_{n=1}^{\infty} b_n\phi_n(x)e^{-\lambda_n\tau} \quad \text{or} \quad I(x,t;c) = \sum_{n=1}^{\infty} b_n\phi_n(x)e^{-\lambda_n\int_0^t c(s)\,ds},$$

where λ_n and ϕ_n are, respectively, the eigenvalues and eigenfunctions of $-\Delta$ on the domain Ω with zero Dirichlet boundary condition and b_n are the components of the initial data u_0 with respect to the basis (ϕ_n), that is $b_n = \int_\Omega u_0(x)\phi_n(x)\,dx$, $n \geq 1$. Since f is continuous and locally Hölder continuous in $x \in \Omega$ uniformly with respect to t, then $\tilde{u}$ given by (2.13) has continuous second derivatives with respect to $x \in \Omega$, for $0 < t \leq T$ [15, Theorem 4, p. 9] and we have that

$$\int_\Omega \Delta\tilde{u}(x,\tau;c)\,dx = \int_\Omega \Delta u(x,t;c)\,dx = I_\Delta(x,t;c) + H(\tau), \tag{2.14}$$

where

$$I_\Delta(x,t;c) = \sum_{n=1}^{\infty} b_n e^{-\lambda_n\int_0^t c(s)\,ds}\int_\Omega \Delta\phi_n(x)\,dx$$

and

$$H(\tau) = \int_0^\tau ds\int_\Omega\int_\Omega \Delta_x G(x,y;\tau,s)\frac{f(y,\alpha^{-1}(s))}{c(\alpha^{-1}(s))}\,dy\,dx.$$

Let $c_1, c_2 \in C([0,T];[\underline{c},\bar{c}])$ be such that $c_1(t) \leq c_2(t)$ for all $t \in [0,T]$. We have

$$\begin{aligned}\int_\Omega \Delta u(x,t;c_2) - \Delta u(x,t;c_1)\,dx &= \int_\Omega \Delta\tilde{u}(x,\tau_2;c_2) - \Delta\tilde{u}(x,\tau_1;c_1)\,dx,\\ &= (I_\Delta(x,t;c_2) - I_\Delta(x,t;c_1)) + (H(\tau_2) - H(\tau_1)).\end{aligned} \tag{2.15}$$

For the first difference on the right, we have that

$$\begin{aligned} I_\Delta(x,t;c_2) - I_\Delta(x,t;c_1) &= \sum_{n\geq 1} b_n \int_\Omega \Delta\phi_n(x)\,dx \left(e^{-\lambda_n \int_0^t c_2(s)\,ds} - e^{-\lambda_n \int_0^t c_1(s)\,ds}\right) \\ &\leq \sum_{n\geq 1} |b_n| \left|\int_\Omega \Delta\phi_n(x)\,dx\right| \left(1 - e^{-\lambda_n \int_0^t |c_2(s)-c_1(s)|\,ds}\right) e^{-\lambda_n \underline{c} t} \\ &\leq \sum_{n\geq 1} |b_n| \left|\int_\Omega \phi_n(x)\,dx\right| \lambda_n^2 e^{-\lambda_n \underline{c} t} \int_0^t |c_2(s) - c_1(s)|\,ds, \end{aligned}$$

where the first inequality follows from the fact that

$$\underline{c} \leq c_2(t) \leq \bar{c} \tag{2.16}$$

and the second inequality follows from $1 - e^{-x} \leq x$ for all $x \geq 0$. Thus,

$$I_\Delta(x,t;c_2) - I_\Delta(x,t;c_1) \leq C_1 t \sup_{0\leq s\leq t} |c_2(s) - c_1(s)|\,, \tag{2.17}$$

where $C_1 = C_1(u_0, \Omega)$ is independent of $c_1(t)$, $c_2(t)$, and t.

To estimate the difference $H(\tau_2) - H(\tau_1)$, we use the Mean Value Theorem. To that end, we first show that H is continuously differentiable. We write $H(\tau)$ in the form

$$H(\tau) = \int_\Omega \Delta_x V(x,\tau)\,dx,$$

where

$$V(x,\tau) = \int_0^\tau \int_\Omega G(x,y;\tau,s) \frac{f(y,\alpha^{-1}(s))}{c(\alpha^{-1}(s))}\,dy\,ds.$$

By [15, Theorem 5, p. 12], $\partial V/\partial\tau$ exists and is continuous for $x \in \Omega$, $0 < \tau \leq \alpha(T)$. Thus, $H'(\tau)$ exists and is continuous for $0 < \tau \leq \alpha(T)$. By the Mean Value Theorem, for all $\tau_1, \tau_2 \in (0, \alpha(T)]$, there exists $\tau^* \in (\tau_1, \tau_2)$ such that $H(\tau_2) - H(\tau_1) = H'(\tau^*)(\tau_2 - \tau_1)$. Next,

we will compute $H'(\tau)$. To that end, rewrite $H(\tau)$ in the form

$$H(\tau) = \int_0^\tau K(\tau, s)\, ds,$$

where

$$K(\tau, s) = \int_\Omega \int_\Omega \Delta_x G(x, y; \tau, s) \frac{f(y, \alpha^{-1}(s))}{c(\alpha^{-1}(s))}\, dy\, dx.$$

Using the Leibniz rule, we have that

$$\begin{aligned}
H'(\tau) &= K(\tau, \tau) + \int_0^\tau \partial_\tau K(\tau, s)\, ds \\
&= \int_\Omega \Delta_x \left(\lim_{s \to \tau} \int_\Omega G(x, y; \tau, s) \frac{f(y, \alpha^{-1}(s))}{c(\alpha^{-1}(s))}\, dy \right) dx \\
&+ \int_0^\tau \int_\Omega \int_\Omega \partial_\tau \Delta_x G(x, y; \tau, s) \frac{f(y, \alpha^{-1}(s))}{c(\alpha^{-1}(s))}\, dy\, dx\, ds \\
&= \int_\Omega \frac{\Delta f(x, \alpha^{-1}(\tau))}{c(\alpha^{-1}(\tau))}\, dx \\
&+ \int_0^\tau \int_\Omega \int_\Omega \partial_\tau \Delta_x G(x, y; \tau, s) \frac{f(y, \alpha^{-1}(s))}{c(\alpha^{-1}(s))}\, dy\, dx\, ds
\end{aligned}$$

where the last equality follows from [15, Theorem 1, p. 4]. Invoking Assumption A1, we obtain that

$$H'(\tau) \leq \int_0^\tau \int_\Omega \int_\Omega \left| \partial_\tau \Delta_x G(x, y; \tau, s) \frac{f(y, \alpha^{-1}(s))}{c(\alpha^{-1}(s))} \right| dy\, dx\, ds.$$

Recalling the estimates of the fundamental solution for the heat equation on bounded domains (and hence for the Green's function)

$$|\partial_\tau \Delta_x G(x, y; \tau, s)| \leq \frac{C}{(\tau - s)^\gamma |x - y|^{d+4-2\gamma}}, \tag{2.18}$$

which follows from [15, Inequality 3.11, p. 97], where $C = C(d, \gamma)$, and γ is a parameter such that $0 < \gamma < 1 < 2 - \beta/2$, d is the space dimension, and β is the Hölder exponent of f. A derivation of this estimate appears in Appendix A. As in Appendix A, let B be a ball

contained in Ω. We can write

$$\begin{aligned}\int_\Omega \partial_x G(x,y;\tau,s)\frac{f(y,\alpha^{-1}(s))}{c(\alpha^{-1}(s))}\,dy &= \frac{f(\xi,\alpha^{-1}(s))}{c(\alpha^{-1}(s))}\int_\Omega \partial_x G(x,y;\tau,s)\,dy \\ &\quad+\int_\Omega \partial_x G(x,y;\tau,s)\left(\frac{f(y,\alpha^{-1}(s))-f(\xi,\alpha^{-1}(s))}{c(\alpha^{-1}(s))}\right)dy \\ &= \frac{f(\xi,\alpha^{-1}(s))}{c(\alpha^{-1}(s))}\int_{\partial B} G(x,y;\tau,s)\cos(\nu,\eta)\,dS_\eta \\ &\quad+\frac{f(\xi,\alpha^{-1}(s))}{c(\alpha^{-1}(s))}\int_{\Omega\setminus B} \partial_x G(x,y;\tau,s)\,dy \\ &\quad+\int_\Omega \partial_x G(x,y;\tau,s)\left(\frac{f(y,\alpha^{-1}(s))-f(\xi,\alpha^{-1}(s))}{c(\alpha^{-1}(s))}\right)dy,\end{aligned}$$

where, we used the divergence theorem for the first integral. Differentiating both sides with respect to x and choosing $\xi = x$ we have that

$$\begin{aligned}\int_\Omega \Delta_x G(x,y;\tau,s)\frac{f(y,\alpha^{-1}(s))}{c(\alpha^{-1}(s))}\,dy &= \frac{f(x,\alpha^{-1}(s))}{c(\alpha^{-1}(s))}\int_{\partial B} \frac{\partial}{\partial_x} G(x,y;\tau,s)\cos(\nu,\eta)\,dS_\eta \\ &\quad+\frac{f(x,\alpha^{-1}(s))}{c(\alpha^{-1}(s))}\int_{\Omega\setminus B} \Delta_x G(x,y;\tau,s)\,dy \\ &\quad+\int_\Omega \Delta_x G(x,y;\tau,s)\left(\frac{f(y,\alpha^{-1}(s))-f(x,\alpha^{-1}(s))}{c(\alpha^{-1}(s))}\right)dy.\end{aligned}$$

Notice that, for fixed x lying in the interior of B, each of the first two integrals on the right-hand side in the above equation is a bounded function of τ and s. Thus we obtain that

$$\begin{aligned}&\int_0^\tau\int_\Omega\int_\Omega \left|\partial_\tau\Delta_x G(x,y;\tau,s)\frac{f(y,\alpha^{-1}(s))}{c(\alpha^{-1}(s))}\right|\,dy\,dx\,ds \\ &\qquad\le \int_0^\tau \frac{1}{c(\alpha^{-1}(s))}\int_\Omega\int_\Omega |\partial_\tau\Delta_x G(x,y;\tau,s)|\,|f(y,\alpha^{-1}(s))-f(x,\alpha^{-1}(s))|.\end{aligned}$$

Since $d+4-2\gamma-\beta > d$, using [15, Lemma 2, p. 14], inequality (2.18) and the Hölder continuity of f, we get that

$$\begin{aligned} H'(\tau) &\leq \int_0^\tau \frac{C}{(\tau-s)^\gamma}\,ds \int_\Omega \int_\Omega \frac{|x-y|^\beta}{|x-y|^{d+4-2\gamma}}\,dy\,dx \\ &\leq \int_0^\tau \frac{C}{(\tau-s)^\gamma}\,ds \int_\Omega \frac{dx}{|x|^{4-2\gamma-\beta}}, \quad \text{for } \gamma < 1 < 2-\beta/2 \\ &\leq \int_0^\tau \frac{C}{(\tau-s)^\gamma}\,ds = \frac{C}{1-\gamma}\tau^{1-\gamma}. \end{aligned}$$

where $C = C(d,f)$. Since $(\tau^*)^{1-\gamma} < \tau_2^{1-\gamma} < (\bar{c}T)^{1-\gamma}$, it follows that $H'(\tau^*) \leq C_2(d,T,f)$, where $C_2(d,T,f)$ is a constant depending on the dimension d of the space, the final time T, and on the source f. Therefore

$$H(\tau_2) - H(\tau_1) \leq C_2(d,T,f)(\tau_2-\tau_1) \leq C_2(d,T,f)\,t \sup_{0\leq s\leq t} |c_2(s)-c_1(s)|. \tag{2.19}$$

Substituting (2.17) and (2.19) into (2.15) we get that

$$\left| \int_\Omega \Delta u(x,t;c_2) - \Delta u(x,t;c_1)\,dx \right| \leq C(u_0,\Omega,d,T,f)\,t \sup_{0\leq s\leq t} |c_2(s)-c_1(s)|\,, \tag{2.20}$$

where $C(u_0,\Omega,d,T,f)$ is bounded and independent of $c_1(t)$ and $c_2(t)$. Note that, due to Lemma 2.2, inequality (2.20) is valid with or without the absolute value in the left-hand side. Hence taking the maximum over $[0,T_0]$, for any $T_0 < T$, we obtain that

$$\left\| \int_\Omega \Delta u(x,t;c_2) - \Delta u(x,t;c_1)\,dx \right\|_{C[0,T_0]} \leq C(u_0,\Omega,d,T,f)\,T_0\,\|c_2-c_1\|_{C[0,T_0]}. \tag{2.21}$$

Next, we have that

$$\begin{aligned} |\mathcal{T}[c_1] - \mathcal{T}[c_2]| &= \left| \frac{\mu'(t) - \int_\Omega f(x,t)\,dx}{\int_\Omega \Delta u(x,t;c_1)\,dx} - \frac{\mu'(t) - \int_\Omega f(x,t)\,dx}{\int_\Omega \Delta u(x,t;c_2)\,dx} \right| \\ &= \left| \frac{\left(\int_\Omega \Delta u(x,t;c_2) - \Delta u(x,t;c_1)\,dx\right)\left(\mu'(t) - \int_\Omega f(x,t)\,dx\right)}{\int_\Omega \Delta u(x,t;c_1)\,dx \int_\Omega \Delta u(x,t;c_2)\,dx} \right|. \end{aligned}$$

From Assumption A3 and equality (2.8), we get the estimates

$$\left|\mu'(t) - \int_\Omega f(x,t)\,dx\right| \le M_1 \quad \text{and} \quad \left|\int_\Omega \Delta u(x,t;c)\,dx\right| \le \frac{M_1}{\underline{c}} := M_2,$$

where $M_1 = \bar{c}\left|\int_\Omega \Delta u(x,t;\bar{c})\,dx\right|$. Moreover, from (2.1) and (2.4), we use the following estimate to obtain an upper bound on the integral $\int_\Omega \Delta u(x,t;c)\,dx$,

$$\int_\Omega \Delta u(x,t;c) - \Delta u_0(x)\,dx \le \frac{1}{\underline{c}}\left(\mu'(t) - \int_\Omega f(x,t)\,dx - \underline{c}\int_\Omega \Delta u_0(x)\,dx\right).$$

Thus, using the previous estimates we get that

$$|\mathcal{T}[c_1] - \mathcal{T}[c_2]| \le \frac{M_1\left|\int_\Omega \Delta u(x,t;c_2) - \Delta u(x,t;c_1)\,dx\right|}{\left|\int_\Omega \Delta u_0(x)\,dx\right|^2}.$$

Taking the maximum over $[0,T_0]$ and using (2.21) we obtain that

$$\|\mathcal{T}[c_1] - \mathcal{T}[c_2]\|_{C[0,T_0]} \le C(u_0,\Omega,d,T,f)T_0\|c_1 - c_2\|_{C[0,T_0]}.$$

Thus $\mathcal{T}$ is a contraction mapping provided T_0 is sufficiently small.

The existence and uniqueness of the fixed point in $0 \le t \le T_0$ follows by the Banach fixed point theorem. In a similar way, we can show that $\mathcal{T}$ is a contraction on $C([T_1,T_2],[\underline{c},\bar{c}])$, for any subinterval $[T_1,T_2]$ of $[0,T]$ such that $T_2 - T_1 < \frac{T_0}{2}$. Due to uniqueness, the corresponding fixed points of $\mathcal{T}$ can be patched together smoothly. To see this, let
$0 \le T_1 < T_2 < T_3 < T_4 \le T$ be such that $T_{i+1} - T_i < \frac{T_0}{2}$, $i = 1,2,3$, and define
$\mathcal{T}_{i,j} : C([T_i,T_j];[\underline{c},\bar{c}]) \to C([T_i,T_j];[\underline{c},\bar{c}])$ by

$$\mathcal{T}_{i,j} : (c,u_0) \mapsto \frac{\mu'(t) - \int_\Omega f(x,t)\,dx}{\int_\Omega \Delta u(x,t;c,u_0)\,dx},$$

where $u(x,t;c,u_0)$ is the solution of (2.1)–(2.3) with diffusion coefficient c and initial condition u_0. Denote by $c_{i,j}(u_0)$ the fixed point of $\mathcal{T}_{i,j}(\cdot,u_0)$ in $[T_i,T_j]$, $1 \le i < j \le 4$, and let

$u_{i,j}(\cdot,t;u_0) = u_{i,j}(\cdot,t;c_{i,j}(u_0),u_0)$. Note that for a fixed $u_1 \in C(\overline{\Omega})$ we have by uniqueness that

$$c_{1,2}(u_1) = c_{1,3}(u_1)\big|_{[T_1,T_2]} \quad \text{and, therefore,} \quad u_{1,2}(\cdot,T_2;u_1) = u_{1,3}(\cdot,T_2;u_1)\big|_{[T_1,T_2]} := u_2,$$

where $c_{1,3}(u_1)\big|_{[T_1,T_2]}$ is $c_{1,3}(u_1)$ restricted to the interval $[T_1,T_2]$. Similarly, we get that

$$\begin{aligned} c_{2,3}(u_2) = c_{2,4}(u_2)\big|_{[T_2,T_3]} &= c_{1,3}(u_1)\big|_{[T_2,T_3]}, \\ u_{2,3}(\cdot,T_3;u_2) = u_{2,4}(\cdot,T_3;u_2)\big|_{[T_2,T_3]} &= u_{1,3}(\cdot,T_3;u_1)\big|_{[T_2,T_3]} := u_3, \end{aligned}$$

and

$$c_{3,4}(u_3) = c_{2,4}(u_2)\big|_{[T_3,T_4]}, \quad u_{3,4}(\cdot,T_4;u_3) = u_{2,4}(\cdot,T_4;u_2)\big|_{[T_3,T_4]}.$$

Let $c_{1,4}(u_1)$ be the extension of $c_{1,3}(u_1)$ to $[T_1,T_4]$ by $c_{3,4}(u_3)$ and $u_{1,4}(u_1)$ be the extension to $[T_1,T_4]$ of $u_{1,3}(u_1)$ by $u_{3,4}(u_3)$. Since $c_{1,3}(u_1) \in C[T_1,T_3]$ and $c_{2,4}(u_2) \in C[T_2,T_4]$, it follows that $c_{1,4}(u_1) \in C[T_1,T_4]$. Also, we have that $u_{1,4}(u_1) \in C_1^2(\Omega \times [T_1,T_4])$ due to the corresponding regularity of $u_{1,3}(u_1)$ and $u_{2,4}(u_2)$. Continuing, after finitely many steps the existence and uniqueness remain valid for $0 \le t \le T$.

□

2.4 Continuous dependence on the data

Next, we study the stability of the problem. We show that the solution to the inverse problem depends continuously on the data. The result is summarized in the following

Theorem 2.5. *Suppose Assumptions A1, A2, and A3 hold and let c_1 and c_2 be the coefficients corresponding to the overdetermination data μ_1 and μ_2, respectively. Then*

$$\|c_1 - c_2\|_{C[0,T]} \le C(u_0,\Omega,d,T,f)\|\mu_1' - \mu_2'\|_{C[0,T]}.$$

Proof. We have that

$$|\mathcal{T}[c_1] - \mathcal{T}[c_2]| = \left| \frac{\mu_1'(t) - \int_\Omega f(x,t)\,dx}{\int_\Omega \Delta u(x,t;c_1)\,dx} - \frac{\mu_2'(t) - \int_\Omega f(x,t)\,dx}{\int_\Omega \Delta u(x,t;c_2)\,dx} \right|$$
$$= \left| \frac{\left(\int_\Omega \Delta u(x,t;c_2) - \Delta u(x,t;c_1)\,dx\right)\left(\mu_1'(t) - \int_\Omega f(x,t)\,dx\right) + G}{\int_\Omega \Delta u(x,t;c_1)\,dx \int_\Omega \Delta u(x,t;c_2)\,dx} \right|,$$

where

$$G = (\mu_1'(t) - \mu_2'(t)) \int_\Omega \Delta u(x,t;c_1)\,dx.$$

Thus

$$|\mathcal{T}[c_1] - \mathcal{T}[c_2]| \leq \frac{M_1 \left|\int_\Omega \Delta u(x,t;c_2) - \Delta u(x,t;c_1)\,dx\right| + M_2|\mu_1'(t) - \mu_2'(t)|}{\left|\int_\Omega \Delta u_0(x)\,dx\right|^2}. \tag{2.22}$$

Using (2.22) and (2.20) we have that

$$\begin{aligned}
\|c_1 - c_2\|_{C[0,T]} &\leq \frac{M_1}{|\int_\Omega \Delta u_0(x)\,dx|^2} \left\| \int_\Omega \Delta u(x,t;c_2) - \Delta u(x,t;c_1)\,dx \right\|_{C[0,T]} \\
&\quad + \frac{M_2}{|\int_\Omega \Delta u_0(x)\,dx|^2} \|\mu_1' - \mu_2'\|_{C[0,T]} \\
&\leq \frac{M_1}{|\int_\Omega \Delta u_0(x)\,dx|^2} C(u_0, \Omega, d, T, f) \|c_1 - c_2\|_{C[0,T]} \\
&\quad + \frac{M_2}{|\int_\Omega \Delta u_0(x)\,dx|^2} \|\mu_1' - \mu_2'\|_{C[0,T]}.
\end{aligned}$$

Therefore

$$\|c_1 - c_2\|_{C[0,T]} \leq C(u_0, \Omega, d, T, f) \|\mu_1' - \mu_2'\|_{C[0,T]}.$$

□

2.5 Numerical results

In this section, we present results of some numerical studies. In view of the applications described earlier, we are interested in finding numerical approximation to solutions of the

inverse problem with a source function that depends only on time, i.e $f = f(t)$. First, we develop a scheme which approximates this problem and then outline the steps in its implementation.

2.5.1 Semi-discretization in time

Set $t^0 = 0$, $u^0 = u_0$ and fix $0 < \alpha < 1$. For $k \geq 1$ given u^{k-1}, let $\hat{u}^k$ be the solution of

$$\hat{u}^k - \alpha \Delta \hat{u}^k = u^{k-1}, \quad \text{in } \Omega, \tag{2.23}$$

and

$$\hat{u}^k = 0, \qquad \text{on } \partial\Omega. \tag{2.24}$$

Let $\tilde{u}$ be the solution of

$$\tilde{u} - \alpha \Delta \tilde{u} = 1, \quad \text{in } \Omega, \tag{2.25}$$

and

$$\tilde{u} = 0, \quad \text{on } \partial\Omega. \tag{2.26}$$

We use the integral constraint to solve the following nonlinear equation in one variable for t^k

$$\mu(t^k) = \hat{\mu}^k + \tilde{\mu} \int_{t^{k-1}}^{t^k} f(t)\, dt, \tag{2.27}$$

where

$$\tilde{\mu} = \int_\Omega \tilde{u}\, dx, \quad \hat{\mu}^k = \int_\Omega \hat{u}^k\, dx.$$

See for example, the book by Ascher and Greif [2] for numerical methods for approximating solutions of nonlinear equations in one variable. Finally, we find the approximate solution

u^k, the variable time step τ^k, and the approximate diffusion coefficient c^k as follows:

$$u^k = \hat{u}^k + \tilde{u} \int_{t^{k-1}}^{t^k} f(t)\, dt, \tag{2.28}$$
$$\tau^k = t^k - t^{k-1},$$

and

$$c^k = \alpha/\tau^k. \tag{2.29}$$

We show that the decomposition (2.23)–(2.29) is equivalent to the discrete version of the original differential equation (2.1)–(2.4).

From (2.28) we have that

$$u^k - \tau^k c^k \Delta u^k = \hat{u}^k - \tau^k c^k \Delta \hat{u}^k + (\tilde{u} - \tau^k c^k \Delta \tilde{u}) \int_{t^{k-1}}^{t^k} f(t)\, dt.$$

Using the auxiliary problems (2.23) and (2.25) with α given by (2.29) we have that

$$u^k - \tau^k c^k \Delta u^k = u^{k-1} + \int_{t^{k-1}}^{t^k} f(t)\, dt,$$

or that

$$\frac{u^k - u^{k-1}}{\tau^k} - c^k \Delta u^k = \frac{1}{\tau^k} \int_{t^{k-1}}^{t^k} f(t)\, dt,$$

which we recognize as the discrete version of equation (2.1). Also, from (2.27) and (2.28) it is clear that the discrete equations for the boundary and integral conditions are all satisfied.

2.5.2 Computational algorithm

We outline the necessary steps for the implementation of the scheme we just described. Choose $0 < \alpha < 1$, solve the following elliptic equation

$$\tilde{u} - \alpha \Delta \tilde{u} = 1, \quad x \in \Omega,$$

and

$$\tilde{u} = 0, \quad x \in \partial\Omega,$$

and compute $\tilde{\mu} = \int_\Omega \tilde{u}\, dx$.

Next we set $t^0 = 0$, $u^0 = u_0$ and repeat the steps below for $k \geq 1$.

Step 1. Solve $\hat{u}^k - \alpha\Delta\hat{u}^k = u^{k-1}$, $x \in \Omega$, $\quad \hat{u}^k = 0$, $x \in \partial\Omega$ $\quad$ and compute $\hat{\mu}^k$.

Step 2. Solve the nonlinear equation $\mu(t^k) = \hat{\mu}^k + \tilde{\mu} \int_{t^{k-1}}^{t^k} f(t)\, dt$ $\quad$ for t^k.

Step 3. Compute the approximate solution $u^k = \hat{u}^k + \tilde{u} \int_{t^{k-1}}^{t^k} f(t)\, dt$.

Step 4. Find the time step $\tau^k = t^k - t^{k-1}$ and the approximate diffusion coefficient $c^k = \alpha/\tau^k$.

We repeat the Steps 1–4 as long as t^k satisfies $t^k \leq T$.

2.5.3 Numerical examples and convergence rates

We consider several examples to illustrate the accuracy of our scheme. The domain Ω is the square $-1 \leq x, y \leq 1$ in $\mathbb{R}^2$. The final time is taken to be $T = 1$, the source function is $f(t) = e^{-t}$, and the initial data is $u_0(x, y) = \cos\frac{\pi}{2}x \cos\frac{\pi}{2}y$. Obviously, Assumption A1 is satisfied for this choice of source. Moreover, $\Delta u_0(x, y) = -2\left(\frac{\pi}{2}\right)^2 \cos\frac{\pi}{2}x \cos\frac{\pi}{2}y < 0$ for all $-1 \leq x, y \leq 1$, so that Assumption A2 is satisfied. The choices of coefficients c we use in our experiments are given in Table 2.1. They are chosen to be continuous and have the same maximum value of 3 on the temporal interval $[0, T]$. We specified a maximum mesh size of 0.4 in our experiments, resulting in 82 elements and 52 unknowns. To generate the data, we specify the diffusion coefficient as provided in Table 2.1 and run the forward model to obtain a numerical approximation of the solution of the direct problem, which we treat as the exact solution. We then compute the numerical integral of this solution and use it as the data for our scheme. In our computational algorithm, we use the MATLAB built-in functions *parabolic* to solve the parabolic system (2.1)–(2.3), *assempde* to solve the

Table 2.1: Rate of convergence estimates from the slopes s_c and s_u in inverse coefficient scheme.

c	$2t+1$	$\frac{9}{4}t^2+\frac{3}{4}$	$2\sin\left(\frac{\pi}{2}t\right)+1$	e^t+3-e
s_c	1.0088	1.0130	1.0090	1.0031
s_u	0.8935	0.9828	0.8918	0.8929

elliptic systems (2.23)–(2.24) and (2.25)–(2.26), and *fzero* to find roots of the nonlinear equation (2.27). In Figure 2.1, we use the diffusion coefficient $c(t) = 2\sin\left(\frac{\pi}{2}t\right)+1$ to graph a 2-D contour plot of the exact and approximate concentrations together with the error (their differences) at the final time (computed with the discretization parameter $\alpha = 0.005$). The values of the concentration and its approximation as well as the error could be read on the color bar plot. The error plot shows that the approximation to the concentration u is quite accurate. Note that the discretization parameter α plays the role of the time step. We plot in Figure 2.2 the four diffusion coefficients from Table 2.1, each with two approximations for values of the discretization parameter $\alpha = 0.1$, and 0.05. We see that the approximations converge to the exact diffusion coefficient as the discretization parameter decreases. Error estimates for the standard implicit scheme suggest that

$$\max_{0\le t\le T} |u(\cdot,t) - u^\alpha(\cdot,t)| = \mathcal{O}(\alpha^{s_u}), \quad \text{and} \quad \max_{0\le t\le T} |c(t) - c^\alpha(t)| = \mathcal{O}(\alpha^{s_c}),$$

for some $s_u, s_c > 0$, where u and c denote the exact concentration and the exact diffusion coefficient, respectively, and u^α is the approximate concentration obtained in Step 3 and c^α is the approximate diffusion coefficient given in Step 4 of the computational algorithm in Section 2.5.2. The log-log plots of the error as a function of the discretization parameter α are depicted in Figure 2.3.

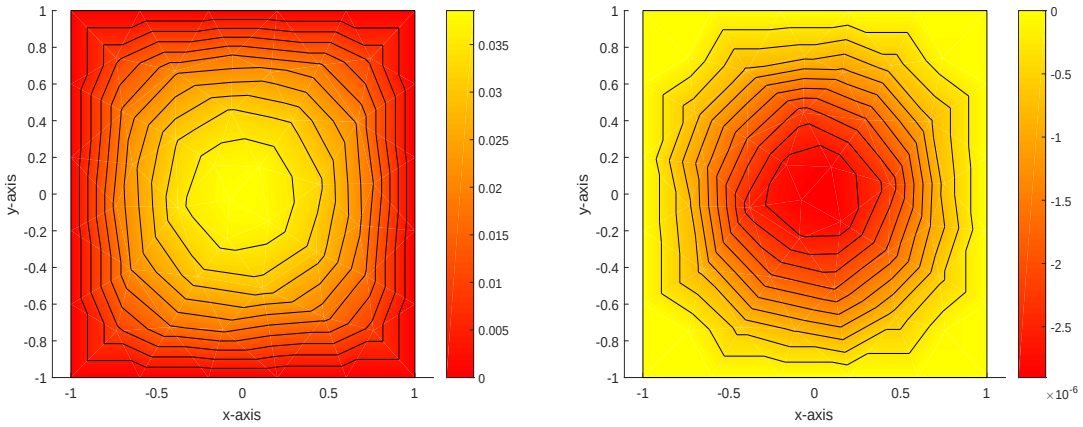

(a) (b)

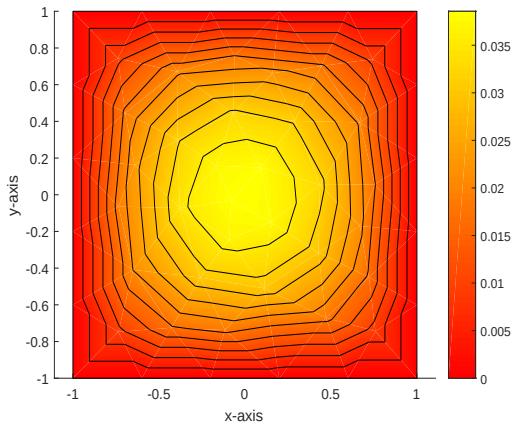

(c)

Figure 2.1: (a) Exact concentration; (b) error for the diffusion coefficient $c(t) = 2\sin\left(\frac{\pi}{2}t\right)+1$; and (c) approximate concentration at the final time.
The concentration is non-dimensionalized.

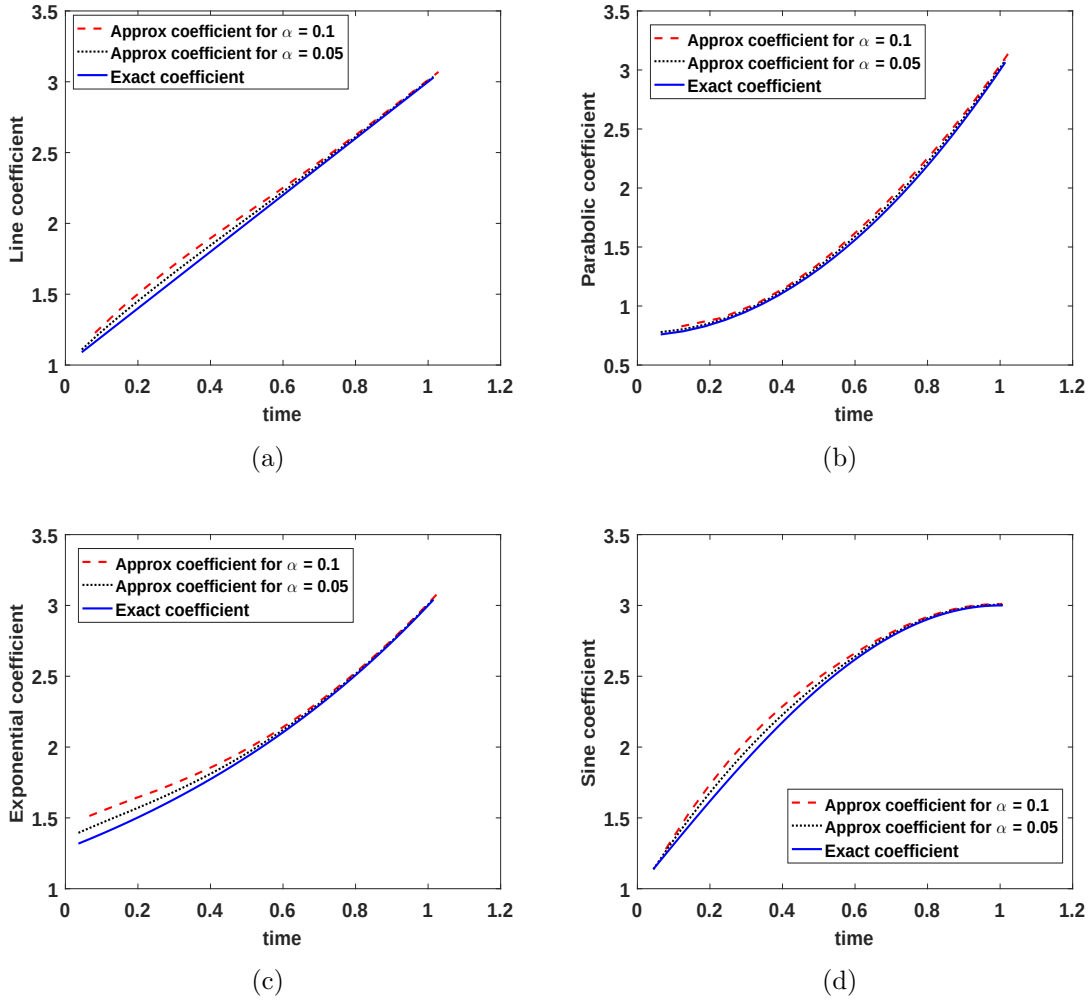

Figure 2.2: Exact coefficients and their approximations: (a) linear; (b) parabolic; (c) exponential; and (d) sine.

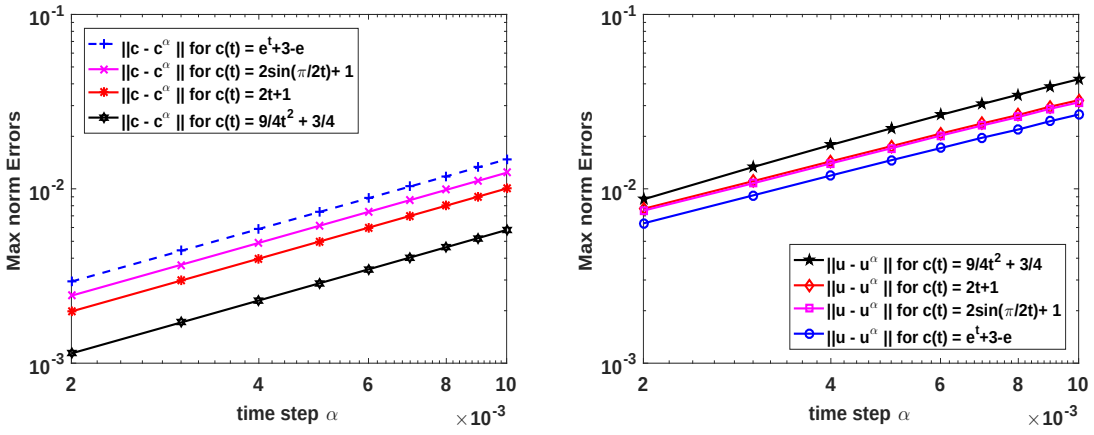

(a) (b)

Figure 2.3: (a) Log-log error plots for the diffusion coefficient; (b) log-log error plots for the concentration.

We also report in Table 2.1 the slopes s_u and s_c which correspond to the rates of convergence estimated using linear regression. These slopes suggest that $s_u \approx 1$ and $s_c \approx 1$, which is consistent with the standard parabolic error estimates.

We present in Table 2.2 and Table 2.3 the values of the errors in the diffusion coefficient c and the values of the errors in the concentration u, respectively, as well as the values of $\alpha = 0.0020, 0.0030, 0.0040, 0.0050, 0.0060, 0.0070, 0.0080, 0.0090, 0.0100$.

Table 2.2: Maximum error in the diffusion coefficient.

	α								
c	0.0020	0.0030	0.0040	0.0050	0.0060	0.0070	0.0080	0.0090	0.0100
$2t+1$	0.0020	0.0030	0.0040	0.0050	0.0060	0.0070	0.0080	0.0090	0.0100
$\frac{9}{4}t^2+\frac{3}{4}$	0.0011	0.0017	0.0023	0.0029	0.0035	0.0040	0.0046	0.0052	0.0058
$2\sin\left(\frac{\pi}{2}t\right)+1$	0.0024	0.0037	0.0049	0.0061	0.0074	0.0086	0.0099	0.0111	0.0124
e^t+3-e	0.0029	0.0044	0.0059	0.0074	0.0088	0.0103	0.0118	0.0133	0.0148

Table 2.3: Maximum error in the concentration for the inverse diffusion coefficient problem.

	α								
c	0.0020	0.0030	0.0040	0.0050	0.0060	0.0070	0.0080	0.0090	0.0100
$2t+1$	0.0077	0.0111	0.0144	0.0175	0.0207	0.0237	0.0265	0.0296	0.0322
$\frac{9}{4}t^2+\frac{3}{4}$	0.0087	0.0133	0.0178	0.0222	0.0265	0.0307	0.0347	0.0387	0.0425
$2\sin\left(\frac{\pi}{2}t\right)+1$	0.0075	0.0108	0.0140	0.0171	0.0202	0.0231	0.0258	0.0288	0.0313
e^t+3-e	0.0063	0.0092	0.0119	0.0146	0.0171	0.0196	0.0219	0.0244	0.0267

Chapter 3

Rothe's method for the inverse source problem

We now show the existence and uniqueness of weak solutions to the following inverse source problem: given the final time $T > 0$ and the integral data $\mu : [0,T] \to \mathbb{R}$, find the source function $f : [0,T] \to \mathbb{R}$ together with the concentration $u : \overline{\Omega} \times [0,T] \to \mathbb{R}$ satisfying

$$\partial_t u(x,t) - \Delta u(x,t) = f(t), \quad (x,t) \in \Omega \times (0,T], \tag{3.1}$$

$$u(x,t) = 0, \qquad (x,t) \in \partial\Omega \times [0,T], \tag{3.2}$$

$$u(x,0) = 0, \qquad x \in \Omega, \tag{3.3}$$

and

$$\int_\Omega u(x,t)\,dx = \mu(t), \quad t \in [0,T]. \tag{3.4}$$

The weak formulation is obtained by multiplying (3.1) and (3.4) by test functions $v \in L^2(0,T;H_0^1(\Omega))$ and $\phi \in L^2(0,T)$ respectively, integrating over Ω and using integration by parts. In this formulation we seek $u \in L^2(0,T;H_0^1(\Omega))$ with $\partial_t u \in L^2(0,T;H^{-1}(\Omega))$ and $f \in L^2(0,T)$ such that

$$\int_0^T \langle \partial_t u, v\rangle + (\nabla u, \nabla v)\,dt = \int_0^T (f,v)\,dt, \qquad \text{for all } v \in L^2(0,T;H_0^1(\Omega)), \tag{3.5}$$

and

$$\int_0^T (\phi(t), u(\cdot,t))\,dt = \int_0^T \phi(t)\mu(t)\,dt, \quad \text{for all } \phi \in L^2(0,T). \tag{3.6}$$

Note that this definition is equivalent to finding u and f as above satisfying for a.e. $t \in (0,T)$

$$\langle \partial_t u, v\rangle + (\nabla u, \nabla v) = (f,v), \quad \text{for all } v \in H_0^1(\Omega), \tag{3.7}$$

and

$$(\phi, u(\cdot, t)) = \phi\mu(t), \quad \text{for all } \phi \in \mathbb{R}. \tag{3.8}$$

3.1 Semi-discretization in time

We use the implicit Euler method for the time discretization of this system. To that end, denote the time step by τ and divide the interval $[0, T]$ into N subintervals $[t_{k-1}, t_k]$ of the same length τ where $k = 1, \cdots, N$. Let $\tilde{u}$ be the weak solution of

$$\tilde{u} - \tau\Delta\tilde{u} = \tau, \quad \text{in } \Omega, \tag{3.9}$$

and

$$\tilde{u} = 0, \quad \text{on } \partial\Omega. \tag{3.10}$$

Define $L\tilde{u} = \tilde{u} - \tau\Delta\tilde{u}$. Then $L\tilde{u} > 0$. By the maximum principle [14, Theorem 2, p. 346],

$$\min_{\bar{\Omega}} \tilde{u} > -\max_{\partial\Omega} \tilde{u}^- = 0, \quad \text{where } \tilde{u}^- = -\min(\tilde{u}, 0). \text{ Thus } \tilde{u} > 0 \text{ in } \Omega.$$

In particular, we have that

$$0 < \int_\Omega \tilde{u}\, dx = \tilde{\mu}.$$

Set

$$t^0 = 0, \quad u^0 = 0, \quad \hat{u}^0 = u^0, \quad \text{and} \quad f^0 = \frac{\mu(t^0) - \hat{\mu}^0}{\tilde{\mu}}, \tag{3.11}$$

where

$$\mu(t^0) = \int_\Omega u^0\, dx \quad \text{and} \quad \hat{\mu}^0 = \int_\Omega \hat{u}^0\, dx.$$

For $k \geq 1$, given u^{k-1}, let $\hat{u}^k$ be the weak solutions of the problems

$$\hat{u}^k - \tau\Delta\hat{u}^k = u^{k-1}, \quad \text{in } \Omega, \tag{3.12}$$

and

$$\hat{u}^k = 0, \qquad \text{on } \partial\Omega. \tag{3.13}$$

Define

$$f^k = \frac{\mu(t^k) - \hat{\mu}^k}{\tilde{\mu}}, \tag{3.14}$$

where

$$\hat{\mu}^k = \int_\Omega \hat{u}^k \, dx \quad \text{and} \quad \mu(t^k) = \int_\Omega u^k \, dx.$$

Let

$$u^k = \hat{u}^k + f^k \tilde{u}. \tag{3.15}$$

Next, we show that the decomposition (3.9)–(3.15) is equivalent to the discrete version of the original system. First, note that from (3.10), (3.11), (3.13), and (3.15), the initial and boundary conditions are satisfied. Moreover, from (3.9), (3.12), and (3.15) we have that

$$\begin{aligned} u^k - \tau\Delta u^k &= \hat{u}^k + f^k\tilde{u} - \tau\Delta(\hat{u}^k + f^k\tilde{u}) \\ &= \hat{u}^k - \tau\Delta\hat{u}^k + f^k(\tilde{u} - \tau\Delta\tilde{u}) \\ &= u^{k-1} + \tau f^k. \end{aligned}$$

The weak formulation is as follows: find $u^k \in H_0^1(\Omega)$ and $f^k \in \mathbb{R}$ such that

$$(u^k, v) + \tau(\nabla u^k, \nabla v) = (u^{k-1}, v) + (\tau f^k, v), \quad \text{for all } v \in H_0^1(\Omega), \tag{3.16}$$

and

$$(\phi, u^k) = \phi\mu(t^k), \qquad \text{for all } \phi \in \mathbb{R}, \tag{3.17}$$

which we recognize as the implicit Euler scheme of the weak formulation (3.7)–(3.8) of problem (3.1)–(3.4).

3.2 Existence of solutions

We will use the Rothe method to prove existence of weak solutions to the inverse source problem. The method involves an approximation of the time-dependent problem by a discrete scheme. We prove uniform estimates for the solutions of the discrete equations. These estimates allow us to obtain weakly convergent subsequences, which in turn converge to the solution of the original time-dependent problem.

3.2.1 Estimate of the unknown source

In this section, we will derive an estimate for the unknown source that will allow us to use the Rothe method for proving the existence of solutions. First, we derive a lower bound for the integral $\tilde{\mu}$ of the solution $\tilde{u}$ of problem (3.9)–(3.10) in the following lemma. This lower bound plays a crucial role in establishing the estimate of the unknown source in Lemma 3.2.

Lemma 3.1. *Suppose $\Omega \subset \mathbb{R}^d$ is a domain that contains a ball B of radius r and let $\tilde{u}$ be the weak solution of the problem*

$$\tilde{u} - \tau\Delta\tilde{u} = \tau, \quad in\ \Omega,$$

and

$$\tilde{u} = 0, \quad on\ \partial\Omega.$$

Then we have that

$$\int_\Omega \tilde{u}\, dx = \tilde{\mu} \geq \frac{|B|}{d+2}\tau \quad for\ \tau < \frac{r^2}{2d},$$

where $|B|$ denotes the volume of the ball B.

Proof. Let $\gamma(d)$ denote the volume of the unit ball in $\mathbb{R}^d$, then $R^d\gamma(d) = |B|$ is the volume of a ball with radius R in $\mathbb{R}^d$, and $R^{d-1}d\gamma(d)$ denotes the surface area of the sphere $\partial B(0, R)$ with radius R. We assume without loss of generality that the center of B is at the origin.

Now, define for $x \in B$,

$$v = \frac{\tau}{2}\left(1 - \frac{|x|^2}{r^2}\right).$$

Then

$$v - \tau\Delta v = \frac{\tau}{2}\left(1 - \frac{|x|^2}{r^2} + \frac{\tau}{r^2}\Delta|x|^2\right) = \frac{\tau}{2}\left(1 - \frac{|x|^2}{r^2} + \frac{2\tau d}{r^2}\right) \le \tau = \tilde{u} - \tau\Delta\tilde{u} \quad \text{for } \tau < \frac{r^2}{2d}.$$

Also, on ∂B, $v = 0 < \tilde{u}$. Therefore $0 < v < \tilde{u}$ in B by the comparison principle. Hence

$$\begin{aligned}
\tilde{\mu} &= \int_\Omega \tilde{u}\,dx \ge \int_B \tilde{u}\,dx \ge \int_B v\,dx = \frac{\tau}{2}\int_B \left(1 - \frac{|x|^2}{r^2}\right)\,dx \\
&= \frac{\tau}{2}\left(|B| - \frac{1}{r^2}\int_0^r \int_{\partial B(0,R)} |x|^2 dS(x)\,dR\right) \\
&= \frac{\tau}{2}\left(|B| - \frac{1}{r^2}\int_0^r R^2 R^{d-1} d\gamma(d)\,dR\right) = \frac{\tau}{2}\left(|B| - \frac{d\gamma(d) r^{d+2}}{r^2(d+2)}\right) \\
&= \frac{\tau}{2}\left(|B| - \frac{d\gamma(d) r^d}{d+2}\right) = \frac{\tau}{2}\left(|B| - \frac{d|B|}{d+2}\right) = \frac{|B|}{d+2}\tau.
\end{aligned}$$

□

We proceed to establish an estimate of the unknown source. The tool we use is eigenfunction expansions as described below. The result appears in Lemma 3.2. We write the solutions in $H_0^1(\Omega)$ of the equations

$$\tilde{u} - \tau\Delta\tilde{u} = \tau, \quad \hat{u}^k - \tau\Delta\hat{u}^k = u^{k-1}, \quad u^k - \tau\Delta u^k = u^{k-1} + \tau f^k, \quad -\Delta\bar{u} = 1,$$

in terms of eigenfunctions

$$\tilde{u} = \sum_{j\ge1} \tilde{U}_j w_j, \quad \hat{u}^k = \sum_{j\ge1} \hat{U}_j^k w_j, \quad u^k = \sum_{j\ge1} U_j^k w_j, \quad \bar{u} = \sum_{j\ge1} \overline{U}_j w_j, \tag{3.18}$$

where w_j are eigenfunctions of the Laplace operator in $H_0^1(\Omega)$ with homogeneous Dirichlet boundary conditions corresponding to eigenvalues λ_j, that is $w_j \in H_0^1(\Omega)$ satisfies

$$-\Delta w_j = \lambda_j w_j \quad \text{in } \Omega \quad \text{for } j \geq 1, \tag{3.19}$$

with $0 < \lambda_1 < \lambda_2 \leq \lambda_3 \cdots$ and $\lambda_j \to \infty$ as $j \to \infty$. From (3.9), (3.18), and (3.19) we have that

$$\begin{aligned} \tilde{u} - \tau\Delta\tilde{u} &= \sum_{j\geq 1} \tilde{U}_j w_j + \tau \sum_{j\geq 1} \tilde{U}_j(-\Delta w_j) \\ &= \sum_{j\geq 1} \tilde{U}_j(1+\tau\lambda_j) w_j = \tau \sum_{j\geq 1} (1, w_j) w_j. \end{aligned}$$

Therefore we have that for $j \geq 1$,

$$\tilde{U}_j(1+\tau\lambda_j) = \tau(1, w_j),$$

and hence

$$\tilde{U}_j = \frac{\tau\psi_j}{1+\tau\lambda_j}, \tag{3.20}$$

where we denote

$$\psi_j = (1, w_j) = \int_\Omega w_j \, dx.$$

Consequently,

$$\int_\Omega \tilde{u} \, dx = \tilde{\mu} = \sum_{j\geq 1} \frac{\tau\psi_j^2}{1+\tau\lambda_j}. \tag{3.21}$$

Similarly, (3.12), (3.18), and (3.19) imply that

$$\begin{aligned} \hat{u}^k - \tau\Delta\hat{u}^k &= \sum_{j\geq 1} \hat{U}_j^k w_j + \tau \sum_{j\geq 1} \hat{U}_j^k(-\Delta w_j) \\ &= \sum_{j\geq 1} \hat{U}_j^k(1+\tau\lambda_j) w_j = \sum_{j\geq 1} U_j^{k-1} w_j, \end{aligned}$$

and so

$$\hat{U}_j^k = \frac{U_j^{k-1}}{1+\tau\lambda_j}. \tag{3.22}$$

Finally, from (3.18), we get that

$$-\Delta\bar{u} = \sum_{j\geq 1} \overline{U}_j(-\Delta w_j) = \sum_{j\geq 1} \overline{U}_j \lambda_j w_j = \sum_{j\geq 1} \psi_j w_j,$$

and thus $\overline{U}_j = \psi_j/\lambda_j$, so that

$$\bar{\mu} = \int_\Omega \bar{u}\, dx = \sum_{j\geq 1} \frac{\psi_j^2}{\lambda_j}. \tag{3.23}$$

These calculations allow us to deduce from (3.15) that

$$\sum_{j\geq 1} U_j^k w_j = \sum_{j\geq 1} \hat{U}_j^k w_j + f^k \sum_{j\geq 1} \tilde{U}_j w_j,$$

and we obtain that for $j \geq 1$ and all $k \geq 0$

$$U_j^k = \hat{U}_j^k + f^k \tilde{U}_j.$$

Using this equation together with (3.20)–(3.22) and a recursive procedure we obtain that

$$\begin{aligned}
U_j^k &= f^k \frac{\tau\psi_j}{1+\tau\lambda_j} + \frac{U_j^{k-1}}{1+\tau\lambda_j} \\
&= f^k \frac{\tau\psi_j}{1+\tau\lambda_j} + \frac{\dfrac{U_j^{k-2}}{1+\tau\lambda_j} + f^{k-1}\dfrac{\tau\psi_j}{1+\tau\lambda_j}}{1+\tau\lambda_j} \\
&= f^k \frac{\tau\psi_j}{1+\tau\lambda_j} + f^{k-1}\frac{\tau\psi_j}{(1+\tau\lambda_j)^2} + \frac{U_j^{k-2}}{(1+\tau\lambda_j)^2} \\
&\vdots \\
&= f^k \frac{\tau\psi_j}{1+\tau\lambda_j} + f^{k-1}\frac{\tau\psi_j}{(1+\tau\lambda_j)^2} + \cdots + f^2\frac{\tau\psi_j}{(1+\tau\lambda_j)^{k-1}} + f^1\frac{\tau\psi_j}{(1+\tau\lambda_j)^k} + \frac{U_j^0}{(1+\tau\lambda_j)^k}.
\end{aligned}$$

Since $u^0 = 0$, we have that $U_j^0 = 0$ for all $j \geq 1$ and for all $k, j \geq 1$

$$U_j^{k-1} = f^{k-1}\frac{\tau\psi_j}{1+\tau\lambda_j} + f^{k-2}\frac{\tau\psi_j}{(1+\tau\lambda_j)^2} + \cdots + f^2\frac{\tau\psi_j}{(1+\tau\lambda_j)^{k-2}} + f^1\frac{\tau\psi_j}{(1+\tau\lambda_j)^{k-1}}. \quad (3.24)$$

From (3.12) we have that

$$u^{k-1} - \hat{u}^k = -\tau\Delta\hat{u}^k = \tau\sum_{j\geq 1}\hat{U}_j^k(-\Delta w_j) = \tau\sum_{j\geq 1}\hat{U}_j^k\lambda_j w_j.$$

Integrating over Ω and using (3.22) yield

$$\mu(t^{k-1}) - \hat{\mu}^k = \tau\sum_{j\geq 1}\hat{U}_j^k\lambda_j\psi_j = \sum_{j\geq 1}\frac{\tau\lambda_j\psi_j}{1+\tau\lambda_j}U_j^{k-1}. \quad (3.25)$$

From (3.14), and using (3.24) and (3.25), we derive a recursive relation for f^k independent of U_j^{k-1},

$$\begin{aligned} f^k &= \frac{\mu(t^k) - \hat{\mu}^k}{\tilde{\mu}} = \frac{\mu(t^k) - \mu(t^{k-1})}{\tilde{\mu}} + \frac{\mu(t^{k-1}) - \hat{\mu}^k}{\tilde{\mu}} \quad (3.26)\\ &= \frac{\mu(t^k) - \mu(t^{k-1})}{\tilde{\mu}} + \frac{\tau}{\tilde{\mu}}\sum_{j\geq 1}\frac{\lambda_j\psi_j}{1+\tau\lambda_j}U_j^{k-1}\\ &= \frac{\mu(t^k) - \mu(t^{k-1})}{\tilde{\mu}} + \frac{\tau}{\tilde{\mu}}\sum_{j\geq 1}\frac{\lambda_j\psi_j}{1+\tau\lambda_j}\left(\frac{f^{k-1}\tau\psi_j}{1+\tau\lambda_j} + \frac{f^{k-2}\tau\psi_j}{(1+\tau\lambda_j)^2} + \cdots + \frac{f^1\tau\psi_j}{(1+\tau\lambda_j)^{k-1}}\right)\\ &= \frac{\mu(t^k) - \mu(t^{k-1})}{\tilde{\mu}} + \frac{\tau^2}{\tilde{\mu}}\sum_{j\geq 1}\frac{\lambda_j\psi_j^2}{(1+\tau\lambda_j)^k}\left(\frac{f^{k-1}(1+\tau\lambda_j)^{k-1}}{1+\tau\lambda_j} + \frac{f^{k-2}(1+\tau\lambda_j)^{k-1}}{(1+\tau\lambda_j)^2} + \cdots + f^1\right)\\ &= \frac{\mu(t^k) - \mu(t^{k-1})}{\tilde{\mu}} + \frac{\tau^2}{\tilde{\mu}}\sum_{j\geq 1}\frac{\lambda_j\psi_j^2}{(1+\tau\lambda_j)^k}\left(f^{k-1}(1+\tau\lambda_j)^{k-2} + f^{k-2}(1+\tau\lambda_j)^{k-3} + \cdots + f^1\right). \quad (3.27) \end{aligned}$$

With the above computations, we are now ready to establish an estimate of the unknown source.

Lemma 3.2. *Let $\Omega \subset \mathbb{R}^d$ be a domain containing a ball B of radius r. Suppose μ is Lipschitz continuous with Lipschitz constant L. Then for $C_\Omega = L \max\left\{\dfrac{d+2}{|B|}, \dfrac{1}{\lambda_1 \bar{\mu}}\right\}$ we have that*

$$|f^n| \leq C_\Omega + \frac{L}{\bar{\mu}} n\tau, \quad n = 1, 2, \cdots \tag{3.28}$$

where $\bar{\mu}$ is defined in (3.23).

Proof. We will prove (3.28) by induction. The choice of the first quantity in the expression for C_Ω allows us to establish the basis of induction. Indeed, for $n = 1$, using Lemma 3.1, (3.26), and the Lipschitz continuity of μ, we have that

$$|f^1| = \frac{|\mu(t^1) - \mu(t^0)|}{\tilde{\mu}} + \frac{|\mu(t^0) - \hat{\mu}^0|}{\tilde{\mu}} \leq \frac{d+2}{|B|} L \leq C_\Omega + \frac{L}{\bar{\mu}}\tau.$$

Suppose that (3.28) holds for $n = 1, 2, \cdots, k-1$. Then from (3.27) we get that

$$\begin{aligned} |f^k| \leq \frac{L\tau}{\tilde{\mu}} + \frac{\tau^2}{\tilde{\mu}} C_\Omega \sum_{j \geq 1} \frac{\lambda_j \psi_j^2}{(1+\tau\lambda_j)^k} \left[(1+\tau\lambda_j)^{k-2} + (1+\tau\lambda_j)^{k-3} + \cdots + 1\right] \\ + \frac{L\tau^3}{\tilde{\mu}\bar{\mu}} \sum_{j \geq 1} \frac{\lambda_j \psi_j^2}{(1+\tau\lambda_j)^k} \left[(k-1)(1+\tau\lambda_j)^{k-2} + (k-2)(1+\tau\lambda_j)^{k-3} + \cdots + 1\right]. \end{aligned}$$

Note that $(1+\tau\lambda_j)^{k-2} + (1+\tau\lambda_j)^{k-3} + \cdots + 1$, is a geometric series with common ratio $(1+\tau\lambda_j)$ and whose sum is $\dfrac{(1+\tau\lambda_j)^{k-1} - 1}{\tau\lambda_j}$. Moreover, from the following geometric series with common ratio x

$$\frac{x^k - 1}{x - 1} = x^{k-1} + x^{k-2} + \cdots + x + 1,$$

we have that, on the one hand,

$$\frac{d}{dx}\left[\frac{x^k - 1}{x - 1}\right] = (k-1)x^{k-2} + (k-2)x^{k-3} + \cdots 2x + 1,$$

and, on the other hand, that

$$\frac{d}{dx}\left[\frac{x^k-1}{x-1}\right] = \frac{kx^{k-1}}{x-1} - \frac{x^k}{(x-1)^2}.$$

Combining, we get that

$$(k-1)x^{k-2} + (k-2)x^{k-3} + \cdots + 2x + 1 = \frac{kx^{k-1}}{x-1} - \frac{x^k-1}{(x-1)^2}.$$

Therefore, with $x = 1+\tau\lambda_j$, we obtain that

$$(k-1)(1+\tau\lambda_j)^{k-2}+(k-2)(1+\tau\lambda_j)^{k-3}+\cdots+2(1+\tau\lambda_j)+1 = \frac{k(1+\tau\lambda_j)^{k-1}}{\tau\lambda_j} - \frac{(1+\tau\lambda_j)^k-1}{\tau^2\lambda_j^2}.$$

Continuing with the estimate of f^k,

$$\begin{aligned}
|f^k| &\le \frac{L\tau}{\tilde{\mu}} + \frac{\tau^2}{\tilde{\mu}} C_\Omega \sum_{j\ge 1} \frac{\lambda_j \psi_j^2}{(1+\tau\lambda_j)^k}\left[\frac{(1+\tau\lambda_j)^{k-1}-1}{\tau\lambda_j}\right] \\
&\quad + \frac{L\tau^3}{\tilde{\mu}\bar{\mu}} \sum_{j\ge 1} \frac{\lambda_j \psi_j^2}{(1+\tau\lambda_j)^k}\left[\frac{k(1+\tau\lambda_j)^{k-1}}{\tau\lambda_j} - \frac{(1+\tau\lambda_j)^k-1}{\tau^2\lambda_j^2}\right] \\
&\le \frac{L\tau}{\tilde{\mu}} + \frac{C_\Omega}{\tilde{\mu}} \sum_{j\ge 1} \frac{\tau\psi_j^2}{1+\tau\lambda_j} - \frac{\tau}{\tilde{\mu}} C_\Omega \sum_{j\ge 1} \frac{\psi_j^2}{(1+\tau\lambda_j)^k} \\
&\quad + \frac{Lk\tau}{\tilde{\mu}\bar{\mu}} \sum_{j\ge 1} \frac{\tau\psi_j^2}{1+\tau\lambda_j} - \frac{L\tau}{\tilde{\mu}\bar{\mu}} \sum_{j\ge 1} \frac{\psi_j^2}{\lambda_j} + \frac{L\tau}{\tilde{\mu}\bar{\mu}} \sum_{j\ge 1} \frac{\psi_j^2}{\lambda_j(1+\tau\lambda_j)^k}.
\end{aligned}$$

From (3.21), (3.23), the definition of C_Ω, and using $\dfrac{1}{\lambda_j} \le \dfrac{1}{\lambda_1}$ for $j \ge 1$, we obtain that

$$\begin{aligned}
|f^k| &\le C_\Omega + \frac{\tau}{\tilde{\mu}} \sum_{j\ge 1} \frac{\psi_j^2}{(1+\tau\lambda_j)^k}\left(\frac{L}{\bar{\mu}\lambda_j} - C_\Omega\right) + \frac{L}{\bar{\mu}} k\tau \\
&\le C_\Omega + \frac{\tau}{\tilde{\mu}} \sum_{j\ge 1} \frac{\psi_j^2}{(1+\tau\lambda_j)^k}\left(\frac{L}{\bar{\mu}\lambda_1} - C_\Omega\right) + \frac{L}{\bar{\mu}} k\tau \\
&\le C_\Omega + \frac{L}{\bar{\mu}} k\tau,
\end{aligned}$$

completing the induction step. □

3.2.2 Rothe's method

We now investigate the existence of solutions to the inverse source problem. The estimate (3.28) is key to obtaining uniform bounds for f^k and u^k. We summarize the existence result below.

Theorem 3.3. *Let μ be Lipschitz continuous on $[0,T]$. Then the problem* (3.1)–(3.4) *has a solution $f \in L^2(0,T)$, $u \in L^2(0,T;H^1(\Omega))$ with $\partial_t u \in L^2(0,T;H^{-1}(\Omega))$.*

Proof. We use backward differences to discretize the time-dependent problem (3.1)–(3.4), as in Section 3.1 for $k = 1, 2, \cdots, N$, and $\tau = \dfrac{T}{N}$,

$$u^0 = u_0, \quad \frac{u^k - u^{k-1}}{\tau} - \Delta u^k = f^k, \quad \text{in } \Omega, \tag{3.29}$$

for $u^k = \hat{u}^k + f^k\tilde{u}$, where $\tilde{u}$ and $\hat{u}^k$ are solutions in $H_0^1(\Omega)$ of

$$\hat{u}^k - \tau\Delta\hat{u}^k = u^{k-1}, \quad \text{in } \Omega, \tag{3.30}$$

and

$$\tilde{u} - \tau\Delta\tilde{u} = \tau, \quad \text{in } \Omega, \tag{3.31}$$

with the property that

$$\int_\Omega u^k \, dx = \mu(t^k). \tag{3.32}$$

Clearly, problem (3.31) has a unique weak solution in $H_0^1(\Omega)$. Moreover, given $u^{k-1} \in L^2(\Omega)$, the equation (3.30) has a unique solution in $H_0^1(\Omega)$ for $k = 1, 2, \cdots, N$.

We will establish uniform estimates on the L^2-norms of u^k, ∇u^k, $\dfrac{u^k - u^{k-1}}{\tau}$ and the L^2-norm of f^k. To that end, put $v = u^k$ in the weak form (3.16) to obtain that

$$\|u^k\|^2 + \tau\|\nabla u^k\|^2 = (u^k, u^{k-1}) + (\tau f^k, u^k).$$

Dropping the second term on the left-hand side and applying the Schwarz inequality yields

$$\|u^k\|^2 \leq |(u^k, u^{k-1})| + |(\tau f^k, u^k)| \leq \tau |f^k||\Omega|^{1/2}\|u^k\| + \|u^k\|\|u^{k-1}\|.$$

Therefore

$$\|u^k\| \leq \tau |f^k||\Omega|^{1/2}\| + \|u^{k-1}\|.$$

Using (3.28), the fact that $k\tau \leq T$, and an iterative procedure for all $k = 1, 2, \cdots, N$ yield,

$$\begin{aligned}
\|u^k\| &\leq \|u^{k-1}\| + \tau|\Omega|^{1/2}\left(C_\Omega + \frac{L}{\bar{\mu}}T\right) \\
&\leq \|u^{k-2}\| + 2\tau|\Omega|^{1/2}\left(C_\Omega + \frac{L}{\bar{\mu}}T\right) \\
&\leq \|u^{k-3}\| + 3\tau|\Omega|^{1/2}\left(C_\Omega + \frac{L}{\bar{\mu}}T\right) \\
&\vdots \\
&\leq \|u^0\| + k\tau|\Omega|^{1/2}\left(C_\Omega + \frac{L}{\bar{\mu}}T\right) \\
&\leq \|u^0\| + T|\Omega|^{1/2}\left(C_\Omega + \frac{L}{\bar{\mu}}T\right) = \|u^0\| + C(d, \Omega, L, T). \qquad (3.33)
\end{aligned}$$

Applying the triangle inequality to the second equation in (3.29) we get that

$$\begin{aligned}
\left\|\frac{u^k - u^{k-1}}{\tau}\right\| &\leq \|\Delta u^k\| + |\Omega|^{1/2}\left(C_\Omega + \frac{L}{\bar{\mu}}T\right) \\
&\leq \|u^k\|_{H^2(\Omega)} + |\Omega|^{1/2}\left(C_\Omega + \frac{L}{\bar{\mu}}T\right).
\end{aligned}$$

Standard elliptic estimates, as in [16, Theorem 8.12, p. 186], under the condition that $\partial\Omega$ is of class C^2, yield that the weak solution $u^k \in H_0^1(\Omega)$ of (3.29) is also in $H^2(\Omega)$ and we have that

$$\|u^k\|_{H^2(\Omega)} \leq C(d, \partial\Omega)\left(\|u^k\| + \|u^{k-1}\| + \|f^k\|\right).$$

where d is the space dimension. Hence, (3.33) yields

$$\|u^k\|_{H^2(\Omega)} \leq C(d, \Omega, L, T, u^0),$$

from which we deduce that, since $\|\nabla u^k\| \leq \|u^k\|_{H^2(\Omega)}$,

$$\|\nabla u^k\| \leq C(d, \Omega, L, T, u^0), \quad k = 1, 2, \cdots, N. \tag{3.34}$$

We conclude that

$$\left\| \frac{u^k - u^{k-1}}{\tau} \right\| \leq C(d, \Omega, L, T, u^0), \quad k = 1, 2, \cdots, N. \tag{3.35}$$

Finally, from (3.28),

$$\|f^k\|_{L^2(0,T)} \leq |\Omega|^{1/2} \left(C_\Omega + \frac{L}{\bar{\mu}} T \right) = C(\Omega, d, T, L), \quad k = 1, 2, \cdots, N. \tag{3.36}$$

Define approximations of u and f that are piece-wise linear and piece-wise constant in time, as follows:

$$u^\tau(t) = u^{k-1} + \frac{u^k - u^{k-1}}{\tau}(t - t^{k-1}), \quad t \in [t^{k-1}, t^k], \quad k = 1, 2, \cdots, N,$$

and

$$f^\tau(t) = f^k, \qquad\qquad t \in [t^{k-1}, t^k], \quad k = 1, 2, \cdots, N.$$

Letting $\tau \to 0$, we obtain a solution of (3.1)–(3.4) as a weak limit of functions $\{(u^k, f^k), k = 1, 2, \cdots, N\}$. The functions u^τ are elements of the space $L^2(0, T; H_0^1(\Omega))$ and satisfy $\partial_t u^\tau = \dfrac{u^k - u^{k-1}}{\tau}$, $t \in (t^{k-1}, t^k)$. Due to (3.33), (3.34), (3.35), and (3.36) we obtain

the following uniform bounds

$$\|u^\tau\|_{L^2(0,T;L^2(\Omega))} \le C(d,\Omega,L,T,u^0), \tag{3.37}$$

$$\|\nabla u^\tau\|_{L^2(0,T;L^2(\Omega))} \le C(d,\Omega,L,T,u^0), \tag{3.38}$$

$$\|\partial_t u^\tau\|_{L^2(0,T;L^2(\Omega))} \le C(d,\Omega,L,T,u^0), \tag{3.39}$$

and

$$\|f^\tau\|_{L^2(0,T)} \le C(\Omega,d,T,L). \tag{3.40}$$

From the weak compactness of $L^2(0,T)$ and $L^2(0,T;L^2(\Omega))$, there exist subsequences $\tau_l, l = 1,2,\cdots$, with $\tau_l \to 0$, for which f^{τ_l} converges weakly in $L^2(0,T)$ to some function $f \in L^2(0,T)$, the functions u^{τ_l}, ∇u^{τ_l}, and $\partial_t u^{\tau_l}$ converge weakly in $L^2(0,T;L^2(\Omega))$ to u, ∇u, and $\partial_t u$, respectively, for some function $u \in L^2(0,T;H_0^1(\Omega))$ with $\partial_t u \in L^2(0,T;H^{-1}(\Omega))$. To see, for example, that $\partial_t u^{\tau_l}$ converges weakly to $\partial_t u$, as in [39, Chapter 11], we denote the weak limit of $\partial_t u^{\tau_l}$ by U. Since $U \in L^2(0,T;L^2(\Omega))$, $y(t) = \int_0^t U(s)\,ds$ exists and $y(t)$ is absolutely continuous, that is, $y(t) \in AC(0,T;L^2(\Omega))$ with $\partial_t y(t) = U(t)$ in $L^2(0,T;L^2(\Omega))$. Using the definition of u^τ, we have that

$$\int_0^t \partial_t u^{\tau_l}(s)\,ds = u^{\tau_l}(t) - u^{\tau_l}(0).$$

By uniqueness of the weak limit, we obtain that

$$y(t) = u(t) \quad \text{in } L^2(0,T;L^2(\Omega)).$$

Therefore, $u \in AC(0,T;L^2(\Omega))$ and

$$\partial_t u(t) = U(t) \quad \text{in } L^2(0,T;L^2(\Omega)).$$

Moreover, from $u(t) = \int_0^t U(s)\,ds$, we deduce that $u(0) = 0$ in $C(0,T;L^2(\Omega))$. The initial condition (3.3) is satisfied in the classical sense. Furthermore, since $u \in L^2(0,T;H_0^1(\Omega))$, then for a.e. $t \in (0,T)$, $u(t) \in H_0^1(\Omega)$. The boundary condition (3.2) is satisfied in the sense of traces. It remains to show that (u,f) satisfies (3.5)–(3.6). Recall the weak formulation

$$\left(\frac{u^k - u^{k-1}}{\tau}, v\right) + (\nabla u^k, \nabla v) = (f^k, v) \quad \text{for all } v \in H_0^1(\Omega),$$

and

$$(u^k, \phi) = \phi\mu(t^k) \quad \text{for all } \phi \in L^2(0,T).$$

Let $v \in L^2(0,T;H_0^1(\Omega))$ and $\phi \in L^2(0,T)$ be arbitrary functions. Consider the previous equations written for $t = t^k$, $k = 1, 2, \cdots, N$. We have, for a.e. $0 \le t \le T$,

$$\langle \partial_t u^\tau(t), v(t)\rangle + (\nabla u^\tau(t), \nabla v(t)) = (f^\tau(t), v(t))\,,$$

and

$$(u^\tau(t), \phi(t)) = \phi(t)\mu(t).$$

Selecting convergent subsequences and integrating from 0 to T, we get that

$$\int_0^T \langle \partial_t u^{\tau_l}(t), v(t)\rangle\ dt + \int_0^T (\nabla u^{\tau_l}(t), \nabla v(t))\ dt = \int_0^T (f^{\tau_l}(t), v(t))\ dt, \tag{3.41}$$

and

$$\int_0^T (u^{\tau_l}(t), \phi(t))\ dt = \int_0^T \phi(t)\mu(t)\,dt. \tag{3.42}$$

Due to the weak convergence of u^{τ_l}, $\partial_t u^{\tau_l}$, ∇u^{τ_l}, and f^{τ_l}, we have that, for $\tau_l \to 0$

$$\int_0^T \langle \partial_t u^{\tau_l}, v(t) \rangle \, dt \to \int_0^T \langle \partial_t u(t), v(t) \rangle \, dt,$$
$$\int_0^T (u^{\tau_l}, \phi(t)) \, dt \to \int_0^T (u(t), \phi(t)) \, dt,$$
$$\int_0^T (\nabla u^{\tau_l}(t), \nabla v(t)) \, dt \to \int_0^T (\nabla u(t), \nabla v(t)) \, dt,$$

and

$$\int_0^T (f^{\tau_l}(t), v(t)) \, dt \to \int_0^T (f(t), v(t)) \, dt.$$

Combining these limits with (3.41)–(3.42) we have that, for $v(t) \in L^2(0,T;H_0^1(\Omega))$ and $\phi \in L^2(0,T)$,

$$\int_0^T \langle \partial_t u(t), v(t) \rangle \, dt + \int_0^T (\nabla u(t), \nabla v(t)) \, dt = \int_0^T (f(t), v(t)) \, dt,$$

and

$$\int_0^T (u(t), \phi(t)) \, dt = \int_0^T \phi(t)\mu(t) \, dt.$$

The couple (u, f) satisfies the differential equation (3.1) and the integral constraint (3.4) in the sense of (3.5) and (3.6) completing the proof. □

3.3 Uniqueness of solutions to the inverse source problem

Theorem 3.4. *The weak solution $u \in L^2(0,T;H_0^1(\Omega))$ with $\partial_t u \in L^2(0,T;H^{-1}(\Omega))$ and $f \in L^2(0,T)$ to the inverse source problem (3.1)–(3.4) is unique.*

Proof. Suppose (u_1, f_1) and (u_2, f_2) are two solutions to the inverse source problem (3.1)–(3.4). Let $u = u_1 - u_2$ and $f = f_1 - f_2$. Then (u, f) satisfies

$$\partial_t u(x,t) - \Delta u(x,t) = f(t), \quad (x,t) \in \Omega \times (0,T], \tag{3.43}$$

$$u(x,t) = 0, \qquad (x,t) \in \partial\Omega \times [0,T], \tag{3.44}$$

$$u(x,0) = 0, \qquad x \in \Omega, \tag{3.45}$$

and

$$\int_\Omega u(x,t)\,dx = 0, \qquad t \in [0,T]. \tag{3.46}$$

Taking $v = u$ in (3.7) we obtain that

$$\langle \partial_t u, u\rangle + \|u\|^2 = f(t)\int_\Omega u(x,t)\,dx = 0 \quad \text{by (3.46)}.$$

That is,

$$\langle \partial_t u, u\rangle = -\|u\|^2. \tag{3.47}$$

Since $u \in L^2(0,T;H_0^1(\Omega))$ with $\partial_t u \in L^2(0,T;H^{-1}(\Omega))$, from [14, Theorem 3, p. 303], $u \in C([0,T];L^2(\Omega))$ and the mapping $t \mapsto \|u(t)\|^2$ is absolutely continuous with

$$\frac{d}{dt}\|u(t)\|^2 = 2\langle \partial_t u(t), u(t)\rangle \quad \text{for a.e } 0 \le t \le T.$$

Using (3.47), we get that

$$\frac{d}{dt}\|u(t)\|^2 = -2\|u(t)\|^2 \le 0 \quad \text{for a.e } 0 \le t \le T.$$

Since $u(0) = 0$, applying the differential form of Gronwall's inequality [14, p. 708], we have that

$$u(t) = 0 \quad \text{for a.e.} \quad 0 \le t \le T.$$

Substituting in (3.43), it follows that $f = 0$. Therefore $u_1 = u_2$ and $f_1 = f_2$. □

3.4 Numerical implementation and convergence studies

We now present several numerical results. We recall (see Section 3.1) that the solution (u^k, f^k) of the discrete problem can be obtained by the iteration

$$u^k = \hat{u}^k + f^k \tilde{u}, \quad \text{with} \quad f^k = \frac{\mu(t^k) - \hat{\mu}^k}{\tilde{\mu}}, \tag{3.48}$$

where $\hat{u}^k$ and $\tilde{u}$ are $H_0^1(\Omega)$ solutions of

$$\hat{u}^k - \tau \Delta \hat{u}^k = u^{k-1}, \quad \text{in } \Omega, \tag{3.49}$$

and

$$\tilde{u} - \tau \Delta \tilde{u} = \tau, \quad \text{in } \Omega. \tag{3.50}$$

We denote

$$\mu(t^k) = \int_\Omega u^k \, dx, \quad \tilde{\mu} = \int_\Omega \tilde{u} \, dx, \quad \text{and} \quad \hat{\mu}^k = \int_\Omega \hat{u}^k \, dx.$$

3.4.1 Finite element approximation

To obtain a fully discrete approximation, the equations are discretized using a finite element formulation in space as we described in Section 1.3.1. Let u_h^k, $\tilde{u}_h$, and $\hat{u}_h^k$ be the finite element approximations to u^k, $\tilde{u}$, and $\hat{u}^k$, respectively. The functions u_h^k, $\tilde{u}_h$, and $\hat{u}_h^k$ are continuous in the finite element space V_h. They are piecewise linear approximations to u^k, $\tilde{u}$, and $\hat{u}^k$, respectively, linear on each triangle in the triangulation T_h of the domain Ω and vanishing on the boundary $\partial\Omega$. From (3.49) and (3.50), we obtain the following weak formulations, for every test function $v \in V_h$,

$$\int_\Omega v \tilde{u}_h \, dx + \tau \int_\Omega \nabla v \cdot \nabla \tilde{u}_h \, dx = \int_\Omega \tau v \, dx,$$

and

$$\int_\Omega v\hat{u}_h^k\,dx + \tau\int_\Omega \nabla v\cdot\nabla\hat{u}_h^k\,dx = \int_\Omega vu_h^{k-1}\,dx.$$

The functions u_h^k, $\tilde{u}_h$, and $\hat{u}_h^k$ have representations

$$u_h^k(x) = \sum_{j=1}^{N_p} u_j^k\phi_j(x), \quad \tilde{u}_h(x) = \sum_{j=1}^{N_p}\tilde{u}_j\phi_j(x), \quad \text{and} \quad \hat{u}_h^k(x) = \sum_{j=1}^{N_p}\hat{u}_j^k\phi_j(x),$$

with unknown $u_j^k = u^k(x_j)$, $\tilde{u}_j = \tilde{u}(x_j)$, and $\hat{u}_j^k = \hat{u}^k(x_j)$, where $\{\phi_j\}_{j=1}^{N_p}$ are basis functions for V_h and $\{x_j\}_{j=1}^{N_p}$ are the interior vertices of T_h. Taking test functions $v = \phi_i$, $i = 1,\cdots,N_p$, and using the representations above, after combining terms, we have that

$$\sum_{j=1}^{N_p}\left(\int_\Omega \phi_i\phi_j + \tau\nabla\phi_i\cdot\nabla\phi_j\,dx\right)\tilde{u}_j = \int_\Omega \tau\phi_i\,dx,$$

and

$$\sum_{j=1}^{N_p}\left(\int_\Omega \phi_i\phi_j + \tau\nabla\phi_i\cdot\nabla\phi_j\,dx\right)\hat{u}_j^k = \sum_{j=1}^{N_p} u_j^{k-1}\int_\Omega \phi_i\phi_j\,dx,$$

or

$$\sum_{j=1}^{N_p}(M_{ij}+\tau K_{ij})\tilde{u}_j = \int_\Omega \tau\phi_i\,dx, \quad i = 1,\cdots,N_p,$$

and

$$\sum_{j=1}^{N_p}(M_{ij}+\tau K_{ij})\hat{u}_j^k = \sum_{j=1}^{N_p} M_{ij}u_j^{k-1}, \quad i,j = 1,\cdots,N_p,$$

where M_{ij} and K_{ij} are respectively the mass and stiffness matrices defined by

$$M_{ij} = \int_\Omega \phi_j\phi_i\,dx \quad \text{and} \quad K_{ij} = \int_\Omega \nabla\phi_j\cdot\nabla\phi_i\,dx, \quad i,j = 1,\cdots,N_p.$$

We obtain the linear systems of N_p equations in N_p unknown written in matrix form

$$(M + \tau K)\tilde{U} = F, \tag{3.51}$$

and

$$(M + \tau K)\hat{U}^k = MU^{k-1}, \tag{3.52}$$

where M, K and F are defined as follows

$$M = (M_{ij}), \quad K = (K_{ij}), \quad F = (F_i), \quad \text{and} \quad F_i = \int_\Omega \tau\phi_i(x)\,dx, \quad i, j = 1, \cdots, N_p, \tag{3.53}$$

and

$$\tilde{U} = (\tilde{u}_j)^t, \quad \hat{U}^k = (\hat{u}_j^k)^t, \quad i, j = 1, \cdots, N_p, \quad k = 1, 2, \cdots, N.$$

As a consequence of (3.48),

$$\sum_{j=1}^{N_p} u_j^k \phi_j(x) = \sum_{j=1}^{N_p} (\hat{u}_j^k + f^k\tilde{u}_j)\phi_j(x), \quad \text{that is,} \quad u_j^k = \hat{u}_j^k + f^k\tilde{u}_j,$$

and therefore,

$$U^k = \hat{U}^k + f^k\tilde{U}, \quad \text{where} \quad U^k = (u_j^k)^t, \quad j = 1, 2, \cdots, N_p, \quad k = 1, 2, \cdots, N.$$

3.4.2 The algorithm

We outline the steps in the numerical experiment. To test the convergence of the algorithm, we first supply a source function $f(t)$ and find the solution u of the direct problem (3.1)–(3.3). Then we compute the integral data $\mu(t^k) = \int_\Omega u^k\,dx$, $k = 1, 2, \cdots, N$.

Step 1. Assemble the matrices K, M, and F.

Step 2. Calculate $\tilde{U} = (\tilde{u}_1, \tilde{u}_2, \cdots, \tilde{u}_{N_p})^t$ and compute its integral $\tilde{\mu}$ over Ω.

For $k = 1, 2, \cdots, N$, we follow the steps below.

Step 3. Given $U^{k-1} = (u_1^{k-1}, u_2^{k-1}, \cdots, u_{N_p}^{k-1})^t$, find $\hat{U}^k = (\hat{u}_1^k, \hat{u}_2^k, \cdots, \hat{u}_{N_p}^k)^t$ and compute its integral $\hat{\mu}^k$ over Ω.

Step 4. Determine the approximate source $f^k = \dfrac{\mu(t^k) - \hat{\mu}^k}{\tilde{\mu}}$.

Step 5. Determine the approximate solution $U^k = (u_1^k, u_2^k, \cdots, u_{N_p}^k)^t$ with $u_j^k = \hat{u}_j^k + f^k \tilde{u}_j$, $j = 1, 2, \cdots, N_p$.

We briefly describe the computation of the rates of convergence. Let (u, f) and (u^τ, f^τ) denote the exact and approximate solutions of the inverse source problem (3.1)–(3.4), respectively. We expect error for parabolic problems to satisfy estimates of the form

$$\|u - u^\tau\| \le C_1 \tau^{\delta_1} \quad \text{and} \quad \|f - f^\tau\| \le C_2 \tau^{\delta_2},$$

where C_1, C_2, δ_1, and δ_2 are constants. To determine C_1, C_2, δ_1, and δ_2, we take the logarithm of both sides of the above inequalities to get

$$\log \|u - u^\tau\| \le C_1 + \delta_1 \log \tau, \quad \log \|f - f^\tau\| \le C_2 + \delta_2 \log \tau.$$

We recognize the rates of convergence as the slopes δ_1 and δ_2 of the linear functions $\log \|u - u^\tau\|$ and $\log \|f - f^\tau\|$, respectively, as functions of $\log \tau$. We estimate the slopes using the least squares.

3.4.3 Numerical studies and rates of convergence

We consider several examples to illustrate the accuracy of our scheme. To show how the scheme handles domains with complicated geometries, we consider a muscovite crystal from Hames and Andresen [23], plotted in Figure 3.1. The final time is taken to be $T = 1$. The examples of the sources we use in our experiments are given in Table 3.1. All selected sources attain the same maximum value of 4 on the temporal interval $[0, T]$. In our experiments, we chose a maximum mesh size of 0.05, resulting in 27,888 elements and 14,145 unknowns. In

Table 3.1: Rate of convergence estimates from the slopes s_f and s_u in inverse source scheme.

f	$4t$	$3t^2+t$	$8\sin\left(\frac{\pi}{6}t\right)$	5^t-1
s_f	0.9930	0.9829	0.9923	0.9968
s_u	0.9781	0.9770	0.9767	0.9962

order to generate the data, we supplied a source function from Table 3.1 and ran the forward model to obtain a numerical approximation to solutions of the direct problem, which we treated as the exact solution. We then computed the numerical integral of the solution and used it as the data for our scheme. In the computational algorithm, we use the built-in MATLAB functions *parabolic* to solve the parabolic problem (3.1)–(3.3), and *assempde* to assemble the matrices M, K, F and solve the elliptic equations (3.49) and (3.50). We plot in Figure 3.1, the exact and approximate concentrations at the final time and the error, computed with the source function $f(t) = 8\sin(\frac{\pi}{6}t)$. The graphs indicate that the error is of order 10^{-3} in the approximation. In Figure 3.2, we depict the four source functions from Table 3.1. In each case, we plot the exact source and approximate source using time steps $\tau = \frac{1}{5}, \frac{1}{15}, \frac{1}{25}$. These graphs illustrate that as the time step τ decreases, the approximate source converges to the exact source uniformly. In Figure 3.3, we present the errors in the approximate concentrations, and in the approximate sources for a time step in the range $[10^{-1}, 10^{-2}]$. Error estimates for the standard implicit scheme suggest that

$$\left(\int_0^T \|u(\cdot,t)-u^\tau(\cdot,t)\|^2_{L^2(\Omega)}\,dt\right)^{1/2} = \mathcal{O}(\tau^{s_u}), \quad \text{and} \quad \left(\int_0^T |f(t)-f^\tau(t)|^2\,dt\right)^{1/2} = \mathcal{O}(\tau^{s_f}),$$

for some $s_u, s_f > 0$, where u and f denote the exact concentration and the exact source, respectively, and u^τ and f^τ are the approximate concentration and the approximate source. The slopes s_u and s_f which correspond to the estimated rates of convergence obtained using the linear regression are given in Table 3.1. These slopes suggest that $s_u \approx 1$ and $s_f \approx 1$, which is consistent with standard parabolic error estimates.

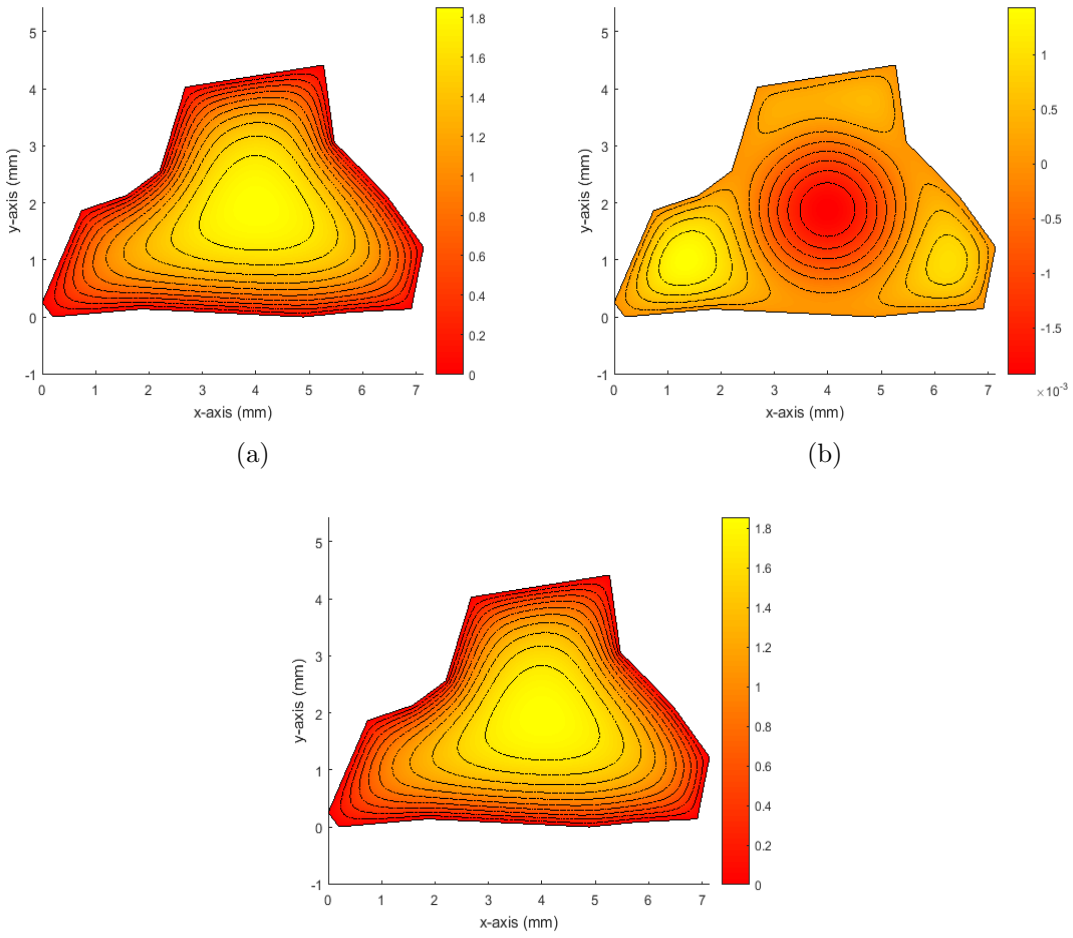

Figure 3.1: (a) Exact concentration; (b) error for the source $f(t) = 8\sin(\frac{\pi}{6}t)$; and (c) approximate concentration at the final time.
The concentration is non-dimensionalized.

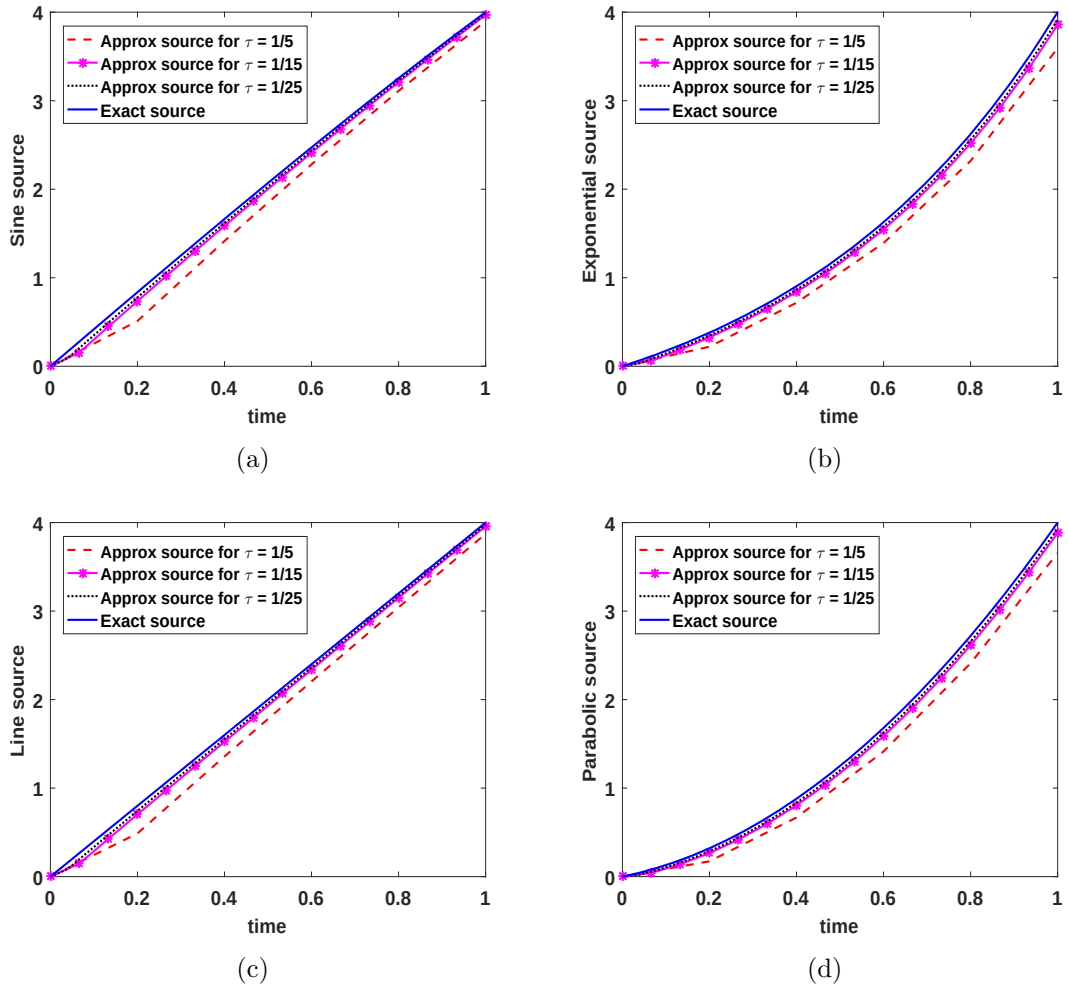

Figure 3.2: Exact sources and their approximations: (a) sine; (b) exponential; (c) linear; and (d) parabolic.

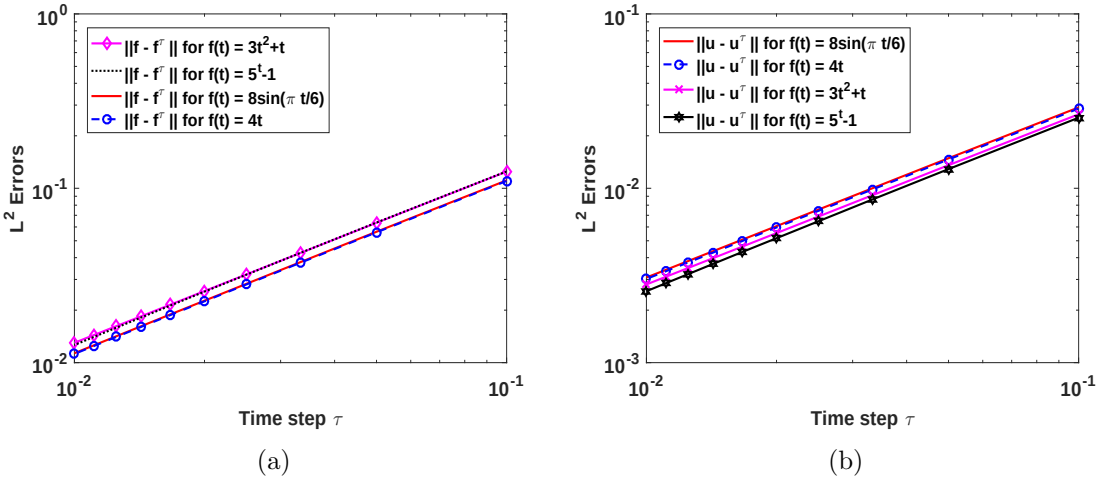

Figure 3.3: (a) Log-log error plots for the source; (b) log-log error plots for the concentration.

Table 3.2 and Table 3.3 below contain the values of the errors in the source f and the values of the errors in the concentration u, respectively, together with the values of the time step τ.

Table 3.2: $L^2(0,T)$ error in the source for the inverse source problem.

	f			
τ	$4t$	$3t^2+t$	$8\sin\left(\frac{\pi}{6}t\right)$	5^t-1
0.1000	0.1101	0.1247	0.1110	0.1250
0.0500	0.0559	0.0634	0.0563	0.0636
0.0333	0.0374	0.0426	0.0377	0.0426
0.0250	0.0281	0.0321	0.0283	0.0320
0.0200	0.0225	0.0257	0.0227	0.0255
0.0167	0.0187	0.0215	0.0189	0.0213
0.0143	0.0161	0.0185	0.0162	0.0182
0.0125	0.0140	0.0162	0.0142	0.0159
0.0111	0.0125	0.0144	0.0126	0.0141
0.0100	0.0112	0.0130	0.0113	0.0126

Table 3.3: $L^2(0,T;L^2(\Omega))$ error in the concentration.

	f			
τ	$4t$	$3t^2+t$	$8\sin\left(\frac{\pi}{6}t\right)$	5^t-1
0.1000	0.0286	0.0266	0.0291	0.0254
0.0500	0.0146	0.0136	0.0149	0.0129
0.0333	0.0098	0.0091	0.0100	0.0086
0.0250	0.0074	0.0069	0.0075	0.0065
0.0200	0.0060	0.0055	0.0061	0.0052
0.0167	0.0050	0.0046	0.0051	0.0043
0.0143	0.0043	0.0040	0.0044	0.0037
0.0125	0.0038	0.0035	0.0038	0.0032
0.0111	0.0033	0.0031	0.0034	0.0029
0.0100	0.0030	0.0028	0.0031	0.0026

Chapter 4

A semigroup approach to the inverse source problem

We now return to the inverse source problem: given the final time $T > 0$, the boundary data $g : \partial\Omega \times (0,T) \to \mathbb{R}$, the initial data $u_0 : \Omega \to \mathbb{R}$, and the integral data $\mu : [0,T) \to \mathbb{R}$, find the time-dependent source function $f : [0,T] \to \mathbb{R}$ together with the concentration $u : \overline{\Omega} \times [0,T) \to \mathbb{R}$ satisfying

$$\partial_t u(x,t) - \Delta u(x,t) = f(t), \qquad \text{in } \Omega \times (0,T), \tag{4.1}$$

$$u(x,t) = g(x,t), \quad \text{in } \partial\Omega \times (0,T), \tag{4.2}$$

$$u(x,0) = u_0(x), \quad \text{in } \Omega, \tag{4.3}$$

and

$$\int_\Omega u(x,t)\,dx = \mu(t), \qquad \text{for all } t \in [0,T). \tag{4.4}$$

We start by giving the meaning of solution (u,f) to the inverse source problem (4.1)–(4.4).

Definition 4.1. The pair (u,f) is a solution of (4.1)–(4.4) if:

1. The source function $f(t)$ is continuous for $0 \le t \le T$.
2. The concentration $u(x,t)$ is continuous for $(x,t) \in \Omega \times [0,T)$.
3. The derivatives $\partial_t u$, ∇u, $\partial^2 u/\partial x_i \partial x_j$ exist and are continuous for $(x,t) \in \Omega \times (0,T)$, $1 \le i,j \le d$.
4. The equations (4.1)–(4.4) hold in the classical sense.

We make the following assumptions on the data:

A1. The boundary data $g(x,t)$ is continuous for $(x,t) \in \partial\Omega \times (0,T)$.

A2. The initial condition u_0 is of class $C^2(\Omega)$.

A3. The integral data μ is of class $C^2[0,T]$.

4.1 Existence of classical solutions

We show the existence and uniqueness of solutions to the inverse source problem (4.1)–(4.4) using semigroup method. We summarize the result in the following

Theorem 4.1. *Suppose Assumptions A1-A3 hold. Then the inverse source problem* (4.1)–(4.4) *has a unique solution* (u,f) *in the sense of Definition 4.1.*

Proof. The idea is to decompose the solution (u,f) of the inverse problem (4.1)–(4.4) into the solution w of a heat equation and a solution (v,f) to an inverse problem. We then apply perturbation theory for semigroups to the inverse problem (v,f). To that end, let w be the unique classical solution of the direct problem

$$\partial_t w(x,t) - \Delta w(x,t) = 0, \qquad (x,t) \in \Omega \times (0,T), \tag{4.5}$$

$$w(x,0) = u_0(x), \quad x \in \Omega, \tag{4.6}$$

and

$$w(x,t) = g(x,t), \quad (x,t) \in \partial\Omega \times [0,T). \tag{4.7}$$

Define

$$\psi(t) := \int_\Omega w(x,t)\,dx, \quad t \in [0,T). \tag{4.8}$$

This choice of w allows us to homogenize the initial and boundary conditions of the inverse source problem (4.1)–(4.4). Consider the following inverse source problem for (v, f),

$$\partial_t v(x,t) - \Delta v(x,t) = f(t), \qquad (x,t) \in \Omega \times (0,T), \tag{4.9}$$

$$v(x,0) = 0, \qquad x \in \Omega, \tag{4.10}$$

$$v(x,t) = 0, \qquad (x,t) \in \partial\Omega \times [0,T), \tag{4.11}$$

and

$$\int_\Omega v(x,t)\,dx = \mu(t) - \psi(t), \quad t \in [0,T). \tag{4.12}$$

We note that $u = w + v$. We integrate the terms in equation (4.9) over Ω and use Green's Theorem to obtain

$$\int_\Omega \partial_t v(x,t)\,dx - \int_\Omega \Delta v(x,t)\,dx = \mu'(t) - \psi'(t) - \int_{\partial\Omega} \frac{\partial v}{\partial \nu}\,dS = f(t)|\Omega|,$$

and conclude that

$$f(t) = \frac{1}{|\Omega|}\left(\mu'(t) - \psi'(t) - \int_{\partial\Omega} \frac{\partial v}{\partial \nu}\,dS\right), \quad t \in [0,T). \tag{4.13}$$

Using (4.13), equations (4.9)–(4.12) become

$$\partial_t v(x,t) - \Delta v(x,t) = \frac{1}{|\Omega|}\left(\mu'(t) - \psi'(t) - \int_{\partial\Omega} \frac{\partial v}{\partial \nu}\,dS\right), \quad (x,t) \in \Omega \times (0,T), \tag{4.14}$$

$$v(x,0) = 0, \qquad x \in \Omega, \tag{4.15}$$

and

$$v(x,t) = 0, \qquad (x,t) \in \partial\Omega \times [0,T). \tag{4.16}$$

Since the term $\int_{\partial\Omega} \frac{\partial v}{\partial \nu}\,dS$ is not known, we apply perturbation analysis to the system (4.14)–(4.16). We interpret system (4.14)–(4.16) as the flow determined by a semigroup acting on

$L^2(\Omega)$. Let

$$D(A) = H_0^1(\Omega) \cap H^2(\Omega), \quad D(B) = H^2(\Omega),$$

and define

$$Av = \Delta v, \quad \text{if } v \in D(A), \tag{4.17}$$

and

$$Bv = -\frac{1}{|\Omega|} \int_{\partial\Omega} \frac{\partial v}{\partial \nu}\, dS, \quad \text{if } v \in D(B).$$

Therefore problem (4.14)–(4.16) can be written as

$$v'(t) = (A + B)v(t) + \frac{1}{|\Omega|}(\mu'(t) - \psi'(t)), \quad t \in (0, T), \tag{4.18}$$

and

$$v(0) = 0. \tag{4.19}$$

We will show that this inhomogeneous initial value problem has a unique solution v. This in turn will imply the existence and uniqueness of the solution (u, f) of the inverse source problem (4.1)–(4.4), where a representation of the source $f(t)$ is given by (4.13) and the existence and uniqueness of the function u is obtained from the decomposition $u = v + w$, where w is the solution of (4.5)–(4.7). We divide the proof into three steps.

1. We first show that A is a closed operator. Note that A and B are linear operators on $L^2(\Omega)$. Moreover, the domain $D(A)$ is dense in $L^2(\Omega)$. To show that A is closed, let $\{v_k\}_{k=1}^{\infty} \subset D(A)$ be a sequence such that

$$v_k \to v \quad \text{and} \quad Av_k \to h \quad \text{in } L^2(\Omega). \tag{4.20}$$

We must show that $v \in D(A)$ and $Av = h$. By using the H^2-regularity for the elliptic operator in (4.17) we have that [14, Theorem 4, p. 334]

$$||v_k - v_l||_{H^2(\Omega)} \leq C(\Omega)(||Av_k - Av_l||_{L^2(\Omega)} + ||v_k - v_l||_{L^2(\Omega)}) \quad \text{for all } k, l.$$

From (4.20), it follows that $\{v_k\}_{k=1}^{\infty}$ is a Cauchy sequence in $H^2(\Omega)$. The completeness of $H^2(\Omega)$ implies that $v_k \to v$ in $H^2(\Omega)$. Thus $v \in D(A)$ and $Av_k \to Av$ in $L^2(\Omega)$. Therefore $Av = h$.

2. Next, we will show that the operators A and $A + B$ are infinitesimal generators of analytic semigroups. To that end, let $\rho(A)$ denote the resolvent set of A and, for $0 < \delta < \frac{\pi}{2}$, define

$$\sum = \{\lambda \in \mathbb{C} : \, |\arg \lambda| < \pi/2 + \delta\} \cup \{0\}. \tag{4.21}$$

Using the result stated in [37, Theorem 5.2, p. 61] that a closed densely defined operator A with $0 \in \rho(A)$ generates an analytic semigroup if and only if there exist $0 < \delta < \frac{\pi}{2}$ and a number $M > 0$ such that $\rho(A) \supset \sum$ and $||(\lambda I - A)^{-1}|| \leq M/\lambda$ for $\lambda \in \sum$, $\lambda \neq 0$.

From the spectral theory for the operator A, it is known that $\rho(A) \supset \sum$. Consider

$$(\lambda I - A)v = h, \quad \text{for } h \in L^2(\Omega), \ \lambda \in \sum, \ \lambda \neq 0. \tag{4.22}$$

Multiplying this equation by v and integrating over Ω, we see that

$$\int_\Omega \lambda v^2 \, dx - \int_\Omega v \, \Delta v \, dx = \int_\Omega h \, v \, dx.$$

Using Green's theorem (in the second term) and Hölder's inequality we get that

$$\left| (\mathrm{Re}\lambda) \int_\Omega v^2 \, dx + i(\mathrm{Im}\lambda) \int_\Omega v^2 \, dx + \int_\Omega |\nabla v|^2 \, dx \right|^2 = \left| \int_\Omega h \, v \, dx \right|^2,$$

and

$$\left[(\mathrm{Re}\lambda)\int_\Omega v^2\,dx+\int_\Omega|\nabla v|^2\,dx\right]^2+\left[(\mathrm{Im}\lambda)\int_\Omega v^2\,dx\right]^2\le\|h\|^2\|v\|^2, \tag{4.23}$$

where $\mathrm{Re}z$ and $\mathrm{Im}z$ denote the real and imaginary parts of the complex number z. If $\mathrm{Re}\lambda\ge 0$ then

$$\left[(\mathrm{Re}\lambda)\int_\Omega v^2\,dx\right]^2\le\left[(\mathrm{Re}\lambda)\int_\Omega v^2\,dx+\int_\Omega|\nabla v|^2\,dx\right]^2.$$

Adding the above inequality to (4.23), we obtain that

$$|\lambda|^2\|v\|^4\le\|v\|^2\|h\|^2.$$

That is,

$$\|v\|\le\frac{1}{|\lambda|}\|h\|.$$

Since (4.22) implies that $\|v\|=\|(\lambda I-A)^{-1}h\|$, it follows that

$$\|(\lambda I-A)^{-1}h\|\le\frac{1}{|\lambda|}\|h\|.$$

This inequality holds for all $h\in L^2(\Omega)$. Hence

$$\|(\lambda I-A)^{-1}\|\le\frac{1}{|\lambda|}.$$

If $\mathrm{Re}\lambda<0$, we can find some $K>0$ such that

$$|\mathrm{Re}\lambda|\le K|\mathrm{Im}\lambda|. \tag{4.24}$$

As a consequence of (4.23),

$$|\mathrm{Im}\lambda|\|v\|^2\le\|v\|\|h\|.$$

Thus, using (4.24),

$$||v|| \leq \frac{\|h\|}{|\mathrm{Im}\lambda|} = \frac{\|h\|}{|\lambda|}\frac{|\mathrm{Re}\lambda|^2 + |\mathrm{Im}\lambda|^2}{|\mathrm{Im}\lambda|} \leq \frac{M\|h\|}{|\lambda|}.$$

Hence

$$||(\lambda I - A)^{-1}|| \leq \frac{M}{|\lambda|}.$$

This shows that A is the infinitesimal generator of an analytic semigroup.

Next, we show that $A+B$ is the infinitesimal generator of an analytic semigroup. From the definitions of $D(A)$ and $D(B)$ it is clear that $D(A) \subset D(B)$. Furthermore, for $v \in D(A)$, we have that

$$||Bv|| = \frac{1}{|\Omega|}\left\|\int_\Omega Av\,dx\right\| \leq \frac{1}{|\Omega|}\int_\Omega \|Av\|\,dx \leq ||Av||. \tag{4.25}$$

Since A generates an analytic semigroup, using [40, Theorem 12.37, p. 420], we conclude that $A + B$ is also an infinitesimal generator of an analytic semigroup.

3. We now show that the inhomogeneous initial value problem (4.18) has a unique solution v. Since analytic semigroups are strongly continuous semigroups (C_0 semigroups), $A + B$ is the infinitesimal generator of a C_0 semigroup $S(t)$.

The initial value problem

$$v'(t) = (A + B)v(t) \quad t \in (0, T), \tag{4.26}$$

and

$$v(0) = 0, \tag{4.27}$$

has a unique solution $S(t)v(0)$ on $[0, T)$ for every $v(0) \in D(A + B)$. We use
[37, Theorem 1.3, p. 102], which says that a densely defined linear operator with nonempty resolvent set is the infinitesimal generator of a C_0 semigroup if and only if for every initial data in the domain of the operator, the homogeneous initial value problem has a unique solution. Note that the resolvent set $\rho(A+B)$ of $A+B$ is nonempty since $\rho(A)$ is nonempty.

Moreover, the domain of $A+B$, $D(A+B)=D(A)$ is dense in $L^2(\Omega)$ since $D(A)$ is dense in that space. For $v(0)\in D(A+B)$, using the semigroup property, we have that

$$\begin{aligned}\lim_{s\to 0^+}\frac{S(s)S(t)v(0)-S(t)v(0)}{s} &= \lim_{s\to 0^+}\frac{S(t)S(s)v(0)-S(t)v(0)}{s}\\ &= S(t)\lim_{s\to 0^+}\frac{S(s)v(0)-v(0)}{s}\\ &= S(t)(A+B)v(0).\end{aligned}$$

Thus, $S(t)v(0)\in D(A+B)$ and $(A+B)S(t)v(0)=S(t)(A+B)v(0)$. Moreover, we have that

$$\frac{d}{dt}S(t)v(0)=(A+B)S(t)v(0)=S(t)(A+B)v(0).$$

Since $v(0)=0$, zero is the only solution of the initial value problem (4.26)–(4.27). Finally, we show that the initial value problem (4.18)–(4.19) has a unique solution v. This follows from [37, Corollary 3.3, p. 113], which states that if a linear operator is an infinitesimal generator of an analytic semigroup and the source function is locally Hölder continuous on $(0,T]$, then for every initial data in the space under consideration, the inhomogeneous initial value problem has a unique solution. First, note that $v(0)=0\in L^2(\Omega)$. Also, the source function $\dfrac{\mu'(t)-\psi'(t)}{|\Omega|}$ is Hölder continuous on $[0,T]$ since $\mu\in C^2[0,T]$ and $\psi\in C^\infty(0,T]$ using (4.8). See [14, Theorem 8, p. 59]. Moreover, if (4.18)–(4.19) has a solution v, then this solution is given by

$$v(t)=S(t)v(0)+\frac{1}{|\Omega|}\int_0^t S(t-s)(\mu'(s)-\psi'(s))\,ds=\frac{1}{|\Omega|}\int_0^t S(s)(\mu'(t-s)-\psi'(t-s))\,ds,$$

where $S(t)v(0)$ is the solution of the initial value problem (4.26)–(4.27). It follows that $v(t)$ is differentiable for $t > 0$ and its derivative

$$\begin{aligned} v'(t) &= \frac{1}{|\Omega|} S(t)(\mu'(0) - \psi'(0)) + \frac{1}{|\Omega|} \int_0^t S(s)(\mu''(t-s) - \psi''(t-s))\, ds \\ &= \frac{1}{|\Omega|} S(t)(\mu'(0) - \psi'(0)) + \frac{1}{|\Omega|} \int_0^t S(t-s)(\mu''(s) - \psi''(s))\, ds \end{aligned}$$

is continuous. The existence and uniqueness of (u, f) follows from the fact that $u = v + w$ and the representation (4.13) for the source function f. □

4.2 Alternative method for the uniqueness of classical solutions

While the semigroup methods provide the existence and uniqueness of solutions, we give an alternative proof of uniqueness of solutions of this problem. Using an energy argument, we now show that the inverse source problem (4.1)–(4.4) has a unique solution. The method used here is similar to the energy method employed to prove uniqueness of the weak solution in Section 3.3. The distinction is that the differentiation of the energy function is done using a differentiation rule, rather than applying Gronwall's inequality as in Section 3.3. The result is summarized as

Theorem 4.2. *Suppose Assumptions A1-A3 hold. Then the solution* (u, f) *in the sense of Definition 4.1 to the inverse source problem* (4.1)–(4.4) *is unique.*

Proof. Suppose that (u_1, f_1) and (u_2, f_2) are two distinct solutions to the inverse source problem (4.1)–(4.4). Let

$$u = u_1 - u_2 \quad \text{and} \quad f = f_1 - f_2. \tag{4.28}$$

Then the pair (u, f) satisfies

$$\partial_t u(x,t) - \Delta u(x,t) = f(t), \quad \text{in } \Omega \times (0,T], \tag{4.29}$$

$$u(x,t) = 0, \qquad \text{in } \partial\Omega \times (0,T], \tag{4.30}$$

$$u(x,0) = 0, \qquad \text{in } \Omega, \tag{4.31}$$

and

$$\int_\Omega u(x,t)\,dx = 0, \qquad \text{for all } t \in [0,T]. \tag{4.32}$$

Define

$$E(t) = \int_\Omega u^2(x,t)\,dx, \quad \text{for all} \quad 0 \le t \le T. \tag{4.33}$$

As a result of (4.31) and (4.33), we have that

$$E(t) \ge 0, \quad \text{for all} \quad 0 \le t \le T \quad \text{and} \quad E(0) = 0. \tag{4.34}$$

Differentiating (4.33) with respect to time and using (4.29) and (4.32) we get that

$$\begin{aligned} E'(t) &= \int_\Omega 2u(x,t)\partial_t u(x,t)\,dx \\ &= 2f(t)\int_\Omega u(x,t)\,dx + 2\int_\Omega u(x,t)\Delta u(x,t)\,dx \\ &= 2\int_\Omega u(x,t)\Delta u(x,t)\,dx. \end{aligned}$$

Integrating the last expression by parts and using (4.30) yields

$$E'(t) = -2\int_\Omega |\nabla u(x,t)|^2\,dx, \quad \text{for all} \quad 0 \le t \le T.$$

Thus,

$$E'(t) \le 0 \quad \text{for all} \quad 0 \le t \le T. \tag{4.35}$$

From (4.34) and (4.35), we get that $E(t) = 0$ for all $0 \leq t \leq T$. Substituting this in (4.33) implies that $u(x,t) = 0$ in $\overline{\Omega} \times [0,T]$. Consequently, using (4.29),

$$f(t) = 0 \quad \text{for all} \quad 0 \leq t \leq T.$$

Therefore, we conclude from (4.28) that

$$u_1 = u_2 \quad \text{and} \quad f_1 = f_2.$$

□

Chapter 5

Inverse source problem with a Neumann boundary condition

We consider the following system

$$\partial_t u(x,t) - c(t)\Delta u(x,t) = f(t), \qquad (x,t) \in \Omega \times (0,T], \tag{5.1}$$

$$\frac{\partial u}{\partial \nu}(x,t) = g(x,t), \quad (x,t) \in \partial\Omega \times [0,T], \tag{5.2}$$

$$u(x,0) = u_0(x), \quad x \in \Omega, \tag{5.3}$$

and

$$\int_\Omega u(x,t)\,dx = \mu(t), \qquad t \in [0,T], \tag{5.4}$$

where ν is the outward unit vector normal to the boundary $\partial\Omega$. The problem we solve is as follows: given the final time T, the diffusion coefficient $c : [0,T] \to (0,\infty)$, the initial data $u_0 : \Omega \to \mathbb{R}$, the Neumann boundary data $g : \partial\Omega \times [0,T] \to \mathbb{R}$, and the integral data $\mu : [0,T] \to \mathbb{R}$, find the time-dependent source function $f : [0,T] \to \mathbb{R}$ together with the concentration $u : \overline{\Omega} \times [0,T] \to \mathbb{R}$ satisfying (5.1)–(5.4). We first give a definition of a solution (u,f).

Definition 5.1. The couple (u,f) is a solution of (5.1)–(5.4) if:

1. The source $f(t)$ is continuous for $0 \le t \le T$.

2. The concentration $u(x,t)$ is continuous for $(x,t) \in \Omega \times [0,T)$.

3. The derivatives $\partial_t u$, ∇u, $\partial^2 u/\partial x_i \partial x_j$ exist and are continuous for $(x,t) \in \Omega \times (0,T)$, $1 \le i,j \le d$,

4. The equations in (5.1)–(5.4) are satisfied in the classical sense.

For a given source function $f(t)$, we denote by $u(x,t;f)$ the solution of the direct problem (5.1)–(5.3). We assume that the data satisfies the following hypotheses:

H1. The coefficient $c(t)$ is continuous for $0 \leq t \leq T$.

H2. The boundary condition $g(x,t)$ is continuous for $(x,t) \in \partial\Omega \times (0,T)$.

H3. The initial data u_0 is of class $C^2(\Omega)$.

H4. The integral condition μ is of class $C^1[0,T]$.

The following existence and uniqueness result for the inverse source problem (5.1)–(5.4) holds.

Theorem 5.1. *Suppose Hypotheses H1-H4 hold. Then the inverse source problem* (5.1)–(5.4) *has a unique solution* (u,f) *in the sense of Definition 5.1.*

Proof. We use the transformation

$$v(x,t) = u(x,t;f) - \int_0^t f(\tau)\, d\tau, \tag{5.5}$$

to homogenize equation (5.1) and use the data (5.4) to recover u and f. To that end, differentiate the terms in (5.5) with respect to time t to get,

$\partial_t v(x,t) = \partial_t u(x,t;f) - f(t)$ and apply the Laplace operator to get $\Delta v(x,t) = \Delta u(x,t;f)$.

Thus, v is a solution of the direct problem

$$\partial_t v(x,t) - c(t)\Delta v(x,t) = 0, \qquad (x,t) \in \Omega \times (0,T], \tag{5.6}$$

$$\frac{\partial v}{\partial \nu}(x,t) = g(x,t), \quad (x,t) \in \partial\Omega \times [0,T], \tag{5.7}$$

and

$$v(x,0) = u_0(x), \quad x \in \Omega. \tag{5.8}$$

It is well known that problem (5.6)–(5.8) has a unique solution v. Integrating the terms in (5.5) over Ω we have that

$$\int_\Omega v(x,t)\,dx = \int_\Omega u(x,t;f)\,dx - |\Omega| \int_0^t f(\tau)\,d\tau = \mu(t) - |\Omega| \int_0^t f(\tau)\,d\tau.$$

Thus,

$$\int_0^t f(\tau)\,d\tau = \frac{1}{|\Omega|}\left(\mu(t) - \int_\Omega v(x,t)\,dx\right). \tag{5.9}$$

Differentiating the terms in the above equation with respect to time yields

$$f(t) = \frac{1}{|\Omega|}\left(\mu'(t) - \int_\Omega \partial_t v(x,t)\,dx\right). \tag{5.10}$$

Using (5.9) and the transformation (5.5), we have that

$$u(x,t) = v(x,t) + \frac{1}{|\Omega|}\left(\mu(t) - \int_\Omega v(x,t)\,dx\right), \tag{5.11}$$

where v is the solution to the direct problem (5.6)–(5.8). □

Chapter 6

Discussion, future work, and conclusion

In this chapter, we summarize the work carried out throughout this dissertation and outline some possible future work. We considered an inverse diffusion coefficient problem subject to an integral constraint and the corresponding direct problem for a parabolic partial differential equation. Moreover, we investigated an inverse source problem for a parabolic equation with an integral constraint.

The direct problem describes a phenomenon in geochronology, in which the dating of minerals is of significant interest. We have developed a numerical implementation of a 2-D model using the finite element method to describe argon diffusion in mica crystals at the grain scale for crystals of arbitrary shape with the assumption of (isotropic) diffusion within the layers and no diffusion between them. Although we focused on $^{40}\mathrm{Ar}/^{39}\mathrm{Ar}$ ages in micas, the results could be used for diffusion in any mineral at the scale of single crystals. Our model is based on *in situ* laser measurements of diffusion gradients in the plane of diffusion that form in micas in nature. We presented some examples of mica crystals with *in situ* $^{40}\mathrm{Ar}/^{39}\mathrm{Ar}$ age distribution and geometries described in the geology literature. Compared to analytical and numerical techniques for this problem found in the geological literature, our model provides a better fit for describing the actual, natural systems than previous models. The better fit is due to modeling the entire age distribution within a 2-D geometry that describes the natural shape more closely. Our 2-D modeling shows the promise for future investigation of diffusion parameters for micas and points to the ability to inform strategies for direct laboratory measurements of intracrystalline age gradients. In this work, we prescribed the Dirichlet and Neumann boundary conditions for the examples we presented, however, the model also allows the specification of a *mixed* or *Robin boundary condition*. One of the key assumptions

in this study is that the diffusion coefficient is spatially homogeneous. A possible future work may be to consider the case of spatially heterogeneous diffusion coefficient. With such heterogeneity, we can model fast diffusion pathways in crystals. Heterogeneous diffusion coefficients could be expected in mixed phases or lattice structures with zones of high defect concentration, as would occur in exsolved or altered K-feldspars. Another direction for future work might be to expand the 2-D geometries to 3-D geometries that allow modeling for such crystals as feldspars and biotites.

We showed the existence and uniqueness of classical solutions to the inverse diffusion coefficient problem using fixed point theory. In the context of geochronology, this problem amounts to reconstructing the temperature history of rocks. Moreover, we proved the existence of weak and classical solutions to the inverse source problem with the Dirichlet boundary condition using the Rothe method and the semigroup theory, respectively. While the semigroup method yielded uniqueness, we also proved uniqueness using an energy method. Furthermore, we established the existence and uniqueness of the inverse source problem with a Neumann boundary condition via a certain transformation.

For both the inverse source problem subject to the Dirichlet boundary condition and the inverse diffusion coefficient problem, we developed and implemented numerical algorithms to approximate their solutions. From model problems, we calculated the errors and reported the rates of convergence, which we estimated using the linear regression. These rates are consistent with the standard parabolic error estimates. The numerical results we presented show the accuracy of our schemes.

We mention that our proof of uniqueness of solutions to the inverse source problem with the Dirichlet boundary condition can be extended to prove uniqueness of solutions to

non-linear problems of the form

$$\partial_t u(x,t) - \Delta u(x,t) + h(x,t,u) = f(t), \quad (x,t) \in \Omega \times (0,T], \tag{6.1}$$

$$u(x,0) = 0, \quad x \in \Omega, \tag{6.2}$$

$$u(x,t) = 0, \quad (x,t) \in \partial\Omega \times [0,T], \tag{6.3}$$

and

$$\int_\Omega u(x,t)\,dx = \mu(t), \quad t \in (0,T]. \tag{6.4}$$

Specifically, we have, under the assumption that h is Lipschitz continuous with respect to u, a weak solution (u,f) to the inverse problem (6.1)–(6.4) where $f \in L^2(0,T)$ and $u \in L^2(0,T;H_0^1(\Omega))$ with $\partial_t u \in L^2(0,T;H^{-1}(\Omega))$ is unique. It is expected that the proof will follow by mimicking the argument in Section 3.3. However, the existence of this problem using the Rothe method as in Chapter 3 is not easily extendable. In particular, we have not been able to obtain an estimate for the source as in Lemma 3.2 using the eigenfunction expansion.

While this dissertation is focused on the applications of the integral overdetermination in geology, we note that inverse problems with integral overdetermination are widely used in science and engineering. Another physical interpretation of the integral overdetermination arises in measuring a physical parameter by a sensor. Any sensor, due to its finite size, always performs some averaging of measured quantities. In the context of system (1.2)–(1.4), the function u is measured by a sensor making some averaging over the domain Ω. From a mathematical point of view, the results of such measurements can be interpreted as integral data. See for instance, the book by Prilepko, Orlovsky, and Vasin [38, p. 60] for more details. The results of this dissertation could then be applied to any application where the integral data arises. Specifically, if we are given the data $\mu(t)$ for all time t, then we can use the algorithms in Chapters 2 and 3 to recover the unknown functions.

Below are several directions that we are interested in pursuing for future work.

- Develop a numerical scheme that takes into account the spatial dependence of the source function for the diffusion coefficient problem. This generalization is relevant, for example, when potassium has a non-constant initial concentration.

- Approximate solutions for a non-constant boundary condition.

- Perform rigorous error analysis and stability analysis for the two schemes introduced in this dissertation.

- Find solutions of the inverse source problem with a source depending on both the space variable and time. The case of multiplicative source, for example, could be considered in the equation $\partial_t u(x,t) - \Delta u(x,t) = f(t)h(x)$ subject to initial and boundary conditions together with an integral constraint of the form (6.4), where $h(x)$ is known and $f(t)$ is to be determined.

- Investigate numerical solutions to the inverse source problem with a Neumann boundary condition including error analysis and stability analysis.

- Study the regularity of solutions of the two inverse problems. As an illustration for the inverse diffusion coefficient problem, note that, using the fixed point method in Chapter 2, we obtained that the coefficient $c \in C[0,T]$ and the concentration $u \in C_1^2(\Omega \times [0,T])$. Formally, since

$$c(t) = \frac{\mu'(t) - \int_\Omega f(x,t)\,dx}{\int_\Omega \Delta u(x,t)\,dx},$$

we get by differentiation that

$$c'(t) = \frac{\left[\mu''(t) - \int_\Omega \partial_t f(x,t)\,dx\right] \int_\Omega \Delta u(x,t)\,dx - I}{\left(\int_\Omega \Delta u(x,t)\,dx\right)^2}, \tag{6.5}$$

where

$$I = \left[\mu'(t) - \int_\Omega f(x,t)\,dx\right] \int_\Omega \partial_t(\Delta u(x,t))\,dx.$$

If we assume that $\mu \in C^2[0,T]$ and $f \in C^1[0,T]$ for all $x \in \Omega$, then in addition to the assumptions on the data in Chapter 2 and $\Delta u \in C^1[0,T]$ for all $x \in \Omega$, we have that $c \in C^1[0,T]$ and $u \in C^2[0,T]$ for all $x \in \Omega$. We note that the regularity of Δu and the regularity of u, as stated above, follow by the corresponding regularity of f, just as in the proof of Lemma 2.1, namely by decomposing the system into two problems. The representation (6.5) suggests that f and c on one hand, u and μ on the other hand have the same regularity in the time variable. We anticipate that this observation could be generalized. Our conjecture is as follows: *in addition to the assumptions on the data in Chapter 2, suppose $\mu \in C^k[0,T]$ and $f \in C^{k-1}[0,T]$ for all $x \in \Omega$, then we expect that $c \in C^{k-1}[0,T]$ and $u \in C^k[0,T]$ for all $x \in \Omega$ and for any integer $k \geq 1$.*

Another important problem to consider is to recover a diffusion coefficient that depends only on the space variable. That is, find c and u in the problem

$$\partial_t u(x,t) - c(x)\Delta u(x,t) = f(x,t), \quad \text{for all } (x,t) \in \Omega \times (0,T),$$

subject to an initial data u_0 and some Dirichlet boundary condition. To solve this problem, we assume that the final overdetermination is given, that is, we know the solution of the direct problem at the final time. Namely,

$$u(x,T) = E(x), \quad \text{for all } x \in \Omega, \tag{6.6}$$

where E is a given function defined on Ω. Following the idea of Chapter 2, to account for the overdetermination condition (6.6), we define a map

$$\mathcal{T} : c \mapsto \frac{E(x) - u_0(x) - \int_0^T f(x,t)\,dt}{\int_0^T \Delta u(x,t;c)\,dt}, \tag{6.7}$$

and show that *the mapping $\mathcal{T}$ given by* (6.7) *has a fixed point c if and only if the overdetermination condition* (6.6) *is satisfied for that function c.* Therefore if we show that the mapping

$\mathcal{T}$ has a fixed point, we will prove the existence (and uniqueness) of this problem. In order to apply the Banach fixed point method to show that the mapping $\mathcal{T}$ is a contraction, we form the following difference for coefficients c_1 and c_2 as in Chapter 2:

$$\mathcal{T}[c_1] - \mathcal{T}[c_2] = \frac{\left(\int_0^T \Delta u(x,t;c_2) - \Delta u(x,t;c_1)\,dt\right)\left(E(x) - u_0(x) - \int_0^T f(x,t)\,dt\right)}{\int_0^T \Delta u(x,t;c_2)\,dt \int_0^T \Delta u(x,t;c_1)\,dt}. \quad (6.8)$$

We note that to handle the term similar to $\int_0^T \Delta u(x,t;c_2) - \Delta u(x,t;c_1)\,dt$ in Chapter 2, we used the Green representation formula for the system (2.5)–(2.7), which we obtain from the original system (2.1)–(2.3) by a transformation of the time variable that transferred the time-dependent coefficient to the source. However, in the case when the coefficient depends only on the space variable, the transformation is not obvious. The other terms in (6.8) could be taken care of with arguments similar to those in Chapter 2. A possible alternative approach to this problem is via Carleman estimates, as considered in the book by Klibanov and Timonov [32] about inverse coefficient problems, with coefficients depending on the space variable.

Finally, inverse problems are almost always ill-posed. In real life applications, the data contains noise. One possibility for future work is to add noise to the numerical data and use regularization techniques to stabilize the numerical approximations.

Appendices

Appendix A

Estimates of the fundamental solution for the heat equation

Following [15], we recall and derive some estimates for the fundamental solution (and hence, for the Green function). These estimates are used in Section 2.3. Let

$$w(x,t;\xi,\tau) = (t-\tau)^{-d/2} \exp\left[-\frac{|x-\xi|^2}{4(t-\tau)}\right],$$

and

$$Z(x,t;\xi,\tau) = (2\sqrt{\pi})^{-d} w(x,t;\xi,\tau).$$

Given f, consider the volume potential $V(x,t)$ defined by

$$V(x,t) = \int_0^t \int_\Omega Z(x,t;\xi,\tau) f(\xi,\tau)\, d\xi\, d\tau.$$

Note that

$$\lim_{\tau \to t} \int_\Omega Z(x,t;\xi,\tau) f(\xi,\tau)\, d\xi = f(x,t)$$

and that the volume potential is an improper integral since the integrand has a singularity at $x=\xi$, $t=\tau$. However, the singularity is integrable. To see that, we write w in the form

$$w(x,t;\xi,\tau) = (t-\tau)^{-\gamma} (|x-\xi|^2)^{\gamma - d/2} \left[\frac{|x-\xi|^2}{t-\tau}\right]^{d/2-\gamma} \exp\left[-\frac{|x-\xi|^2}{4(t-\tau)}\right].$$

Then,

$$\begin{aligned} |w(x,t;\xi,\tau)| &= \frac{1}{(t-\tau)^\gamma |x-\xi|^{d-2\gamma}} \left[\frac{|x-\xi|^2}{t-\tau}\right]^{d/2-\gamma} \exp\left[-\frac{|x-\xi|^2}{4(t-\tau)}\right] \\ &\leq \frac{C}{(t-\tau)^\gamma |x-\xi|^{d-2\gamma}}, \quad 0 < \gamma < 1, \end{aligned} \tag{A.1}$$

where the last inequality follows from the bound $s^m e^{-\epsilon s} \leq C$, with $s = \dfrac{|x-\xi|^2}{t-\tau}$, $m = d/2-\gamma$, $\epsilon = 1/4$, and C depends only on m and ϵ. Thus, $C = C(d,\gamma)$. Similarly

$$\frac{\partial}{\partial x_i} w(x,t;\xi,\tau) = (t-\tau)^{-d/2} \left(\frac{-2(x_i-\xi_i)}{4(t-\tau)} \right) \exp\left[-\frac{|x-\xi|^2}{4(t-\tau)} \right]$$

and therefore

$$\begin{aligned}
\left| \frac{\partial}{\partial x_i} w(x,t;\xi,\tau) \right| &= (t-\tau)^{-d/2-1} \left| \frac{(x_i-\xi_i)}{2} \right| \exp\left[-\frac{|x-\xi|^2}{4(t-\tau)} \right] \\
&= \frac{|(x_i-\xi_i)|}{2(t-\tau)^{\gamma}} \left(|x-\xi|^2 \right)^{\gamma-d/2-1} \left[\frac{|x-\xi|^2}{t-\tau} \right]^{d/2+1-\gamma} \exp\left[-\frac{|x-\xi|^2}{4(t-\tau)} \right] \\
&\leq \frac{C}{(t-\tau)^{\gamma}|x-\xi|^{d+1-2\gamma}}, \quad \frac{1}{2} < \gamma < 1.
\end{aligned}$$

In a similar fashion, we obtain that

$$\frac{\partial^2 w(x,t;\xi,\tau)}{\partial x_i^2} = (t-\tau)^{-d/2} \left(-\frac{1}{2(t-\tau)} + \frac{(xi-\xi_i)^2}{4(t-\tau)^2} \right) \exp\left[-\frac{|x-\xi|^2}{4(t-\tau)} \right], \tag{A.2}$$

and hence

$$\left| \frac{\partial^2 w(x,t;\xi,\tau)}{\partial x_i^2} \right| \leq \frac{C}{(t-\tau)^{\gamma}|x-\xi|^{d+2-2\gamma}}. \tag{A.3}$$

Let

$$J(x,t,\tau) = \int_{\Omega} Z(x,t;\xi,\tau) f(\xi,\tau)\, d\xi,$$

then

$$V(x,t) = \int_0^t J(x,t,\tau)\, d\tau.$$

To estimate the second order derivative of J assume that $f(x,t)$ is a continuous function on $\Omega \times [0,T]$ and locally Hölder continuous in $x \in \Omega$ with exponent β, uniformly with respect to t. For a second order parabolic operator in general form, see [15, Theorems 3-4, p. 8-12].

Using [15, Theorem 3, p. 8] we have that

$$\frac{\partial V(x,t)}{\partial x_i} = \int_0^t \frac{\partial J(x,t,\tau)}{\partial x_i}\, d\tau.$$

We write $\partial J(x,t,\tau)/\partial x_i$ in the form

$$\frac{\partial J(x,t,\tau)}{\partial x_i} = f(y,\tau)\int_\Omega \frac{\partial}{\partial x_i} w(x,t;\xi,\tau)\, d\xi + \int_\Omega \frac{\partial}{\partial x_i} Z(x,t;\xi,\tau)[f(\xi,\tau) - f(y,\tau)]\, d\xi,$$

where y is a fixed point. Let B be a fixed ball in Ω. We have that

$$\begin{aligned}\int_\Omega \frac{\partial}{\partial x_i} w(x,t;\xi,\tau)\, d\xi &= \int_B \frac{\partial}{\partial x_i} w(x,t;\xi,\tau)\, d\xi + \int_{\Omega\setminus B} \frac{\partial}{\partial x_i} w(x,t;\xi,\tau)\, d\xi \\ &= \int_{\partial B} w(x,t;\eta,\tau)\cos(\nu,\eta_i)\, dS_\eta + \int_{\Omega\setminus B} \frac{\partial}{\partial x_i} w(x,t;\xi,\tau)\, d\xi,\end{aligned}$$

where ν is the outward pointing normal to ∂B. Thus,

$$\begin{aligned}\frac{\partial J(x,t,\tau)}{\partial x_i} &= f(y,\tau)\left[\int_{\partial B} w(x,t;\eta,\tau)\cos(\nu,\eta_i)\, dS_\eta + \int_{\Omega\setminus B} \frac{\partial}{\partial x_i} w(x,t;\xi,\tau)\, d\xi\right] \\ &\quad + \int_\Omega \frac{\partial}{\partial x_i} Z(x,t;\xi,\tau)[f(\xi,\tau) - f(y,\tau)]\, d\xi.\end{aligned}$$

Differentiating the terms in the equation above with respect to x_i, we obtain that

$$\begin{aligned}\frac{\partial^2 J(x,t,\tau)}{\partial x_i^2} &= f(y,\tau)\left[\int_{\partial B} \frac{\partial}{\partial x_i} w(x,t;\eta,\tau)\cos(\nu,\eta_i)\, dS_\eta + \int_{\Omega\setminus B} \frac{\partial^2}{\partial x_i^2} w(x,t;\xi,\tau)\, d\xi\right] \\ &\quad + \int_\Omega \frac{\partial^2}{\partial x_i^2} Z(x,t;\xi,\tau)[f(\xi,\tau) - f(y,\tau)]\, d\xi.\end{aligned}$$

We choose $y = x$ and get that

$$\begin{aligned}\frac{\partial^2 J(x,t,\tau)}{\partial x_i^2} &= f(x,\tau)\int_{\partial B} \frac{\partial}{\partial x_i} w(x,t;\eta,\tau)\cos(\nu,\eta_i)\, dS_\eta \\ &\quad + f(x,\tau)\int_{\Omega\setminus B} \frac{\partial^2}{\partial x_i^2} w(x,t;\xi,\tau)\, d\xi + \int_\Omega \frac{\partial^2}{\partial x_i^2} Z(x,t;\xi,\tau)[f(\xi,\tau) - f(x,\tau)]\, d\xi. \quad \text{(A.4)}\end{aligned}$$

Let x be a fixed point in the interior of B. Then each of the first two integrals in (A.4) is a bounded function of t and τ. Using (A.3) and the fact that f is locally Holder continuous in $x \in \Omega$, uniformly with respect to t, we obtain that

$$\begin{aligned}\left| \int_\Omega \frac{\partial^2}{\partial x_i^2} Z(x,t;\xi,\tau)[f(\xi,\tau) - f(x,\tau)]\, d\xi \right| &\leq \frac{C}{(t-\tau)^\gamma} \int_\Omega \frac{d\xi}{|x-\xi|^{d+2-2\gamma-\beta}} \\ &\leq \frac{C}{(t-\tau)^\gamma},\end{aligned}$$

if $1 - (\beta/2) < \gamma < 1$, and the constant C is independent of (x,t,τ) provided that x is restricted to a closed subset of Ω. From (A.4), we conclude that

$$\left| \frac{\partial^2 J(x,t,\tau)}{\partial x_i^2} \right| \leq \frac{C}{(t-\tau)^\gamma}, \quad 1 - (\beta/2) < \gamma < 1.$$

That is,

$$\left| \int_\Omega \frac{\partial^2}{\partial x_i^2} Z(x,t;\xi,\tau) f(\xi,\tau)\, d\xi \right| \leq \frac{C}{(t-\tau)^\gamma}, \quad 1 - (\beta/2) < \gamma < 1. \tag{A.5}$$

Finally, we derive an estimate for $\partial_\tau \Delta_x w(x,t;\xi,\tau)$. From (A.2), we get that

$$\Delta_x w(x,t;\xi,\tau) = (t-\tau)^{-d/2} \left(-\frac{d}{2(t-\tau)} + \frac{|x-\xi|^2}{4(t-\tau)^2} \right) \exp\left[-\frac{|x-\xi|^2}{4(t-\tau)} \right],$$

and thus,

$$\begin{aligned}\partial_\tau \Delta_x w(x,t;\xi,\tau) = &\frac{d}{2}(d/2+1)(t-\tau)^{-d/2-2} \exp\left[-\frac{|x-\xi|^2}{4(t-\tau)} \right] \\ &- \frac{d}{2}|x-\xi|^2 (t-\tau)^{-d/2-3} \exp\left[-\frac{|x-\xi|^2}{4(t-\tau)} \right] \\ &+ \frac{1}{4}(-d/2-2)(t-\tau)^{-d/2-3} \exp\left[-\frac{|x-\xi|^2}{4(t-\tau)} \right] \\ &+ \frac{1}{16}|x-\xi|^4 (t-\tau)^{-d/2-4} \exp\left[-\frac{|x-\xi|^2}{4(t-\tau)} \right].\end{aligned}$$

Using a decomposition as in (A.1), each of the four terms on the right-hand side of the equation above is bounded by

$$\frac{C(d)}{(t-\tau)^{\gamma}|x-\xi|^{d+4-2\gamma}},$$

with different values of the constant $C(d)$. To see that, we illustrate the process by estimating the fourth term $F := \frac{1}{16}|x-\xi|^4(t-\tau)^{-d/2-4}\exp\left[-\frac{|x-\xi|^2}{4(t-\tau)}\right]$ as follows:

$$\begin{aligned} F &= \frac{|x-\xi|^4}{16(t-\tau)^{\gamma}}\left[\frac{|x-\xi|^2}{t-\tau}\right]^{d/2+4-\gamma}(|x-\xi|^2)^{-d/2-4+\gamma}\exp\left[-\frac{|x-\xi|^2}{4(t-\tau)}\right] \\ &\leq \frac{C(d)\,|x-\xi|^4}{16(t-\tau)^{\gamma}}|x-\xi|^{-d-8+2\gamma} \\ &\leq \frac{C(d)}{(t-\tau)^{\gamma}|x-\xi|^{d+4-2\gamma}}. \end{aligned}$$

Consequently,

$$|\partial_{\tau}\Delta_x w(x,t;\xi,\tau)| \leq \frac{C(d)}{(t-\tau)^{\gamma}|x-\xi|^{d+4-2\gamma}}.$$

Appendix B

Matlab code for the inverse source problem

We present MATLAB code for the main program computing the approximate solutions of the inverse source problem in Chapter 3. We refer to Section 3.4 for an outline of the algorithm. For an illustration of the program output, we plot the exact and approximate exponential source functions in Figure B.1.

Listing B.1: Main program.

```
function [p,e,t,tlist,u_exact,u_approx,source_exact, source_approx, L2u_error, ...
                    sourceL2_error] = inverseSource(N,hmax,T)
% This file shows how to solve the inverse source problem 'ut - laplace(u) = f(t)' subjects
% to zero initial and zero Dirichlet boundary conditions on the domain 'Omega x [0,T]' where
% 'Omega' is a 2D spatial domain implemented in the file 'geometryInverseSource.m'. The mesh
% is discribed by 'p' (matrix of points), 'e'(matrix of edges) and 't'(matrix of triangles).
% 'T' is the final time. 'Hmax' is the max mesh size. 'N' is the total number of time steps.

% Call the geometry considered to solve the PDE
[dl,numberOfEdges] =geometryInverseSource();

% Boundary Condition vector 'dirichletBC' for each edge: MATLAB employs the Dirichlet
% boundary condition h*u = r, and the Generalized boundary conditions
% n\cdot(c*\nabla u) + q*u = g. In our case, u = 0 on the boundary, h = 1, r = q = g = 0.
r = '0';
dirichletBC = [1 1 1 1 1 length(r) '0' '0' '1' r]';
% The first row of dirichletBC represents the number of PDE; the second row contains the
% number of Dirichlet boundary condition; the third row contains the length for the strings
% representing q; the fourth row contains the length for the springs representing g; the
% fifth row contains the length for the strings representing h; the sixth row contains the
% length for the strings representing r. The following rows contain text expressions
% representing the actual boundary conditions for q, g, h, r, respectively.
% b: boundary Condition matrix that represents all of the boundary segments
b = repmat(dirichletBC,1,numberOfEdges);

% 'initmesh' generates a mesh on the domain 'Omega'
```

```
[p,e,t] = initmesh(dl,'Hmax',hmax);
% 'tau' is the time step for the discretization. 'tlist' contains the times at which the
% parabolic solution is computed. 'u0' is the initial condition
tau = T/N; tlist = 0:tau:T;  u0=zeros(size(p,2),1);

% Define coefficients for the PDE 'ut - laplace(u) = f(t)'.
a = 0; c = 1; d = 1; f = @source;

% 'parabolic' solves a parabolic problem. 'u_exact' is the solution of the continuous PDE
u_exact = parabolic(u0,tlist,b,p,e,t,c,a,f,d);

% Interpolate the solution u_exact from node data to triangle midpoints data
u_interp = pdeintrp(p,t,u_exact);

% Compute the area of each triangle in the mesh. 'pdetrg' returns the area of each triangle.
area = pdetrg(p,t);

% Find mu(t), the integral of the solution over the spatial domain 'Omega'.
mu = zeros(1,N+1);  % Allocate mu
for k = 1:N+1
    mu(k) = dot(area,u_interp(k,:));
end

% 'source_exact' is the known source supplied to solve the direct problem
source_exact = source(p,t,u_exact,tlist);

% Define the PDE coefficients for 'u_tilde - tau*laplace(u_tilde) = tau'
c = tau; a = 1; f =  tau;
% 'assempde' assembles stiffness matrix K, the mass matrix M and right side F of PDE
% problem. Q, G, H and R are contributions from the boundary
[K,M,F,Q,G,H,R] = assempde(b,p,e,t,c,a,f);
u_tilde = assempde(K,M,F,Q,G,H,R);

% Interpolate the solution u_tilde from node data to triangle midpoint data
u_tilde_interp = pdeintrp(p,t,u_tilde);

% Find the integral of the solution u_tilde
mu_tilde = dot(area,u_tilde_interp);

% u_hat is the solution of the auxiliary problem 'u_hat^k - tau*Laplace(u_hat^k) = u^{k-1}'
% 'mu_hat' is the integral of 'u_hat^k'
```

```
u_hat = zeros(size(p,2),N+1);
u_hat_interp = pdeintrp(p,t,u_hat);
mu_hat = zeros(1,N+1);

% u_approx is the approximate PDE solution from the scheme
% 'source_approx' is the approximate source term obtained from the scheme
u_approx = zeros(size(p,2),N+1);
source_approx = zeros(1,N+1);

% Calculate the approximate solutions
for k = 1:N
    F = source_approx(k)*M*u_tilde + M*u_hat(:,k);
    u_hat(:,k+1) = assempde(K,M,F,Q,G,H,R);
    u_hat_interp(k+1,:) = pdeintrp(p,t,u_hat(:,k+1));
    mu_hat(k+1) = dot(area,u_hat_interp(k+1,:));
    source_approx(k+1) = (mu(k+1) - mu_hat(k+1))/mu_tilde;
    u_approx(:,k+1) = source_approx(k+1)*u_tilde + u_hat(:,k+1);
end

% Compute the L2 error in u_exact
u_approx_interp = pdeintrp(p,t,u_approx);
u_error = u_interp - u_approx_interp;
L2u_error_square = zeros(1,N+1);
for k=1:N+1
    L2u_error_square(k) = dot(area,(abs(u_error(k,:))).^2);
end
L2u_error = sqrt(trapz(tlist,L2u_error_square));

% Error in the source source_exact
source_difference = source_approx - source_exact;
source_difference_square = (abs(source_difference)).^2;
% 'trapz' returns the approximate integral via the trapezoidal method
source_error_square = trapz(tlist,source_difference_square);
sourceL2_error = sqrt(source_error_square);

% Write the source function as a nested function: here we use an exponential function
    function S = source(p,t,u0,time)
        S = exp(log(5)*time) - 1;
    end
end
```

Listing B.2: Geometry file.

```
function [dl,numberOfEdges] = geometryInverseSource()

% x-coordinates of vertices of the polygon in mm
X =[.201 1.871 4.893 5.757 6.909 7.139 6.477 6.001 5.469 5.268 2.678 2.203 1.583 .737 0];

% y-coordinates of vertices of the polygon in mm
Y =[.000 .139 .000 .083 .139 1.225 2.088 2.562 3.063 4.417 4.029 2.562 2.133 1.866 .250];

% Number of line segments on the boundary of the polygon
numberOfEdges = size(X,2);

% Code for generating the polygon: row 1 contains 2, which is the number code for polygon.
% Row 2 contains the number 'numberOfEdges' of line segments on the
% boundary of the polygon. The next 'numberOfEdges' rows contain the
% x-coordinates of vertices. The next
% 'numberOfEdges' rows contain the y-coordinates vertices
polygon = [ 2 numberOfEdges X Y]';
% 'decsg' analyzes the Constructive Solid Geometry model drawn and
% constructs a set of disjoint minimal regions, bounded by boundary
% segments and border segments...
dl = decsg(polygon);
end
```

Listing B.3: Demonstration file.

```
% This program computes approximate solutions of the inverse source problem.
% We only plot the exact and approximate exponential sources. The main
% function is implemented in "inverseSource.m", which calls the domain implemented in
% "geometryInverseSource.m".
close all
hmax = 0.05; N = 50; T = 1;
[p,e,t,tlist,u_exact,u_approx,source_exact, source_approx, ...
                                    L2u_error,sourceL2_error] = inverseSource(N,hmax,T);
figure;
plot(tlist,source_exact,'b-',tlist,source_approx,'r--')
legend('Exact source','Approx source','Location','north')
xlabel('time')
ylabel('Source functions')
```

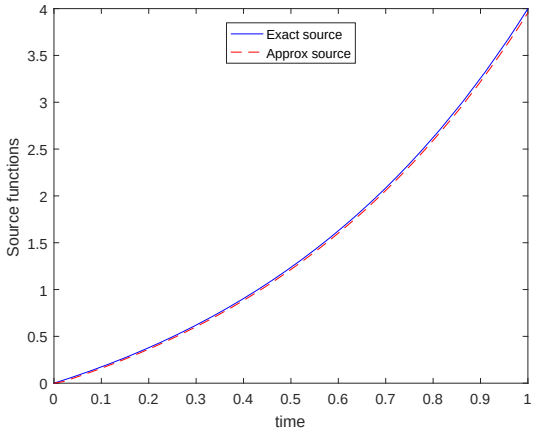

Figure B.1: Output of the program: approximation of the source $f(t) = 5^t - 1$.

Bibliography

[1] Herbert Amann. Fixed point equations and nonlinear eigenvalue problems in ordered banach spaces. *SIAM review*, 18(4):620–709, 1976.

[2] Uri M. Ascher and Chen Greif. *A First Course in Numerical Methods*. SIAM, Computational Science and Engineering, 2011.

[3] Dietrich Braess. *Finite elements: theory, fast solvers, and applications in solid mechanics*. Cambridge University Press, 2007.

[4] Haim Brezis. *Functional analysis, Sobolev spaces and partial differential equations*. Springer, 2010.

[5] John R. Cannon and William Rundell. Recovering a time dependent coefficient in a parabolic differential equation. *Journal of Mathematical Analysis and Applications*, 160(2):572–582, 1991.

[6] Yanzhao Cao, Max Gunzburger, and James Turner. The controllability of systems governed by parabolic differential equations. *Journal of Mathematical Analysis and Applications*, 215(1):174–189, 1997.

[7] Mourad Choulli. *Une introduction aux problèmes inverses elliptiques et paraboliques*. Mathématiques et Applications 65. Springer, 2009.

[8] Philippe G. Ciarlet. *The finite element method for elliptic problems*. Classics in Applied Mathematics 40. SIAM, 2002.

[9] John Crank. *The mathematics of diffusion*. Clarendon Press, 2nd edition, 1975.

[10] Mehdi Dehghan. Fully explicit finite-difference methods for two-dimensional diffusion with an integral condition. *Nonlinear Analysis: Theory, Methods and Applications*, 48(5):637–650, 2002.

[11] Martin H. Dodson. Closure temperature in cooling geochronological and petrological systems. *Contributions to Mineralogy and Petrology*, 40(3):259–274, 1973.

[12] Dean G. Duffy. *Green's Functions with Applications*. Studies in Advanced Mathematics. CRC Press, 2001.

[13] J. Dykstra Eusden and Daniel R. Lux. Slow late paleozoic exhumation in the presidential range of New Hampshire as determined by the $^{40}Ar/^{39}Ar$ relief method. *Geology*, 22(10):909–912, 1994.

[14] Lawrence C. Evans. *Partial differential equations*. American Mathematical Society, 2nd edition, 2010.

[15] Avner Friedman. *Partial differential equations of parabolic type*. Courier Dover Publications, 2008.

[16] David Gilbarg and Neil S. Trudinger. *Elliptic partial differential equations of second order*. Springer, revised third printing edition, 1998.

[17] E. Ginder. Construction of solutions to heat-type problems with time-dependent volume constraints. *Advances in Mathematical Sciences and Applications*, 20(2):467–482, 2010.

[18] Dmitry Glotov, Willis E. Hames, A. J. Meir, and Sedar Ngoma. An integral constrained parabolic problem with applications in thermochronology. *Computers and Mathematics with Applications*, 71(11):2301–2312, 2016.

[19] Dmitry Glotov, Willis E. Hames, A. J. Meir, and Sedar Ngoma. An inverse diffusion coefficient problem for a parabolic equation with integral constraint. *International Journal of Numerical Analysis and Modeling*, accepted, 2017.

[20] Mark S. Gockenbach. *Understanding and implementing the finite element method*. SIAM, 2006.

[21] W. E. Hames and S. A. Bowring. An empirical evaluation of the argon diffusion geometry in muscovite. *Earth and Planetary Science Letters*, 124(1-4):161–169, 1994.

[22] W. E. Hames and K. V. Hodges. Laser $^{40}Ar/^{39}Ar$ evaluation of slow cooling and episodic loss of ^{40}Ar from a sample of polymetamorphic muscovite. *Science*, 261(5129):1721–1724, 1993.

[23] Willis E. Hames and Arild Andresen. Timing of paleozoic orogeny and extension in the continental shelf of north-central Norway as indicated by laser $^{40}Ar/^{39}Ar$ muscovite dating. *Geology*, 24(11):1005–1008, 1996.

[24] T. Mark Harrison, Ian Duncan, and Ian McDougall. Diffusion of ^{40}Ar in biotite: temperature, pressure and compositional effects. *Geochimica et Cosmochimica Acta*, 49(11):2461–2468, 1985.

[25] Alemdar Hasanov and Marián Slodička. An analysis of inverse source problems with final time measured output data for the heat conduction equation: A semigroup approach. *Applied Mathematics Letters*, 26(2):207–214, 2013.

[26] A. Hazanee, M. I. Ismailov, D. Lesnic, and N. B. Kerimov. An inverse time-dependent source problem for the heat equation. *Applied Numerical Mathematics*, 69:13–33, 2013.

[27] Kip V. Hodges, Willis E. Hames, and Samuel A. Bowring. $^{40}Ar/^{39}Ar$ age gradients in micas from a high-temperature-low-pressure metamorphic terrain: evidence for very slow cooling and implications for the interpretation of age spectra. *Geology*, 22(1):55–58, 1994.

[28] Victor Isakov. *Inverse problems for partial differential equations*. Applied Mathematical Sciences 127. Springer, 2nd edition, 2006.

[29] N. I. Ivanchov. Inverse problems for the heat-conduction equation with nonlocal boundary conditions. *Ukrainian Mathematical Journal*, 45(8):1186–1192, 1993.

[30] Sergei Igorevich Kabanikhin. Definitions and examples of inverse and ill-posed problems. *Journal of Inverse and Ill-Posed Problems*, 16(4):317–357, 2008.

[31] Fatma Kanca and Mansur I. Ismailov. The inverse problem of finding the time-dependent diffusion coefficient of the heat equation from integral overdetermination data. *Inverse Problems in Science and Engineering*, 20(4):463–476, 2012.

[32] Michael V. Klibanov and Alexander A. Timonov. *Carleman estimates for coefficient inverse problems and numerical applications*. Inverse and ill-posed problems 46. Walter de Gruyter, 2004.

[33] Jichun Li and Yi-Tung Chen. *Computational partial differential equations using MATLAB*. CRC Press, 2008.

[34] Ian McDougall and T. Mark Harrison. *Geochronology and Thermochronology by the* ^{40}Ar/^{39}Ar *Method*. Clarendon Press, Oxford, 1988.

[35] A. J. Meir and Irad Yavneh. An elliptic problem with integral constraints with application to large-scale geophysical flows. *Computational Geosciences*, 2(4):337–346, 1998.

[36] Nabil Merazga and Abdelfatah Bouziani. Rothe method for a mixed problem with an integral condition for the two-dimensional diffusion equation. *Abstract and Applied Analysis*, 2003(16):899–922, 2003.

[37] Amnon Pazy. *Semigroups of linear operators and applications to partial differential equations*. Applied Mathematical Sciences 44. Springer-Verlag, 1983.

[38] Aleksey I. Prilepko, Dmitry G. Orlovsky, and Igor A. Vasin. *Methods for solving inverse problems in mathematical physics*. Pure and Applied Mathematics. CRC Press, 2000.

[39] Karel Rektorys. *The method of discretization in time and partial differential equations*. Mathematics and its Applications. D. Reidel Publishing Company, 1982.

[40] Michael Renardy and Robert C. Rogers. *An introduction to partial differential equations*. Texts in Applied Mathematics 13. Springer New York, 2nd edition, 2004.

[41] William Rundell. Determination of an unknown non-homogeneous term in a linear partial differential equation from overspecified boundary data. *Applicable Analysis*, 10(3):231–242, 1980.

[42] Karel Švadlenka and Seiro Omata. Construction of solutions to heat-type problems with volume constraint via the discrete morse flow. *Funkcialaj Ekvacioj*, 50(2):261–285, 2007.

[43] Vidar Thomée. *Galerkin Finite Element Methods for Parabolic Problems*. Springer Series in Computational Mathematics. Springer, 2nd edition, 2006.

[44] E. Bruce Watson, Keith H. Wanser, and Kenneth A. Farley. Anisotropic diffusion in a finite cylinder, with geochemical applications. *Geochimica et Cosmochimica Acta*, 74(2):614–633, 2010.

[45] J. Wheeler. Diffarg: a program for simulating argon diffusion profiles in minerals. *Computers and Geosciences*, 22(8):919–929, 1996.

[46] Liu Yang, Mehdi Dehghan, Jian-Ning Yu, and Guan-Wei Luo. Inverse problem of time-dependent heat sources numerical reconstruction. *Mathematics and Computers in Simulation*, 81(8):1656–1672, 2011.